Instituto Tecnológico y de Estudios Superiores de Monterrey

Campus Monterrey

School of Engineering and Sciences

Technical and economic evaluation for two process alternatives of CO_2 mineralization technology using electric arc furnace slag as raw material

A thesis presented by:

Diana Edith Martínez García

Submitted to the School of Engineering and Sciences
in partial fulfillment of the requirements for the degree of

Maestro en Ciencias

con

Especialidad en Ingeniería Energética

Monterrey, Nuevo León, MX May 15th, 2018

Instituto Tecnológico y de Estudios Superiores de Monterrey

Campus Monterrey

School of Engineering and Sciences

The committee members, hereby, certify that have read the thesis Project presented by **Diana Edith Martínez García** and that is fully adequate in scope and quality a partial requirement for the degree of Master of Science in Energy Engineering.

Ph. D. Alejandro Montesinos Castellanos
Tecnológico de Monterrey
School of Engineering and Sciences
Advisor

B. Eng. Maria Teresa Guerra Reyes
Tenova HYL
Advisor

M. Sc. Josué Florencio Guzmán Lozano
Tenova HYL
Committee Member

M. Sc. Juan Antonio Villarcal Treviño
Consultant. Tenova HYL
Committee Member

Dr. Rubén Morales Menéndez
Dean of Graduate Studies
School of Engineering and Sciences

Monterrey, Nuevo León, MX

May 15th, 2018

Declaration of Authorship

I, Diana Edith Martínez García, declare that this thesis titled, "Techno-economic evaluation for two process alternatives of CO_2 mineralization technology using electric arc furnace slag as raw material" and the work presented in it are my own. I confirm that:

- This work was done wholly or mainly while in candidature for a research degree at this University.
- Where any part of this thesis has previously been submitted for a degree or any other qualification at this University or any other institution, this has been clearly stated.
- Where I have consulted the published work of others, this is always clearly attributed.
- Where I have quoted from the work of others, the source is always given. Except for such quotations, this thesis is entirely my own work.
- I have acknowledged all main sources of help.
- Where the thesis is based on work done by myself jointly with others, I have made clear exactly what was done by others and what I have contributed myself.

Diana Edith Martínez García

Monterrey, Nuevo León, MX May 15th, 2018

Acknowledgements

I would first like to thank Tenova HYL and the Industrial Consortium to Foster Applied Research in Tecnológico de Monterrey. In particular, I wish to thank Osvaldo Micheloud, Stefano Magliolino and Manuel Echeverria for giving me the opportunity of pursuing my master thesis. I am grateful and satisfied to have worked in this amazing project and within this collaboration.

I would also like to thank Teresa Guerra, Josué Guzmán, Antonio Villareal, Jorge Becerra and Alejandro Montesinos, as well as the rest of the Engineering Design Team from Tenova HYL, for their scientific advices and instruction with the design and modelling of the processes analyzed in this thesis as well as their introduction to the world of iron and steelmaking. Than you all for your invaluable support and guidance during this research.

I specially want to acknowledge my current and former Consortium colleagues for their help and companion during the last two years, to my closest friends for their understanding and motivation, and to Daniel for his unfailing support and continuous encouragement towards this work; for being there.

I could not finish this section without mentioning my family, my dear parents David Martínez and Alicia García, my sister Dulce Alicia and brother Jesus Alberto who are always in my heart and have supported me all my life.

Technical and economic evaluation for two process alternatives of CO_2 mineralization technology using electric arc furnace slag as raw material

by

Diana Edith Martínez García

Abstract

Carbon dioxide is the major recognized cause of climate change because of its greenhouse properties and continuous accumulation in the atmosphere. It has become attractive for industries that emits great amounts of CO_2 emissions to the atmosphere the application of Carbon Dioxide Utilization (CDU) technologies in their processes. In this thesis, technical, economic and environmental aspects are presented to conceptualize two pilot plants that utilize two waste materials, one being the Electric Arc Furnace (EAF) slag produced during steel making and two the CO_2 removed in a Direct Reduction (DR) plant to produce either Light Weight Aggregate (LWA) for the construction industry or Precipitated Calcium Carbonate (PCC) for the chemical industry. The objective of the research reported was to evaluate the feasibility for the implementation of the CDU processes in an integrated steelmaking facility which includes a Direct Reduction plant.

Keywords: greenhouse

List of figures

List of tables

Abbreviations

BF	Blast Furnace
CCS	Carbon Capture and its Storage
CDU	Carbon Dioxide Utilization
DR	Direct Reduction
DRI	Direct Reduced Iron
DR-EAF	Direct Reduction-Electric Arc Furnace process
EAF	Electric Arc Furnace
GCC	Ground Calcium Carbonate
GHG	Greenhouse Gas
IEA	International Energy Agency
IPCC	Intergovernmental Panel on Climate Change
JRC	Joint Research Centre
LWA	Light Weight Aggregate
MFA	Material Flow Analysis
PCC	Precipitated Calcium Carbonate
PFD	Process Flow Diagram
TRL	Technology Readiness Levels

CONTENTS

CHAPTER 1 INTRODUCTION

1.1 INTRODUCTION

Greenhouse gases (GHG) in the atmosphere have reached the highest levels ever recorded, and concentrations are increasing. Carbon dioxide (CO_2), the most important greenhouse gas, has increased by 90 ppm (480 billion tones) in about 200 years [1]. The Intergovernmental Panel on Climate Change (IPCC), during the 5th Assessment Report (AR5) issued in 2013-14, confirmed that in order to avoid the worst effects of climate change it is necessary to keep the temperature rise less than 2 degrees and that CO_2 emissions should be reduced globally by 41-72% by 2050 respect to 2010 levels [2].

There are four main paths to avoid excessive CO_2 concentration in the atmosphere: (a) the carbon capture and its storage (CCS), (b) energy efficiency improvements, (c) alternative energy sources and (d) carbon dioxide utilization (CDU). The recent interest in CDU technologies stems primarily from the fact that CO_2 is a potentially recyclable material with an interesting application profile and great potential for the chemical industry. A benefit of CDU processes is the possibility to use CO_2 in local effluent streams; in this way, the greenhouse gas can be transformed into a raw material for a material value chain in an industrial facility and allow the manufacturing of a high value-added chemical product [3].

In the steelmaking industry, one of the greatest CO_2 emitters in the world, the conventional Direct Reduction (DR) industrial processes in the world include MIDREX and Tenova HYL technologies which are very similar but differ in detail such as gas production and heat recovery systems. Although Tenova HYL technology operates with lower carbon dioxide emissions, the ironmaking plant usually associated to this process is still one of the most raw material-dependent and energy intensive industry with large waste generations in the world [4]. There is a pressing need to solve these resource and environmental problems associated with the steel manufacture.

A possible feedstock for CO_2 mineralization processes is industrial solid waste, such as slags generated from steel plants. These materials are generally alkaline and rich in calcium which can be easily reacted with CO_2 via ion leaching and carbonation reaction, which is like the natural weathering processes [5]. Moreover, these residues tend to be more reactive for carbonation than primary minerals due to their chemical instability and thus their use might enable a reduction of the energy consumption compare to conventional CO_2 mineralization route [6].

For all reasons mentioned above, this work analyzes two CO_2 mineralization processes in three main parts following engineering and investment analysis principles. The first one aims to confirm the occurrence of the main reactions for the CO_2 mineralization with laboratory tests while. The second part includes simulation of both processes accomplished by Aspen Plus software to solve the mass and energy balances, as well as the economic analysis. Finally, the third part consists in a comprehensive comparison of the two pilot plants (one for each alternative) is developed by evaluating the economic and technical impacts of the deployment of the CO_2 mineralization processes. our research efforts concentrate on ensuring process operability in such a way that a specified PCC.

1.2 BACKGROUND

The CCS technologies have been the conceptual solution to the environmental issue as they capture CO_2 effectively and transport it to where it can be stored for medium to long periods of time avoiding its emission to the atmosphere. Despite of their technological efficiency, they are not yet economically feasible nor mature technologies [7]. As a result, CDU, using the captured CO_2 from industries sources, is becoming more and more recognized worldwide as it not only reduces CO_2 emission to atmosphere but also generates economic profit by producing sellable products.

These two approaches are complementary as CCS aims to capture and storage CO_2 while CDU aims to generate value to the waste CO_2. CDU technologies stand in this thesis for the conversion of CO_2 to produce materials that have the potential to be part of the CO_2 abatement

options of the future, decreasing CO_2 emissions and entailing less fossil fuel consumption [8].

In the process of CO_2 mineralization, the GHG reacts with selected materials containing CaO (and other forms of alkaline compounds as MgO) to form a solid carbonate, which can lead to salable products primarily for the construction industry. Whereas chemicals and fuels typically only offer a short to medium term store of CO_2, using CO_2 in a mineralization process, either by accelerating the carbonation of certain types of industrial waste, or with certain types of minerals, permanently stores CO_2 [9]. This process is thermodynamically favored but is kinetically challenging in nature. Thus, most of the research in the area of carbon mineralization has been focused on the mineral dissolution and carbonation [10].

1.2.1 HYL Direct Reduction process

The DR HYL technology process is designed to convert iron pellet/lump into metallic iron using reducing gases. Oxygen is removed from the iron ore by chemical reactions based on hydrogen (H_2) and carbon monoxide (CO), to produce highly metallized Direct Reduced Iron (DRI). The DR process flow diagram of the HYL technology can be found in Figure 1-1 [12].

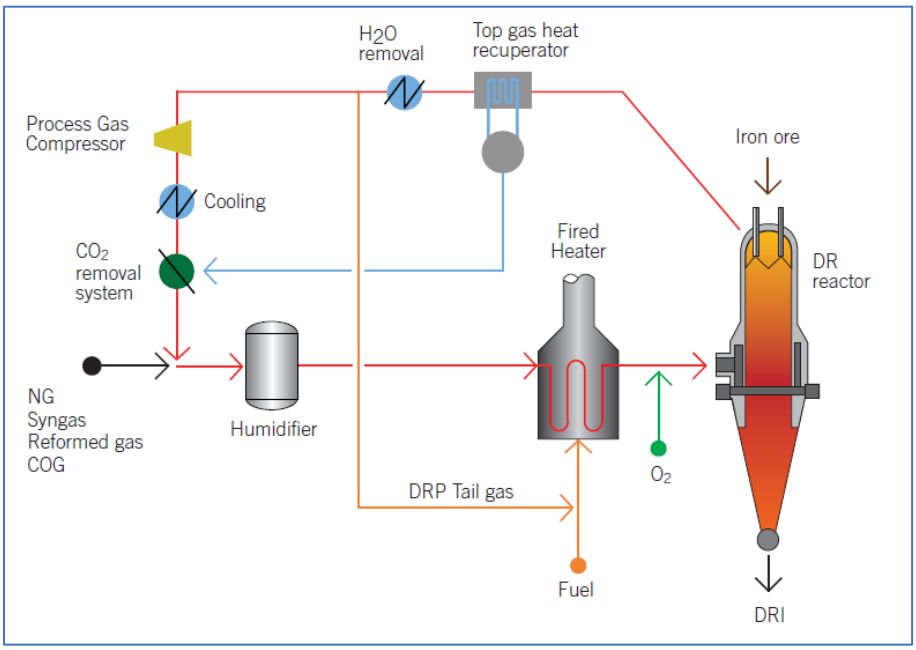

Figure 1- 1 Direct Reduction process flow diagram [12].

The technology offers the flexibility to produce three different product forms, depending on the specific requirements of each user. The basic components of the reduction circuit, aside from the reactor, are a gas heater to increase the reducing gases temperature up to 925° C; a scrubbing unit for dedusting, cooling and H_2O elimination from top gases; the recycle gas compressor and the CO_2 removal unit [12].

Inside the shaft furnace vessel, hot reducing gas is fed to the reduction zone and flows upward to the iron ore moving bed. The exhaust reducing gas (top gas) leaves the reactor at about 400 °C and passes through the top gas heat recuperator, where its energy is recovered to produce steam, or alternatively to preheat the reducing gas stream, and then through the quenching/scrubbing system. In these units, water produced during the reduction process is condensed and removed from the gas stream and most of the dust carried with the gas is also separated. Scrubbed gas is then passed through the process gas recycle compressor, where its pressure is increased. Compressed gas, after being sent to the carbon dioxide removal unit, is mixed with the natural gas make-up, thus closing the reducing gas circuit.

In the CO_2 removal unit, the compound is selectively removed through an amine-based absorption for a more efficient reuse. It consists of a CO_2 absorption column and one stripping column, plus auxiliary equipment. The recycled reduction gas, with high CO_2 concentration,

is fed to the CO_2 removal system at the bottom of the absorption column, as shown in Figure 1-2 [13].

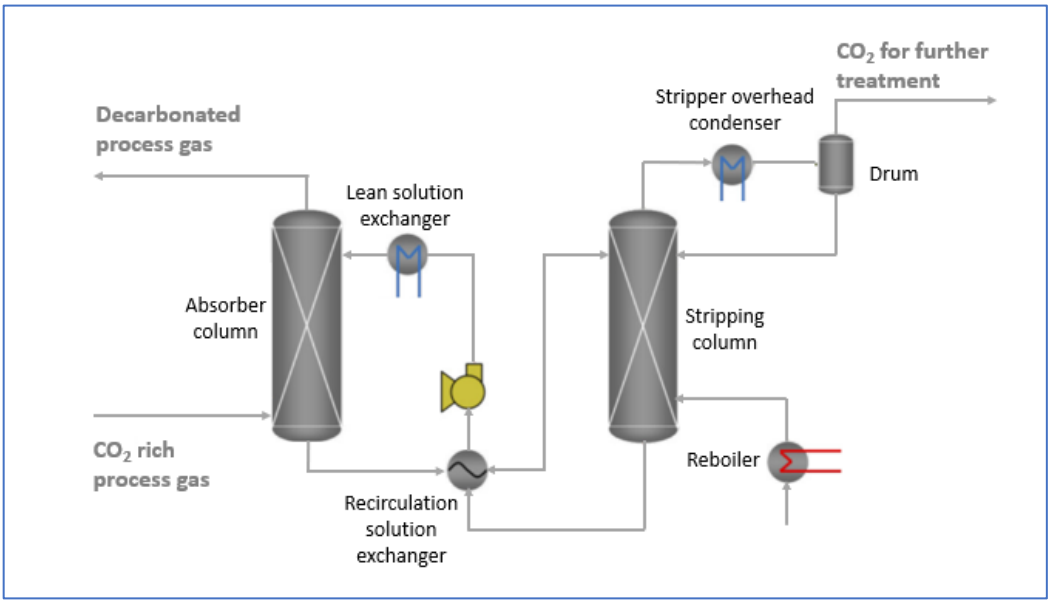

Figure 1- 2 CO_2 absorption system in the HYL DR technology process [13].

In the CO_2 absorption column, the gas is decarbonated by counter-current contact with cold lean absorbing solution coming from the stripping section [13]. Decarbonated gas exits at the top of the absorption column with a lower CO_2 content and then routed back to the reducing gas circuit. Rich solution exits from the bottom of the CO_2 absorption column, and then, the CO_2 is stripped off from the rich solution in the stripping column. The CO_2 rich vapor stream is lastly cooled down and at this point, the rich CO_2 gas stream is ready for commercialization or further treatment.

The International Energy Agency (IEA) has reported that CO_2 emissions of steel produced from 100% natural gas based DRI is between 0.77 to 0.92 tCO_2/tsteel. Different from the Blast Furnace (BF) route, a DR process can use not only natural gas, but also syngas from coal gasification, coke oven gas and hydrogen. For this reason, the DR route emits 40% to 60% less CO_2 as compared with BF [11].

1.2.2 Electric Arc Furnace slag

Electric Arc Furnace (EAF) slags are by-products from iron and EAF steel manufacturing, EAF slags consist primarily on oxides of calcium, magnesium, iron, silicon and aluminum, as well as silicates in various combinations. They also contain several trace elements, which may be freed if the slags are dissolved in a carbonation process [14].

While the chemical composition of the EAF slags is dependent on the compositions of the raw materials and the process step through which they are generated on, their physical characteristics vary depending on the slag processing. In a steel making process via direct reduction and electric arc furnace (DR-EAF), slag has a dual function: (a) It controls the chemical composition of steel via the additives that affect the chemical equilibrium between steel and slag, and (b) as slag foam, it covers the electric arc, thereby decreasing the energy lost through radiation [15].

EAF slags are mainly utilized as a concrete aggregate and in various applications in highway construction. Recently, they have also been deemed as alternatives for mineral sequestration because of its similarity to natural Ca/Mg-bearing silicate minerals. Typically, the slag from DR-EAF has a CaO content of 24-40%; According to Hannu-Petteri and Forsman in [16],this amount could store, ideally, up to 314 Kg of CO_2 per each ton of slag via CO_2 mineralization. While the CO_2 fixation capacity of natural silicate minerals is greater than that, this slag still appealing because, as a waste in the steel plant, it is readily available, removing the need to mine and transport huge amounts of minerals.

After separating steel slags from molten steel, they are transferred to holding locations to be shipped for landfill. While most of the steel slags are currently categorized as unhazardous wastes, stainless steel slags that contain Ni and Cr are labelled as hazardous wastes; these cannot be landfilled without further treatment.

1.3 PROBLEM DEFINITION

For more than 60 years, Tenova HYL has developed technologies designed to improve steelmaking competitiveness and productivity for steel facilities. Although the process efficiency has been significantly improved, the process still emits CO_2 that has no use in the overall system. Some of the CO_2 is selectively removed from the recycled process gases stream and sometimes sold after that to other companies.

Tenova HYL is looking forward to adding value to the selectively removed CO_2 utilizing it directly in a downstream process without any need of an additional purification stage. The downstream process consists in mineralization of this CO_2 utilizing slag for this purpose. To properly validate this alternative, it is needed first to validate the technical feasibility of this CDU technology, via experimental work, and second to completely evaluate the mineralization route via design and simulation of pilot scale unit.

In the present work, the laboratory evaluation is presented and based on the results obtained, the pertinent work to the conceptual design of a pilot installation was performed. For the pilot plants, an estimation of the investments was finally done.

1.4 JUSTIFICATION

The production of steel is not only a very energy intensive process, but a great contributor of carbon dioxide emissions. Tenova HYL DR process technology selectively remove 62% of the total carbon inlet of the system as CO_2. Since this compound has the potential to be used and transformed into a commercial product; CCS and CDU technologies represent a new economy in the use of CO_2 as raw material.

Being the Technology Readiness Levels (TRL) a type of measurement system used to assess the maturity level of technologies, with a range from 1 to 9 (see Appendix A), the Joint Research Centre (JRC) has used it to prioritize five of the main CDU utilization pathways, and their market potential, following the discussions that took place in the CO_2 re-use

workshop, in June 2013 by the European Commission [17]. The CDU products considered, the TRL of the CDU plants and their worldwide production are summarized in Table 1-1.

Table 1- 1 CDU technology products considered by the JRC [17].

CDU products	TRL	Worldwide production (Mt/yr)
Methanol	6-7	61
Formic Acid	3-5	0.62
Urea	9	150
Mineral Carbonates	6-9	14
Polyol for Polyurethanes	3-5	8

Based on the given information, one promising option that can contribute to the reduction of the GHG, is the production of mineral carbonates. The CDU technology that produces mineral carbonates is called CO_2 mineralization and it stands mostly in demonstration stage as the TRL in Table 1- indicates.

A steel plant could benefit from a CO_2 mineralization process by combining two of its own by-products; one hand the slag; which has few useful applications and is partly landfilled, and one the other hand the CO_2 that right now it is sent to the atmosphere from the DR process. The product resulting will be marketable calcium carbonate ($CaCO_3$)-based products. This alternative would not only generate economic benefits but provide a new utilization option for the low-value slag and the anthropogenic gas.

It has been found that success of CO_2 mineralization depends critically on the cost and efficiency with which alkalinity can be extracted from feedstocks, and subsequently carbonated. While various CO_2 mineralization processes have been proposed, an economical and scalable process that could produce carbonated products with enough low energy requirements has not yet been found [18] [19] [20] [21] [22].

Given the information above, this work focuses on the mineralization of CO_2 from EAF slag by conceptualizing the CDU pilot-plants in order to identify whether a commercial product

can be produced. Based on data obtained by the experimental and simulation work, the cost of their implementation in a steel plant with a DR process will be estimated.

1.5 OBJECTIVES

The main scope for the present work is to provide relevant technical and economic aspects of the CO_2 mineralization technology to conceptualize two CDU pilot plants and evaluate their feasibility of implementation as a coupled with the direct reduction process in a steel facility. Objectives could be divided into:

1. Determine the efficiency of Ca^{++} ions extraction from EAF slag and its carbonation via CO_2 absorption.
2. Performance of the pilot plants simulation using Aspen Plus
3. Economic evaluation of both processes
4. Comparison of CDU pilot plants

To ensure the realization of these objectives, the following activities must be developed.

a) Literature review of state of the art and outlook of the Steel Industry and mineralization CDU technology.
b) Experimental work
c) Elaboration of process flow diagrams.
d) Processes simulation
e) Mass and energy balances performance
f) Economic analysis
g) Techno-economic evaluation
h) Pilot plants comparison.

Chapter 2 literature review

For CO_2 utilization, there are physical methods such as capture and sequestration under the ocean and soil, chemical methods such as catalysis/electrochemical reaction, inorganic chemical reaction and carbonation, and biological methods such as forestation/reforestation, plant/algae or microbe usage. Table 2-1 enlists the main Carbon Dioxide Utilization (CDU) technologies and their maturity level.

Table 2- 1 Maturity level of main CDU technologies

CDU category	CDU technology	Maturity level		
		Research	Demonstration	Mature market
Enhanced commodity production	Power cycles ($scCO_2$)	***		
	Urea production			***
Enhanced hydrocarbon recovery	CO_2-EOR			***
	CO_2-EGR		***	
	ECBM		***	
CO_2 to fuel	Renewable methanol		***	
	Formic acid	***	*	
	Algae	***	***	
	Photocatalytic processes	***		
CO_2 mineralization	Cement production	*	***	
	CO_2 concrete curing		*	
	Carbonate mineralization	***	***	
Chemicals production	Sodium carbonate			***
	Polymers	***	*	
	Acetic acid	***		
	Algae		***	

EOR=Enhanced Oil Recovery. EGR=Enhanced Gas Recovery. ECBM=Enhanced Coal Bed Methane.

*Some activities

***Main activities

Within this table “Research” means that while the basic science is understood, the technology is conceptually feasible and some testing at the laboratory or bench scale has been carried out, it has not yet been demonstrated in a pilot plant. “Demonstration” means that the technology has been, or is being, built and operated at the scale of a pilot plant, but that further development is required before the technology is ready for use in a commercial/full scale system.” Mature market” means that the technology is in commercial operation with multiple replications or could be easily modified to accommodate new applications involving non-captive CO_2. Appendix B shows a detailed description of these CDU technologies reviewed.

Among the prospective technologies for CO_2 utilization, this thesis is focused on CO_2 mineralization. To fully understand the problem context, it is convenient to introduce the general mechanism and process of the CDU technology and review its application to manufacture marketable products such as precipitated calcium carbonate (PCC) and Light Weight Aggregates (LWA).

2.1 CO_2 MINERALIZATION

As a promising approach for CO_2 sequestration and utilization, CO_2 mineralization technology captures CO_2 in its mineral form by the reaction of this element with alkaline materials, including calcium- rich oxides and silicates, to form environmental friendly solid carbonate products.

One clear advantage of CO_2 mineralization compared to Carbon Capture and its Storage (CCS) methods is that the product of the first one, $CaCO_3$, is thermodynamically stable under ambient conditions. Thus, this method can store CO_2 for a very long time, making post storage monitoring of carbon dioxide stored as carbonates unnecessary and representing a CDU technology [23]. On the other hand, the main disadvantage of CO_2 mineralization is that although the net carbonation reaction is exothermic, this reaction does not occur spontaneously and requires large amounts of additives and/or energy to actually take place.

Mineral carbonation process is roughly divided into direct and indirect methods. In direct methods, the mineral is carbonated in one step, while in indirect methods, the reactive element (such as Ca or Mg, as ions or oxides, hydroxides, etc.) is first extracted from the mineral prior to carbonation (Figure 2-1) [24].

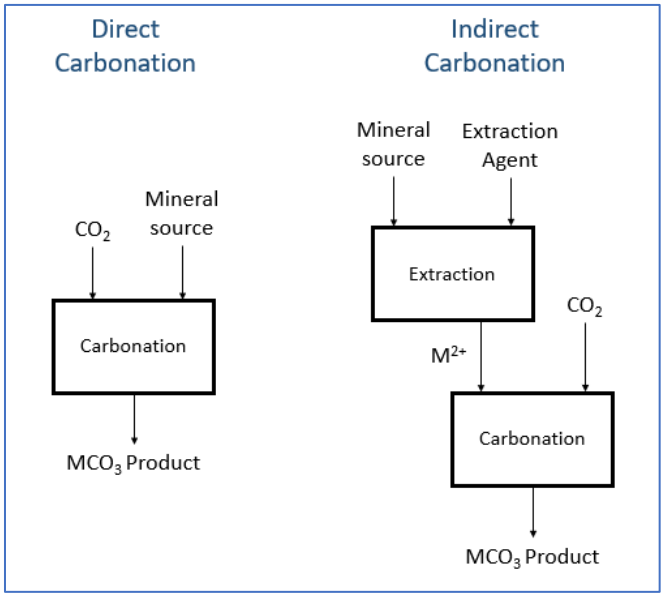

Figure 2- 1 Direct and indirect CO_2 mineralization methods scheme **[25]**.

In indirect carbonation, the solvent agent enhances the extraction of reactive compound (like Ca), the following carbonation reaction step, on the other hand, is dependent on a basic (alkaline) environment [25]. This two-step route allows optimizing the conditions for both the extraction and the carbonation. Most of these processes usually provide a faster carbonation route than direct processes but demand additional energy or chemicals. Moreover, the precipitated end products from the indirect carbonation process, has higher quality compared to the products obtained by direct carbonatation. The higher the quality of the products is, the easier and faster they can be adapted for various industrial and construction applications [26].

Since indirect carbonation route seems to have more advantages than direct carbonation, it was selected as the CO_2 mineralization route for the present work, including the conceptual design of a pilot plant, in the next section are listed and described the current developments on this CO_2 mineralization type.

2.2 STATE OF THE ART

Currently, as established in the previous chapter, CO_2 mineralization is mainly at the level of laboratory-scale research. It has been implemented only by a few companies and their demonstration plants. Blue Planet (previously Calera Corporation) has been operating a demonstration facility that produces the material from CO_2 and carbide residue: an industrial waste that comes from the production of polyvinyl chloride (PVC) [2]. Blue Planet first adds water to the residue to extract calcium hydroxide, then bubbles CO_2-rich flue gas from a nearby industrial plant through the solution to obtain pure calcium carbonate, which is turned into fiber cement boards that can be used in construction.

CarbonCure Technologies Inc. developed a precast concrete manufacturing technology with a concrete curing process utilizing waste CO_2 gas captured in coal fired power plant and cement factory, while Skyonics patented CO_2 mineralization process system converting flue gas CO_2 into bicarbonate (baking soda) as main commercial product [2].

Table 2- 2 Overview of CO_2 mineralization technology

Description	CaO composition (wt%)	Reference
TRL	6-9	[2]
Production plant level scale	10 kton/yr	[8]
Production worldwide scale	0.62 Mton/yr	[27]
Maturity	Demonstration	[28] [29]
Involved companies and organization	Blue Planet, Skyonic Corp, CarbonCure, Carbon8	[24] [30] [31]
Advantages	CO_2 stored for long periods, no risk of CO_2 leakage, Abundant materials (minerals or industrial wastes)	[8]
Disadvantages	Low efficiency, High capital costs anticipated, Not enough information about the durability and stability of the chemically fixed CO_2	[8] [32]
Technical challenges and opportunities	Minerals reserves that can be technically exploited, Meet industrial standards for building materials	-

Some other recent studies in CO_2 mineralization were also reviewed and analyze to generate Table 2-2 which presents summarize for the current advantages and opportunities of the CDU technology.

2.3 LIGHT WEIGHT AGGREGATE

Agglomerating processes are used to increase the grain size of powders, by sticking particulates together with a liquid binder and mechanical agitation, such as tumbling in a revolving drum. This process is controlled by the physio-chemical properties of the input powder, the moisture content of the feed and process parameters such as rotation speed [26]. These energy intensive processes form low-density solid pellets by particle fusion and swelling this structure is called Light Weight Aggregate (LWA).

The UK currently consumes around 280 million tonnes of aggregate annually, 25% of which is derived from secondary and recycled sources. Light aggregates are subject to the Aggregate are currently $220 per tonne produced and there is increasing interest in the use of alternative materials [6]. One of the objectives of the present thesis was to examine the use of CO_2 mineralization process utilizing EAF slag to produce a material suitable for use as LWA, and the validation of the process at pilot scale level. Figure 2-2 shows the main stages for the LWA production process [33].

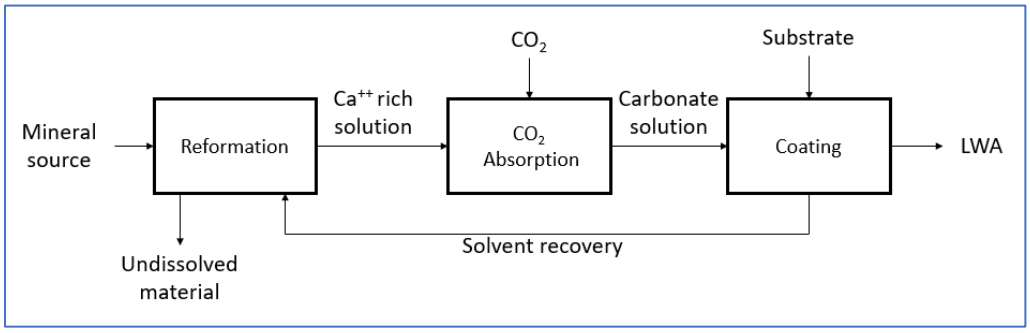

Figure 2- 2 LWA production process concept found in literature [33].

This CO_2 mineralization route consists on a first step called Extraction, where the divalent ions of interest are extracted from the alkaline source with help of an extraction agent

(Depending on the nature of the material). Then a CO_2 absorption stage takes place to generate a carbonate solution; the carbonate generated is used for the agglomeration of the substrate in the final coating stage, producing light weight aggregates.

2.4 PRECIPITATED CALCIUM CARBONATE

The calcium carbonate found in nature and used in industry is called ground calcium carbonate (GCC). Natural calcium carbonate is used for various purposes, such as manufacturing concrete or cement, and producing lime to be used in, for example, soil stabilization and neutralization, glassmaking, water treatment, and flue gas desulphurization [34].

Precipitated calcium carbonate or commonly called PCC has the same chemical formula as GCC ($CaCO_3$) but instead of crushing limestone the PCC is created by precipitation, this makes PCC cleaner and purer than GCC. When precipitating calcium carbonate the crystal forms, structures and size can be adjusted, unlike GCC where the structure is generally calcite with a large size distribution of the rhombohedral particles. PCC is commonly used as a filler and coating pigment in plastics, rubbers, paints, and papers. It is consumed mainly by the paper industry and has quite a high price (>$100/ton). Its total annual consumption is approximately 13 Mt worldwide [35].

There are several ways of producing PCC, some more expensive than others. The most common methods are precipitation with gaseous carbon dioxide, the lime soda process and the Solvay process where the PCC is a by-product from ammonia production [36]. This thesis is focused in its precipitation using carbon dioxide. A description of a PCC production process can be seen in Figure 2-3, where a mineral source containing Ca (i.e. EAF slags) and CO_2 are the main input of the process.

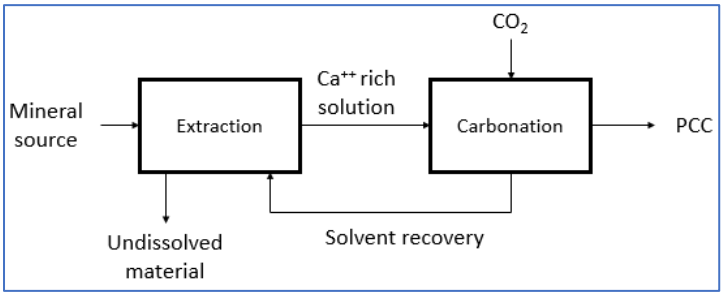

Figure 2- 3 PCC production process found in literature [36].

The calcium-containing material is added to the aqueous solution in the extraction reactor and it reacts with the circulating solvent, after which the residue from the slag is removed from the process product solution. The Ca^{++} rich solution continues to the carbonation reactor where CO_2 is added. During carbonation a two-staged reaction takes place, precipitated after which it is removed from the process while the solvent solution is recirculated to the first step.

The markets for the PCC product are limited; in 2011 the worldwide consumption was estimated at 14 Mt. Measured in Mt of CO_2 captured, and according to Ron Zevenhoven et. al. in [36], if all PCC production was replaced by a CO_2 mineralization technology, 6.2 Mt of CO_2 could be chemically bound to calcium carbonate product.

In both mineralization processes mentioned (for LWA and PCC production), the governing reaction for Ca extraction is simplified as Equation (2.1), which describes the effect of the salt solvent on the dissolution of calcium oxide.

$$\mathrm{Ca}O_{(s)} + 2NH_4Cl_{(aq)} + H_2O_{(l)} \leftrightarrow CaCl_{2(aq)} + 2NH_4OH_{(aq)} \quad (2.1)$$

In this context, CaO represents all water-soluble Ca regardless of the actual crystal form in which it is bound. For the carbonation step, the main reactions can be summarized as Equations (2.2) and (2.3).

$$2NH_4OH_{(aq)} + \mathrm{C}O_{2(g)} \leftrightarrow (NH_4)_2CO_{3(aq)} + H_2O_{(l)} \quad (2.2)$$

$$(NH_4)_2CO_{3(aq)} + CaCl_{2(aq)} \leftrightarrow CaCO_{3(s)} + 2NH_4Cl_{(aq)} \quad (2.3)$$

The crystal shape of the calcium carbonate can be controlled by temperature: a precipitation temperature of 60–80 °C or higher forms aragonite, while a temperature of 20–30 °C will produce rhombohedral calcite. As aragonite is the wanted product in this case study, the carbonator temperature is kept at 60 °C [37].

Chapter 3 methodology

This chapter presents the methodology carried out for the development of this thesis. Figure 3-1 provides a general view of the limitation and scope of this investigation. It describes the main activities presented in each chapter of this thesis as well as their objectives.

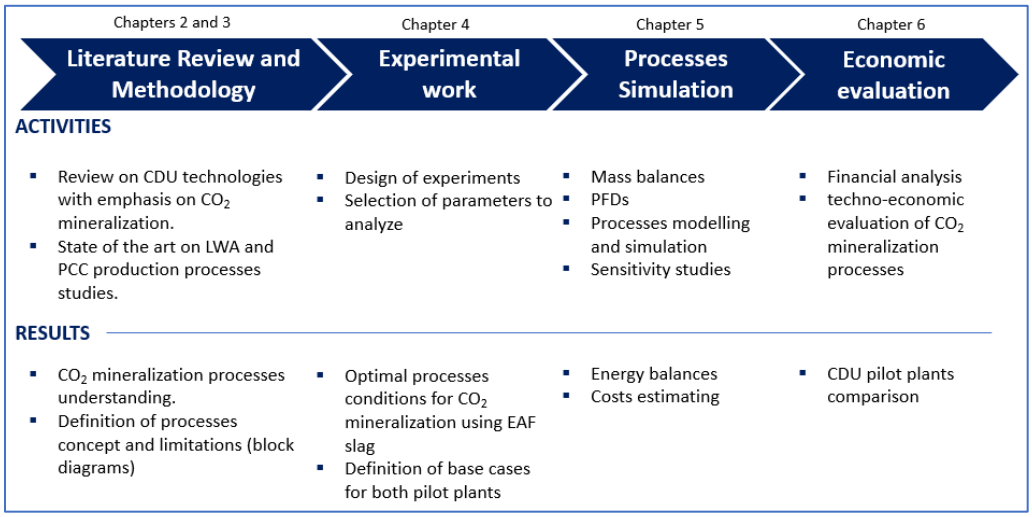

Figure 3- 1 Investigation methodology applied in this study.

The general objective of this thesis was to determine if CO_2 mineralization is a feasible CDU technology to implement with a direct reduction process in a steel plant. This was responded by evaluating two CDU technologies (to produce light weight aggregates and precipitated calcium carbonate) in terms of technical and economic aspects to prove the hypothesis that CO_2 mineralization represents a feasible technology choice. Therefore, the investigation methodology consisted of a literature review of state of the art and outlook of both CO_2 mineralization processes in chapter 2; the experimental work to replicate the main stages of both process in chapter 4; elaboration of process diagrams and mass and energy balances in chapter 5 and economic analysis and technologies evaluation in chapter 6. Additional to the sections previously mentioned which describe the methodology to carry out the project; it is presented, in chapter 7, a brief pilot plant comparison.

3.1 EXPERIMENTAL WORK

As mentioned before, when the research reported in this thesis started, the NH_4Cl process route, found in the literature, seemed to be the most promising carbonation route [37]. Therefore, this was the selected solvent for the study.

The CO_2 mineralization processes proposed in this thesis had not been previously tested for DR-EAF slag. Therefore, the necessity of the experimental work to determine if calcium could actually be extracted from the slag using NH_4Cl. Also, it was of great importance to confirm the precipitation of calcium carbonate. Having stablished these requirements, it was decided to perform two types of laboratory tests: (a) Calcium extraction and (b) Carbonate precipitation tests. Both experiments are described with more details in the next chapters.

The experimental design for Ca extraction tests as well as Carbonation tests are showed in their correspondent section.

3.1.1 Calcium extraction

The experimentation objective of this phase was to confirm the calcium extraction from the slag, in this work, it means the selective solution of 2^{++} ions extracted from the slag using a NH_4Cl aqueous solution. Being Ca^{++} one of the main ions selectively extracted, the ability of NH_4Cl to dissolve Ca from the slag was particularly investigated by dissolving the slag in various concentrations of an aqueous solution of the solvent.

This extraction step in which calcium in the steel slag is dissolved can be described by equations 3.1 and 3.2, as follows.

$$\mathrm{Ca}O_{(s)} + 2NH_4Cl_{(aq)} + H_2O_{(l)} \leftrightarrow CaCl_{2\,(aq)} + 2NH_4OH_{(aq)} \quad (3.1)$$

$$\mathrm{Ca}O_{(s)} + H_2O_{(l)} \leftrightarrow Ca^{2+} + 2OH^{-}_{(aq)} \quad (3.2)$$

Figure 3-2 describe, as an example, the protocol used for these experiments. The slag, previously grounded to specific grain size, was added to a becker containing NH_4Cl aqueous

solution a constant temperature. A magnetic stirrer was used for mixing the solution constantly for 20 minutes and was left to fully precipitate for at least 2 hours. After settlement, the liquid phase was decanted, keeping most of the precipitate in the beaker.

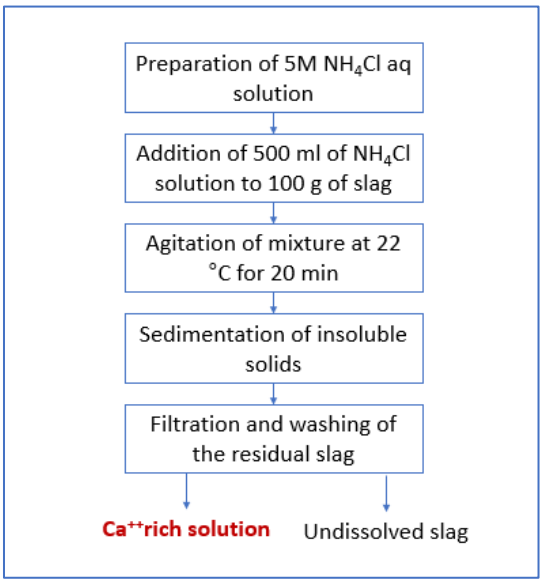

Figure 3- 2 Experimental protocol follow during the Calcium Extraction tests

This Ca-rich solution was separated and stored for further analysis. Filtration process began with a Whatman 3 filter paper until the beaker seemed cleared of mixture. The precipitate was washed with deionized water and dried at 110 °C overnight. A detailed protocol for these experiments can be found in Appendix C.

When the final weights are registered, the percentage of weight lost in the sample is calculated, it was found via analysis that most of the weight lost was the result of Ca^{++} dissolved in the solution, and therefore extracted from the slag. To quantify this percentage, a gravimetric analysis method by precipitation was implemented. The calculation was obtained using Equation 3.3.

$$\%w_t = \frac{w_i - w_f}{w_i}(100) \tag{3.3}$$

$w_i = Initial\ weight$

$w_f = Final\ weight$

$\%w_t = Weight\ loss\ of\ sample$

The liquid phases decanted during the experiments were digested so the Ca, magnesium (Mg) and iron (Fe) contents could be analyzed using Inductively Coupled Plasma-Atomic Emission Spectrometry (ICPAES).

It was decided to run the slag solution (reforming) under different experimental conditions in order to find the optimum. The conditions tested are enlisted in Table 3-1, this was done as already said in order to obtain information that could help us to have the most efficient extraction of Ca from the slag.

Table 3- 1 Experimental parameters varied during Calcium Extraction tests.

Tag	Factor	Low	High
PS	Particle size	<100 mesh	>100 mesh
T	Temperature	22 °C	75 °C
SLR	Solid-liquid Ratio	1:5	1:1
C	Solvent concentration	2M	5M

In total, 12 tests were performed for this experimental phase, as seen in Table 3-2; where different solid-to-liquid ratios (SLR), solvent concentrations (C), particle sizes (PS) and reaction temperatures (T) were studied.

Table 3- 2 Experimental tests developed for the Ca extraction phase

Test Tag	PS (mesh)	T (°C)	SLR	C (M)
L22152	<100	22	1:5	2
L22153	<100	22	1:5	3
L22155	<100	22	1:5	5
L22112	<100	22	1:1	2
L22115	<100	22	1:1	5
L75152	<100	75	1:5	2
L75153	<100	75	1:5	3
L75155	<100	75	1:5	5
M22152	>100	22	1:5	2
M22153	>100	22	1:5	3
M22155	>100	22	1:5	5
M75155	>100	75	1:5	5

The cases considered as base for the second part of the experimental work developed in this investigation, the Carbonation step, were the ones with the best results in terms of Ca extraction efficiency.

3.1.2 Carbonation

In the carbonation process, a gas rich in carbon dioxide is bubbled through the Ca-rich solution, obtained in the previous experimental phase, producing $CaCO_3$. The net carbonation and precipitation reactions are then given as in Equations 3.4 and 3.5.

$$2NH_4OH_{(aq)} + CO_{2\,(g)} \leftrightarrow (NH_4)_2CO_{3\,(aq)} + H_2O_{(l)} \quad (3.4)$$

$$(NH_4)_2CO_{3\,(aq)} + \mathrm{Ca}Cl_{2\,(aq)} \leftrightarrow CaCO_{3\,(s)} + 2\mathrm{NH_4Cl_{(aq)}} \quad (3.5)$$

Based on the stoichiometry of the foregoing reactions, it can be seen that the ammonium salt consumed in the extraction step is regenerated in the carbonation step, allowing it to be reused continuously; Though theoretically, all the solvent used in the extraction stages is regenerated in the carbonation stage with no loses, in fact, some of the solvent is lost in several ways as: (a) precipitated on the solid slag residue during the extraction step, (b) reacted with an impurity forming an insoluble salt removed with the $CaCO_3$ or (c) stripped from the solution as ammonia NH_3.

For this experimental phase, it was first performed the same protocol as in the previous chapter, considering the parameters and conditions of the test with the highest Ca extraction observed. Figure 3-3 displays an example of the protocol used to develop the Carbonation tests.

Once the Ca extraction was made, the Ca-rich solution was stored in a test tube. Using a gas diffuser, the solution was treated with pure CO_2 gas at a rate of 0.4 L/min. After allowing the solution to react with the gas flow for 30– 60 min, the formed precipitates were filtered with a Whatman 589/3 filter paper and dried; and the produced carbonates were dried overnight at 110 °C and weighed to determine the obtained conversions.

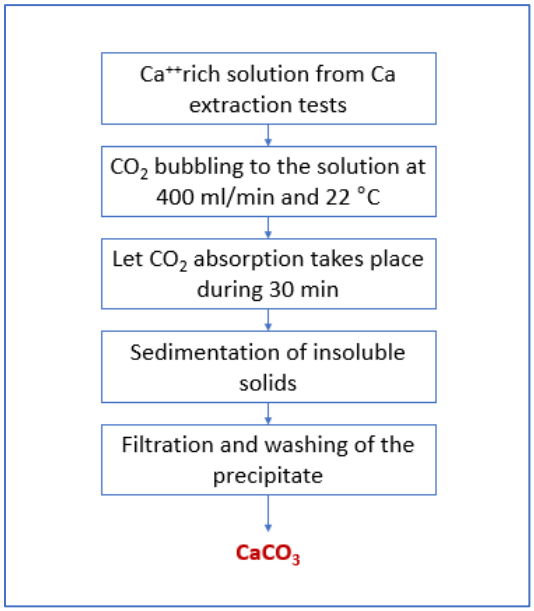

Figure 3- 3 Experimental protocol follow during the Carbonation tests

For each test approximately 400 ml of the Ca-rich solutions were used. The CO_2 flow were set using a rotameter and the temperature and pH of the mixture were recorded and logged at 10-minute intervals during the reaction.

For the specification of the parameters in this experimental phase, the tests with the best extraction efficiency obtained in the prior experiments were considered. Hence, the 2 tests carried out in this phase are the ones listed in Table 3-3.

Table 3- 3 Experimental tests developed for the Ca extraction phase

Test Tag	PS (mesh)	T (°C)	SLR	C (M)
L22152	<100	22	1:5	2
L22155	<100	22	1:5	5

The experimental work concluded once the best extraction and precipitation efficiency was obtained. The conditions with which these results were obtained, were specified as part of the base case used for the simulation in the next section.

3.2 PILOT PLANTS SIMULATION

The objective of a process evaluation is to determine the importance of the technology in relation to a set of criteria. The set of criteria selected here involves investigating the development of the two CO_2 mineralization processes in terms of their technical and economic impact.

Material flow analysis (MFA) has become an increasingly applied method providing a system-oriented view of interlinked processes and flows to support strategic and priority-oriented decisions and to design management measures.

MFA is used in this work to establish the mass balances and Process Flow Diagrams (PFD) of the technologies ensuring that the sum of all inputs into the system must equal all outputs plus changes in stock. For the correct evaluation of the CDU processes, system boundaries in the PFDs are established, based on the conditions of a determined CO_2 effluent from the DR HYL technology process, to set a comparable scenario for the two pilot plants to evaluate and compare.

As a base case, the steel plant with DR process to analyze in this project produces 6,300 tons per day of liquid steel and emits 801 tons of CO_2. 47% of the amount of dioxide carbon produced per day, equivalent to 380 tons, is sold to another industry while the other 53% has no current use.

The analysis is based partly on the current operation conditions of the steel plant, the results obtained in the experimental work and assumptions made during the study. The basis for the entire techno-economic assessment is the modelling of the process, and the application of CCS technologies with auxiliaries.

3.2.1 Technical Key Performance Parameters

For assessing the technical approach, the two alternative processes were modeled using Aspen Plus V8; based on the most detailed sources found in bibliography describing the CO_2

mineralization. It is assumed that the pilot plants work under the same conditions and are designed to convert 207 kg/h of CO_2 into the respective final products. The main parameters affecting the reactions were selected from the results of the experimental work.

Material balances are the basis of process design. Based on material balances, the quantities of raw materials required, and the quality and quantity of products can be estimated. Like mass, energy can be transferred from, and to a system. There are two principles that govern how energy can be transferred: (a) heat or energy that flows through a temperature gradient and (b) work, or energy that flows in response to any driving force other than a temperature gradient. The relevant stream is taken from the result of the simulation work and the energy and material balances obtained represent the starting point to calculate the Key Performance Indicators (KPI) for the technical analysis:

Product purity (wt%)

This indicator refers to the wt% that either the LWA or the PCC represent in the product stream of the two plant configurations modeled.

CO_2 converted

This indicator evaluates the CO_2 that is transformed in the reactor of the mineralization (carbonation) process and the CO_2 transformed into product through the whole process. These are expressed as a percentage of the total amount of CO_2 that enters as raw material (Eq. 3.6).

$$\mathbf{CO_2 conv} = \left(\frac{\mathbf{CO_2 in} - \mathbf{CO_2 out}}{\mathbf{CO_2 in}}\right)_{\mathbf{Process}} \quad (3.6)$$

Energy required

This indicator evaluates the energy consumptions and requirements obtained from the pilot plants simulation.

3.2.2 Simulation assumptions

The EAF slag used in this process, as mentioned in chapter 4, was supplied by an DR-EAF steel plant located in Monterrey, México. Since the slag used in the experimental work had a 26% of CaO equivalent, it was assumed in this study that the slag entering the processes contains 0.64 Kmol of CaO per every 100 kgs. of slag.

Some of the properties of all the components included in the CO_2 mineralization system are given in 3-5.

Table 3- 4 Properties of main compounds presented during CO_2 mineralization processes

Component	Molecular formula	Molar mass (g/mol)	Boiling point (°C)
Water	H_2O	18.015	99.98
Calcium oxide	CaO	56.077	2850
Carbon dioxide	CO_2	44.010	--
Ammonium chloride	NH_4Cl	53.490	520
Ammonium hydroxide	NH_4OH	35.040	37.7
Calcium chloride	$CaCl_2$	110.980	1935
Calcium carbonate	$CaCO_3$	100.087	--
Calcium hydroxide	$Ca(OH)_2$	74.093	--

Based on the effect of particle size presented before, prior to being diluted, the slag was grinded to a desire particle size below mesh 100, nevertheless, the milling stage is not considered as part of the pilot plant, this will be done by an external company. Therefore, in this study, slag has a temperature of 25 °C, it is at atmospheric pressure and is already grinded.

CO_2 an NH_4Cl solutions streams are also fed to the process. The CO_2 enters the process at a temperature and pressure of 42 °C and 1.2 bars, respectively, these are the normal conditions at which the it exits the DR plant. NH_4Cl is added as an aqueous recycled solution at 1 bar and 107 °C because is the solvent assumed in both pilot plants. In the feed, the concentration of the NH_4Cl solution is 5M and the ratio between it and the slag is 5:1 in order to enable the best Ca extraction efficiency experienced during the experimental work.

The main assumptions for the mass balance and the simulations of the pilot plants are described in Table 3-6.

Table 3- 5 General assumptions made for the technical analysis of both LWA and PCC pilot plant.

Parameter	Assumption
Production rate of LWA and PCC	1 ton/h
CaO present in slag	26%
H_2O present in CO_2 stream	4%
NH_4Cl solution recovery efficiency	99.99%
Filtration settling efficiency *	100%
Moisture *	20%
Coating target **	33%
Coating efficiency **	70%

*Specifications by Tenova HYL design Team

**Assumptions considered just for the LWA pilot plant technical analysis

Both production capacities for LWA and PCC processes were established as 1 ton/h of the final product (either LWA or PCC) for a calculus base. Detailed processes descriptions are presented in the following sections. For simulation purposes, variability of the slag composition was not considered and reactants (NH_4Cl, CO_2) were added under the best experimental results in order to ensure the maximum conversion in each of the reactive stages.

The simulation strategy consisted first in modelling each individual unit in the process instead of the whole plant, thus avoiding problems with calculations and numerical results, and a further compilation of all units were made. Table 3-7 shows the Aspen Plus models for simulated stages of both mineralization processes.

Table 3- 6 Aspen Plus models for simulated stages of the mineralization processes.

Stage	Unit	Aspen Plus model	
		LWA pilot plant	PCC pilot plant
Extraction	Reactor	Rstoic	Rstoic
Separation	Stripping tower	RadFrac	NA
CO_2 absorption	Absorber column	RadFrac	Flash2

An electrolyte system is defined as one in which some of the molecular species dissociate partially or completely into ions in a liquid solvent, and/or some of the molecular species precipitate as salts. Therefore, an Electrolyte-NRTL activity coefficient model, ELECNRTL, was selected for the processes simulation. ELECNRTL can represent aqueous and aqueous/organic electrolyte systems over the entire range of electrolyte concentrations with a single set of binary interaction parameters. In Aspen Plus V8, the dissociation and precipitation reactions obtained with the model have fast kinetic and can be considered to be at chemical equilibrium under the conditions present. The liquid phase equilibrium reactions that describe this behavior are referred to as the solution chemistry.

Given the non-ideal behavior of the electrolyte system to analyze, the electrolyte–NRTL property method is used to predict the activity coefficients, enthalpies, and Gibbs energies for liquid phase thermodynamic behavior. On the other hand, the Redlich–Kwong equation of state calculates the fugacity coefficients for the vapor phase properties [38].

It is worth mentioning that due to the lack of some of the components properties in the Aspen's database, in the simulation, a value of -151.7 kcal/mol of CaO Standard Heat of Formation (DHFRM) was loaded.

Equation 3.7 show how the indirect emissions for electricity consumption was calculated.

$$CO_2\ emitted = (EEF)(Electricity) \tag{3.7}$$

Where

$CO_2\ emitted = emissions\ of\ CO_2\ by\ elecrticity\ usage\ (kg/h)$

$EEF = Electricity\ Emission\ Factor = 0.4562\ in$ [44]

$Electricity = Electricity\ required\ by\ the\ pilot\ plant\ (kWh)$

The Electricity Emission Factor (EEF) used in this thesis was selected from [44]. It is a value that varies every year depending on the mix of fuels used to generate the electricity in Mexico.

On the other hand, Equation 3.8 shows how the indirect emissions for thermal energy consumption was calculated.

$$CO_2\ emitted = (NGEF)(Thermal\ energy) \tag{3.8}$$

Where

$CO_2\ emitted = emissions\ of\ CO_2\ by\ elecrticity\ usage\ (kg/h)$

$NGEF = Natural\ Gas\ Emission\ Factor = 2.69\ in$ [45]

$Thermal\ energy = Heat\ required\ by\ the\ pilot\ plant\ (kcal/h)$

3.2.2 Economical Key Performance Parameters

The purpose of the economic analysis is to calculate the capital investment cost and the Net Present Value (NPV) to assess the feasibility of the pilot plant and identify its uncertainties.

Materials and products prices were assumed based on the literature review [--] while operations, equipment, utilities and installation costs were calculated from the Activated Economics tool of Aspen Plus V8. The economic assumptions required for the elaboration of cash flows are summarized in Table 3-8.

Table 3- 7 Cashflows analysis assumptions for both LWA and PCC pilot plants.

Parameter	Assumption
Financing	100% owned capital
Discount rate	8%
Plant availability	8760 h/year
Plant depreciation method	SLN
Plant depreciation period	7 years
Income tax rate	30%
Project life	20 years

Once this information is obtained by the simulation and the calculations from the Tenova HYL engineers, economic KPIs are calculated as in Equations 3.7 and 3.8 [42].

$$\text{Cap. Inv.} = f(C_{\text{financial funding}},\ C_{\text{operation}},\ C_{\text{installation}}, C_{\text{utilities}}) \quad (3.7)$$

$$\mathbf{NPV = f(Initial\ investment, Cash\ flow, Discount\ rate, Time)} \quad (3.8)$$

Net present value (NPV) is the difference between the present value of cash inflows and the present value of cash outflows over a period of time. NPV is used in capital budgeting to analyze the profitability of a projected investment or project.

Payback period, or "payback method," is one popular metric that is frequently used as an alternative to net present value. It is much simpler than NPV, mainly gauging the time required after an investment to recoup the initial costs of that investment. Unlike NPV, the payback period fails to account for the time value of money. For this reason, payback periods calculated for longer investments have a greater potential for inaccuracy, as they encompass more time during which inflation may occur and skew projected earnings and, thus, the real payback period as well [43].

Moreover, the payback period is strictly limited to the amount of time required to earn back initial investment costs. As such, it also fails to account for the profitability of an investment after that investment has reached the end of its payback period. It is possible that the investment's rate of return could subsequently experience a sharp drop, a sharp increase or anything in between. Comparisons of investments' payback periods, then, will not necessarily yield an accurate portrayal of the profitability of those investments.

The economics of the CO_2 utilization technology pilot plant rely on the CO_2 captured and the production capacity. Based on the energy and material balances obtained from the modelling and the technical feasibility of investigated solutions, the economic profitability is further evaluated. As for the boundaries used for the economical evaluations, are the same as those defined in the technical assessment and based on similar justifications as in section 3.2.1.

Internal rate of return (IRR) is another metric commonly used as an NPV alternative. Calculations of IRR rely on the same formula as NPV does, except with slight adjustments. IRR calculations assume a neutral NPV (a value of zero) and solve for the discount rate. The discount rate of an investment when NPV is zero is the investment's IRR, essentially representing the projected rate of growth for that investment. Because IRR is necessarily annual — it refers to projected returns on a yearly basis — it allows for the simplified comparison of a wide variety of types and lengths of investments.

CHAPTER 4 EXPERIMENTAL RESULTS

The objective of the experimental work developed during this investigation was confirm and extent the Ca^{++} ions extraction from electric arc furnace slag and its further carbonation using CO_2. This chapter includes the experimental protocols that were elaborated based on reviewed bibliography and the selection of parameters of interest to analyze during the laboratory tests. This was made to obtain the laboratory conditions at which the tests carried out result in the best Ca^{++} extraction efficiency, which is later used as part of the design basis for the material balances in chapter 5. Also, the effect that each parameter has on the Ca++ ions extraction is presented.

As mentioned before, the solvent selected for the experimental work is ammonium chloride (NH_4Cl). The decision was made based on the results of similar studies reviewed on literature where NH_4Cl showed a higher Ca^{++} ions extraction compared with other salts. In addition, it is commonly used in extraction processes due to its relative ease of recycling and low cost [39].

The slag used in the experiments was provided by a DR-EAF steel plant. The composition of the slag was analyzed using X-ray diffraction (XRD) and is presented in Table 4-1.

Table 4- 1 Chemical composition of the EAF slag determined by XRF.

	Al_2O_3	CaO	Cr_2O_3	FeT	MgO	MnO	P_2O_5	SiO_2	TiO_2	V_2O_5	K_2O	Na_2O
%	6.01	26	0.27	33.22	7.61	1.46	0.23	16.74	1.24	0.21	0.09	0.36

The compound of interest is the CaO as the source of Ca^{++} ions. From the XRF analysis, it is assumed that the CaO reported in Table 4-1 is calcium that can be dissolved. Since the XRF is an analytical technique that measures the Ca atoms present in the sample, there is a possibility that a portion of the element is in the form of silicate (or more complex structures) instead of oxide, therefore, the 26% wt of slag is a CaO equivalent amount and not strictly calcium in form of oxide.

All reagents used during the experiments were not of analytical grade.

4.1 CALCIUM EXTRACTION

As shown in previous chapter, in Table 3-2, 12 tests were developed to confirm the Ca^{++} ions extraction from de EAF slag. Table 4-2 displays the main results obtained during the experimental work.

Table 4- 2 Ca extraction tests results in terms of weight loss of slag and Ca^{++} ions present in the after-extraction solution.

Tag	PS (mesh)	T (°C)	SLR	C (Molarity)	Weight loss (%)	Ca extracted (%)
L22152	<100	22	1:5	2	11.61	7.19
L22153	<100	22	1:5	3	11.94	7.04
L22155	<100	22	1:5	5	12.76	6.72
L22112	<100	22	1:1	2	6.84	4.18
L22115	<100	22	1:1	5	8.11	4.39
L75152	<100	75	1:5	2	11.79	*
L75153	<100	75	1:5	3	12.03	*
L75155	<100	75	1:5	5	12.84	*
M22152	>100	22	1:5	2	6.61	3.02
M22153	>100	22	1:5	3	6.93	2.87
M22155	>100	22	1:5	5	7.96	2.81
M75155	>100	75	1:5	5	8.13	*

*Results not available. PS=particle size. T=Temperature. C=Solvent concentration

The percentage of Ca extracted showed above is calculated by comparing the concentrations in liquid samples after extraction (analyzed through ICP) to the total equivalent amount present in fresh slag (26% wt) prior to experiments. As mentioned above, not all Ca in slag is present in a reactive form, but because the overall degree of Ca conversion is of high interest, all the efficiency calculations in this paper are made according to this method.

The discussion of these results take place in the following section with the purpose of conclude in the effect of each parameter tested (particle size, reaction temperature, solid-liquid ratio and solvent concentration) over the calcium extraction efficiency during extraction tests.

4.1.1 Effect of particle size

The first parameter effect analyzed in the extractions test was the particle size (PS). Four experiments, grouped in 2 pairs, were carried out. The varying parameter between each of the tests in the pairs was the PS specified by the mesh used, and the other parameters (temperature, solid-to-liquid ratio and solvent concentration) were constant. Two slag samples with different particle sizes were analyzed. One sample had passed through a 100-mesh screen (tag as >100 mesh), hence its particles measured less than 149 μm. The other sample had passed through an 8-mesh screen but not through the 100-mesh screen (tag as <100 mesh), so it had a particle size in the range of 149-2,380 μm.

The results obtained are the percentages of weight loss in the slag after the extraction process. These experiments were performed at room temperature and with a SLR of 1:5 and a 5M solvent concentration. Both <100 and >100 mesh slag samples were tested, and the percentages of weight loss obtained are displayed by Figure 4-1.

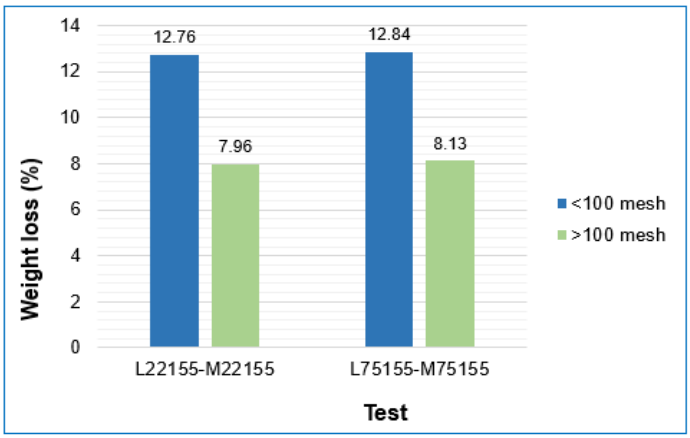

Figure 4- 1 Effect of slag particle size on its weight loss during Extraction tests.

The particle size of the slag has a significant effect on the percentage of weight loss as it increased approximately 58% with decreasing particle size range from 149–2,380 µm to lower than 149 µm after 20 minutes of mixing. It is inferred by the results that a smaller particle size improves the percentage of weight loss, hence the Ca^{++} ions leaching, during the extraction process. This result is in line with theorical reasoning since the smaller the particle size, the larger the surface area, and the better the mass transfer rate which in turn results in

higher extraction efficiency. Once the slag is reduced to fine particles, its increase in total available surface area lends to optimum interaction of the CaO with the solvent.

Another experiment was realized with a slag sample from a 325-mesh (less than 44 μm), a reaction temperature of 75 °C, SLR of 1:5 and 5M NH_4Cl. The experiment resulted in weight loss percentage equals 13.26 (see L75155* results in Apendix __). This means that there was an increment in the weight loss of only 3% when changing from <100-mesh to >325-mehs and the difference in the energy required for grinding the slag to that particle size would be more significant and less favorable for the process economics.

The results obtained so far indicate that there might be a limitation in the amount of calcium that can be extracted from the slag. A possible reason is the deposition of other non-reactive compounds on the surface of the particle which limits the interaction area between the CaO and the solvent. Another potential reason is a part of CaO trapped inside the crystal structure of the particles. Both theories can be confirmed by SEM analysis (Scanning Electron Microscopy)

4.1.2 Effect of reaction temperature

To analyze the effect of temperature, 6 extractions test were carried out and then grouped together in pairs where each couple has the same conditions of particle size (PS<100 mesh), solid-to-liquid ratio (SLR=1:5) and solvent concentration; the only variable within the two tests was the temperature. The studied temperatures were 22°C (room temperature) and 75°C and the results shown in Figure 4-1 correspond to the percentage of weight loss in the slag considering the initial weight of the sample and the final weight of the undissolved slag.

It was found a small increase (approximately 1%) in the weight loss percentage when the extraction test was carried out at a higher temperature. This result leads to the premise that the ions extraction efficiency is slightly greater when the temperature is increased.

From phase equilibrium, it is known that both solubility and dissolution rate of solids in liquids can be increased by raising the temperature since the addition of more heat facilitates the dissolving reaction by making the particles move faster and collide more frequently.

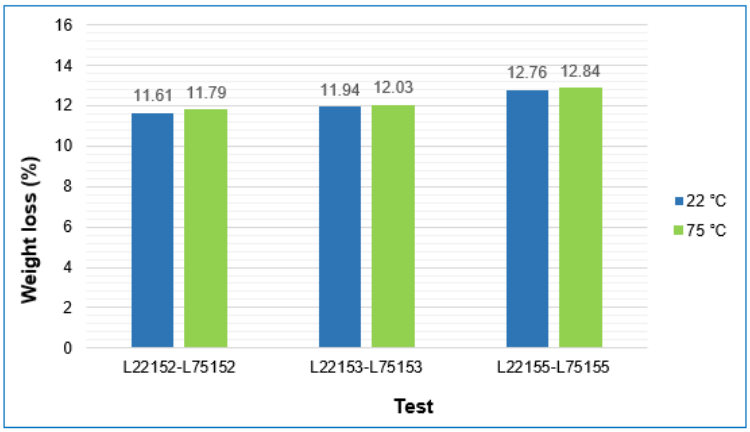

Figure 4- 2 Effect of reaction temperature on slag weight loss during extraction tests.

It has been found in recent similar studies [19], [40], that the extraction of calcium from slags was, indeed, faster when increasing the temperature; almost all the calcium from slag dissolved after 15 minutes when reaction temperature was set at 20 °C while at higher temperatures, between 60-80°C, it took only 10 minutes. Regarding the solubility of CaO, these studies also showed that calcium extraction efficiency had an increase of approximately 7% when using 2M NH_4Cl and increasing from 30°C and 70°C the reaction temperature.

As mentioned before, a minimum mixing time of 20 min was set in these tests, as well as a further sedimentation time of ~2h. Hence, the results presented in Figure 4-1 were taken once all the calcium that could be dissolved did so and the mixture had returned to room temperature. It is concluded that the protocol stablished did not allow an accurate visualization of the effect of temperature during the extraction and that more tests might be required. Nevertheless, from the bibliography review and the data obtained in this thesis, it is inferred that the influence of this parameter is not significant compared with the effect of other parameters tested, as the particle size and solid-to-liquid ratio.

4.1.3 Effect of solid-to-liquid ratio

The ratio of solid slag to liquid solvent (SLR) is defined by Equation (4.1) where m_{slag} is the mass, in g, of the slag sample used in the experiments (in g), and V_s is the volume of the solvent solution in ml.

$$\text{SLR} = \frac{m_{slag}}{V_s} \tag{4.1}$$

To observe the effect of the SLR parameter during extraction tests, 2 pairs of experiments were developed and analyzed. The solvent concentration, particle size and NH_4Cl aqueous solution volume (500 ml) were maintained constant within each experiment; only, the weight of the slag samples used in the tests were changed (100 g, 500 g) to observe the effect of two solid-to-liquid ratios, 1:1 y 1:5. All the tests were carried out at room temperature since there was no need of increasing temperature as concluded in the previous section.

This parameter had a strong influence on calcium extraction as can be seen in Figure 4-3. The data obtained from the experiments was the concentration of Ca (mg/l) in the liquid phases after the mixing. The results shown below were calculated in terms of the percentage of Ca extracted from the slag sample.

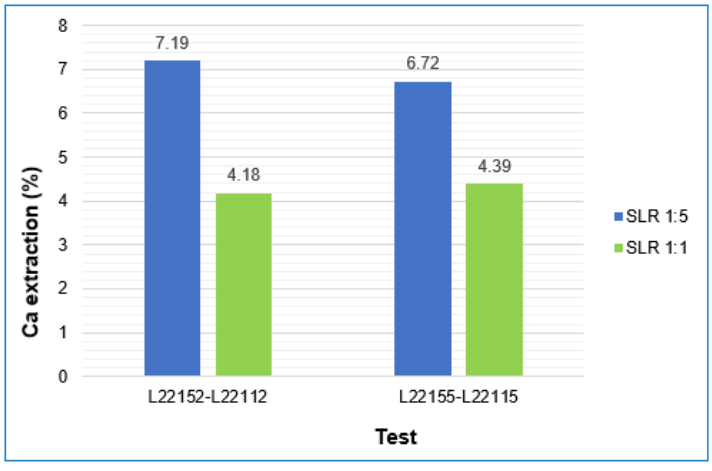

Figure 4- 3 Effect of solid-to-liquid ratio (SLR) on calcium extraction efficiency

The results presented above show that a smaller SLR of 1:5 results in a higher calcium extraction efficiency (38% of the Ca present in the EAF slag) while the highest solid to liquid ratio tested of 1:1 resulted in a lower extraction (23%). Similarly, it was found that lower values of SLR, as 1:20, leads to greater Ca^{++} extraction (around 60% of Ca present in the slag).

The results obtained, and data reviewed indicate that the extraction efficiency improves with decreasing solid-to-liquid ratio, as it brings a relative higher volume of solvent solution corresponding to unit mass of slag and increases the reaction probabilities between solvent and solute. Nevertheless, a natural consequence for reducing the SLR is that a high amount of NH_4Cl solution would be needed per unit of slag, as well as a bigger extraction tank in order to achieve such values of extraction efficiency. On the other hand, the SLR can be increased if there exist an economical or operational limitation for the NH_4Cl solution flow in the process, though it would have a negative impact in the Ca^{++} extraction efficiency.

4.1.4 Effect of solvent concentration

The final parameter studied in the laboratory was the solvent concentration. In this case, 100 g of slag from a <100 mesh was dissolved in 2M, 3M and 5M NH_4Cl solutions at 22 °C in a 1:5 SLR. ICP-EAS the results obtained are presented in Figure 4-4, where the percentages of Ca, Mg and Fe ions in the solution are specified.

The final parameter studied during the extraction tests was the solvent concentration. In this case, 100 g of slag from a <100 mesh was dissolved in 2M, 3M and 5M NH_4Cl solutions at 22 °C in a 1:5 SLR. The results obtained are presented in Figure 4-4, where the percentages of Ca, Mg and Fe ions dissolved were calculated based on the ICP-EAS analysis on the liquid phase and the percentage of weight loss experienced during the test.

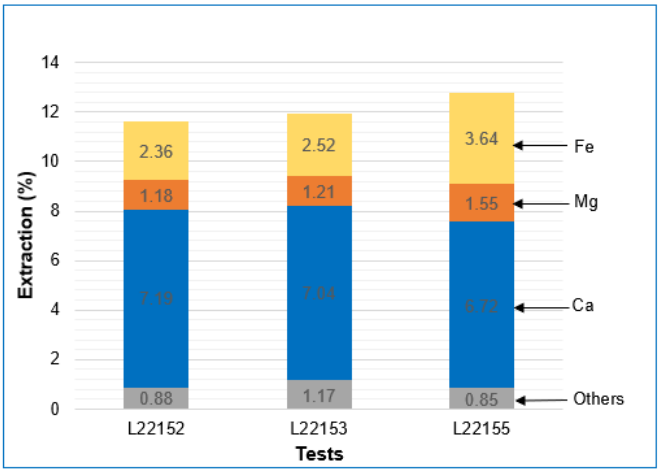

Figure 4- 4 Percentage of Ca, Mg and Fe ions extraction at different solvent concentrations.

Increasing the ammonium chloride concentration in the solution from 2M into 3 or 5M did not increase dissolution of Ca. Moreover, the dissolution of other elements as Fe and Mg increased with the increase of the solvent concentration.

As already mentioned, the EAF slag not also contains easy-reacting Ca (e.g., CaO, $Ca(OH)_2$) but also difficult-reacting Ca (e.g., Ca_2SiO_4). Once all the easy-reacting Ca that could be dissolved did, the excess of NH_4Cl in solution starts dissolving other elements as Fe and Mg. This is undesirable, because a commercial calcium carbonate product should contain as few impurities as possible, especially if it is intended to commercialize as Precipitated Calcium Carbonate (PCC). It was found during the literature review [41] that raising the pH (by the addition of a basic solution) after the slag dissolution and prior carbonation, allows impurities (Mg, Fe, Al) to precipitate as hydroxides. This precipitation could lead to a separation of the non-desired elements before the CO_2 is bubbled and the $CaCO_3$ is produced.

4.2 CARBONATION

The second step in the experimental work was to confirm the precipitation of $CaCO_3$ as via carbonation of the Ca-rich solution from the extraction stage. This section begins with some background theory and data for the NH_4Cl-CO_2-Ca system which are necessary to provide a basis for the discussion of the experimental work results.

The mechanism by which $CaCO_3$ is formed during carbonation of calcium-rich solution is reportedly well known [39]. It involves several steps as summarized by Equations (4.2) to (4.5)

$$CO_{2(g)} \leftrightarrow CO_{2(aq)} \tag{4.2}$$

$$CO_{2(aq)} + OH^-_{(aq)} \leftrightarrow HCO^-_{3(aq)} \tag{4.3}$$

$$HCO^-_{3(aq)} + OH^-_{(aq)} \leftrightarrow H_2O_{(l)} + CO^{2-}_{3(aq)} \tag{4.4}$$

$$CO^{2-}_{3(aq)} + Ca^{2+}_{(aq)} \leftrightarrow CaCO_{3(s)} \tag{4.5}$$

Ionic reactions such as (4.3), (4.4) and (4.5) are usually very fast. Reaction (4.2) occurs at the gas-liquid interface and reaction (4.3), which is a relatively fast reaction, can occur at the interface. Thus, the controlling step in carbonation reactions is usually the absorption of CO_2 into solution.

Once the CO_2 dissolves, it will react with OH^- at the interface. However, if OH^- is exhausted at due to steps reactions (4.3) and (4.4) then the rate of absorption of CO_2 can be significantly reduced. Apparently, this result in a competition between the reactions of CO_2 with H_2O and with OH^- to form carbonic acid or bicarbonate. According to X. Wang et al. in [40], at high pH, the hydroxide path is faster, whereas at low pH the water path is faster, hence the need for a pH monitoring in these experiments.

To confirm the carbonation during the carbonation step, two separate carbonation tests (L22152 and L22155) were performed with the best result obtained in Ca extraction tests. The same conditions were used for each test (T = 22°C, CO2 flow = 0.4 L/min) and Table 4-3 below shows the results for each test performed.

Table 4- 3 Main results obtained from Carbonation tests

Test	Weight loss during extraction test (%)	$CaCO_3$ precipitated (g)
L22152	14.16	14.28
L22155	16.02	14.25

The tests shown above were developed from EAF slag samples of 100 g. This means that a great amount of waste material is needed in order to fixed CO_2 in carbonate products.

4.1.1 Effect of pH

Figure 4-5 shows the recorded temperature and pH during carbonation. The initial pH for each test was 9.5.

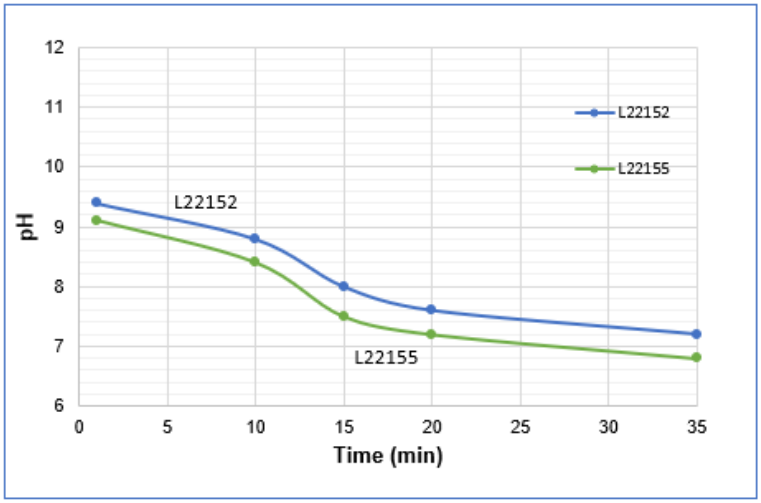

Figure 4- 5 pH values recorded during Carbonation tests

The initial pH value of Ca-rich solution (9.5) began to decrease after CO_2 was introduced. After 30 minutes of CO_2 absorption, the pH value of the solution decreased to between 7.3 and 6.8. It is confirmed that the dissolution of gaseous CO_2 depends on the pH value, since the precipitation was observed once the pH was recorded lower than 8.5. According to literature (mentioned previously) carbonate (CO_3^{2-}) ion is the dominant species in the solution when pH is higher than 9.2. Since carbonate is the main species in carbonation reaction, it can be concluded that the efficiency of carbonation decreases as the pH value deceases.

4.3 DESIGN BASIS

The objective of this work was to design two pilot plants for their economic evaluation and comparison. Although the experimental work yields attractive results, the CO_2 mineralization

technology is not currently mature enough, so it is advisable to verify these results with the operation of the pilot plant. Results of the laboratory studies were used to choose the most suitable design basis, but the pilot plants must be understood not as a scale-up of laboratory experiments, but as small-scale simulations of the future industrial operations. These design basis for both pilot plants is presented in Table 3-8.

Table 3- 8 General assumptions made for the technical analysis of both LWA and PCC pilot plant.

Parameter	Assumption
Particle size of EAF slag	>100 mesh
Ca^{++} extraction efficiency	40%
NH_4Cl concentration	5M
SLR	1:5

It is also presented in this chapter that a lower solvent concentration (2M, 3M) can be used to achieve the same Ca^{++} extraction efficiency of the one obtained by a 5M NH_4Cl solution. Nevertheless, the latter was established as part of the design basis to assure the CaO dissolution happens as quickly as possible. This also enable the pilot plant to handle high concentrations and allow the tests of operating conditions once it is implemented.

-

CHAPTER 5 PROCESSES SIMULATION RESULTS

This section summarizes the systematic methodology used to evaluate the potential impact of the CDU processes addressed in this thesis. The main objective is to elaborate the conceptual designs of two pilot plants by their using Aspen Plus and confirm the final mass and energy balances, as well as the operational conditions and the technical key parameters needed for the further comparison of the CO_2 mineralization processes.

The conceptual designs of both CO_2 mineralization processes were developed according to a pilot plant size suggested by Tenova HYL design team. The boundaries, assumptions and results of the CDU pilot plants and thus of the model, are presented on next sections.

5.1 THERMODYNAMICS AND REACTIONS

In these simulations some components existed as solids, e.g., CaO, $CaCO_3$. The rest of the compounds exist in aqueous or liquid phase. As mentioned earlier in this thesis, in both processes simulation there were aqueous solutions of electrolytes such as salts and $Ca(OH)_2$, as well as polar and non-polar organic components. Therefore, the ELECNRTL property method was selected for the simulation.

To properly study, understand and eventually model the pilot plant it was necessary to know the chemical species that could be formed and to have an appreciation of the potential reactions and relevant chemical equilibria in the system. The global components specified for the processes simulation are presented in Table 5-1. For both pilot plants simulation, the components were the same, as well as the dissociations and salt reactions.

Based on information gathered from the literature [38], and the ELECTNRTL model used in the simulation, the following chemical reactions and equilibria were considered relevant for the mineralization system studied.

Table 5- 1 Components definition for simulation of chitosan production process.

Component ID	Type	Name
H_2O	Conventional	Water
CaO	Solid	Calcium-oxide
CO_2	Conventional	Carbon-dioxide
NH_4Cl	Solid	Ammonium-chloride
NH_4OH	Conventional	Ammonium-hydroxide
$CaCl_2$	Conventional	Calcium-chloride
Ca^{++}	Conventional	Ca^{++}
H_3O^+	Conventional	H_3O^+
NH_4^+	Conventional	NH_4^+
HCl	Conventional	Hydrogen-chloride
$CaCO_{3(S)}$	Solid	Calcium-carbonate
$CaCl_{2(S)}$	Solid	Calcium-chloride
HCO_3^-	Conventional	Water
Cl^-	Conventional	Cl^-
CO_3^{--}	Conventional	CO_3^{--}
NH3	Conventional	Ammonia
$CaOH^+$	Conventional	$CaOH^+$
$AMCARB_{(S)}$	Solid	Ammonium-carbamate
$CA(OH)_2$	Solid	Calcium-hydroxide
OH^-	Conventional	OH^-
$NH2COO^-$	Conventional	Carbamate
$AMBIC_{(S)}$	Solid	Ammonium-hydrogen-carbonate

$$CO_{2\,(g)} \leftrightarrow CO_{2\,(aq)} \tag{5.1}$$

$$NH_{3\,(g)} \leftrightarrow NH_{3\,(aq)} \tag{5.2}$$

$$H_2O_{(g)} \leftrightarrow H_2O_{(l)} \tag{5.3}$$

$$HCl + H_2O \leftrightarrow Cl^- + H_3O^+ \tag{5.4}$$

$$NH_3 + HCO_3^- \leftrightarrow H_2O + NH_2COO^- \tag{5.5}$$

$$NH_3 + H_2O \leftrightarrow OH^- + NH_4^+ \tag{5.6}$$

$$H_2O + HCO_3^- \leftrightarrow CO_3^{--} + H_3O^+ \quad (5.7)$$

$$2\,H_2O + CO_2 \leftrightarrow HCO_3^- + H_3O^+ \quad (5.8)$$

$$CaOH^+ \leftrightarrow Ca^{++} + OH^- \quad (5.9)$$

$$2\,H_2O \leftrightarrow OH^- + H_3O^+ \quad (5.10)$$

$$Ca(OH)_{2\,(S)} \leftrightarrow CaOH^+ + OH^- \quad (5.11)$$

$$CaCO_{3(S)} \leftrightarrow CO_3^{--} + Ca^{++} \quad (5.12)$$

$$NH_4HCO_3 \leftrightarrow HCO_3^- + NH_4^+ \quad (5.13)$$

$$NH_4Cl \leftrightarrow Cl^- + NH_4^+ \quad (5.14)$$

$$CaCL_{2(S)} \leftrightarrow Ca^{++} + 2\,Cl^- \quad (5.15)$$

$$NH_2COONH_{4\,(S)} \leftrightarrow NH_2COO^- + NH_4^+ \quad (5.16)$$

$$CaCl_2 \leftrightarrow Ca^{++} + 2\,Cl^- \quad (5.17)$$

In the species and reactions generated by the model in the simulation, there are three types of reactions: ionic equilibrium, complete dissociation, and salt precipitation. Equations (5.1) and (5.2) represent the equilibrium between the CO_2 and NH_3 present in the gas and liquid phase. Liquid water is also considered in equilibrium with water vapor in Equation (5.3). Equations (5.4) to (5.10) describe the aqueous molecular and ionic equilibria which exist between the liquid species. Equations (5.11) to (5.16) represent salt precipitations and finally Equation (5.17) shows the $CaCl_2$ dissociation. Although the equilibrium constants for some of the formation reactions are very small and these components are unlikely to form in any significant quantity (e.g. $NH_4Cl(aq)$), they have still been listed for completeness as they are commonly encountered in the literature and should be considered in equilibrium calculations.

As shown in next sections (Figures 5-1 and 5-4), the CO_2 mineralization processes are similar; however, one considers an intermediate separation stage, while the other one does not. Since the aim of the investigation was to explore through simulation the technical

performance of both processes, the next sections correspond to the simulation of each pilot plant with their respective mass and energy balances.

5.2 LWA PILOT PLANT

A general block diagram of the proposed LWA pilot plant with NH_4Cl recycle is presented in Figure5-1, including the system boundaries for its simulation. The overall process consists of 6 stages: calcium extraction, NH_4OH separation, CO_2 absorption, substrate coating, final product washing and solvent recovery system. In this work, the first 3 stages were the ones of most interest to simulate in order to confirm both Ca ions leaching, and carbonation reactions occurred.

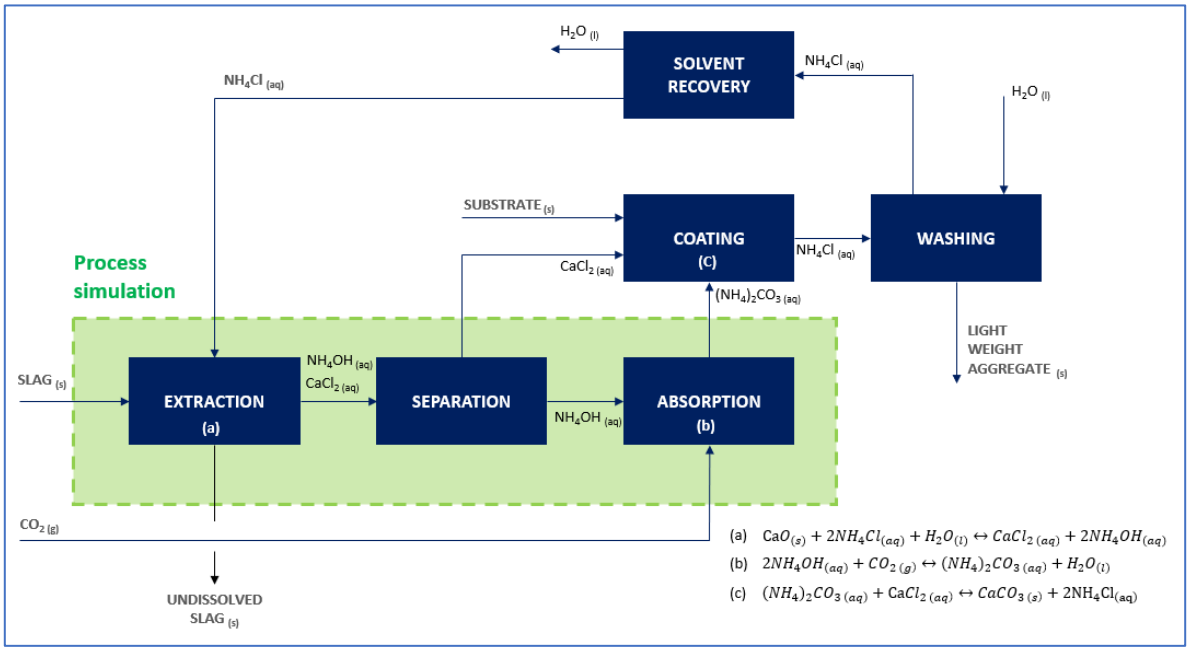

Figure 5- 1 Block Process Diagram of LWA pilot plant

The six stages of the CO_2 mineralization pilot plant with LWA as final product are described as follows. This is a brief description of the purpose of each stage and the explanation of what is expected to occur with the main components of the process.

Calcium extraction

In the extraction stage, the slag and the NH_4Cl are fed to the extraction tank. The slag is mixed with the NH_4Cl solution and Ca^{++} ions are extracted from in the form of $CaCl_2$. Consequently, the NH_4Cl is converted to NH_4OH. The undissolved slag exits the process while the stream of interest, which contains the Ca^{++} ions, continues to the next stage. As it was concluded in the previous chapter, the success of the whole mineralization process depends critically on efficiency, and cost, with which alkalinity can be extracted from the slag, and subsequently carbonated, hence the need to simulate this stage.

$CaCl_2$-NH_4OH Separation

As it is mentioned in chapter 2, the Light Weight Aggregate (LWA) produced in this pilot plant concept consist o a substrate that is coated by $CaCO_3$. An immediate absorption of CO_2 is inconvenient because of the inevitable precipitation of $CaCO_3$ without the presence of the substrate. To address this issue, an intermediate stage is needed to separate the $CaCl_2$ of the NH_4OH solution from extraction stage. This separation is required to assure that the $CaCO_3$ is produced once the substrate is present and not before. In this way, the solution rich in NH_4OH, and free from $CaCl_2$, is pumped into the CO_2 absorption stage and the desired coating can be controlled.

CO_2 absorption

Now the carbonation takes place; the NH_4OH aqueous solution encounters the carbon dioxide stream deriving from the Direct Reduction (DR) plant. When the carbonation is completed, based on the stoichiometry of the reactions, a certain amount of $(NH_4)_2CO_3$ is produced, without precipitation. The mix of these two continue its way into the coating stage while the unreacted gases, if any, exit the process.

Substrate coating

The substrate, the $CaCl_2$ and the $(NH_4)_2CO_3$ containing solutions (from separation and absorption stages, respectively) are fed to an agglomeration unit. Here, the compounds react

based on Equation 3.5 and produce a $CaCO_3$ precipitate on the substrate surface generating the LWA product. Along with the $CaCO_3$, the interaction between the ammonium carbonate and the calcium chloride also leads to the regeneration of the NH_4Cl.

LWA washing

When the carbonation and agglomeration is completed, the LWA needs to be washed and separated from residual solids, unreacted material and the recovered NH_4Cl solution. At this point is where the final product exits the mineralization process and can be storage or directly transport for commercialization.

NH_4Cl solution recycle

Since the optimal Ca^{++} extraction efficiency obtained in experimental work was only 40%, with a liquid solid ratio of 5:1. It is inferred that the CO_2 mineralization process proposed would demand a large flow of solvent solution. This condition does not represent any problem if the solvent can be recycled efficiently. In order to achive this, the excess of liquid in the recovered solution, if any, needs to be evaporated from the stream to obtain the NH_4Cl concentration required for the extraction stage (5M). After this condition is reached, the solvent is finally recycled to extraction stage.

5.2.1 Mass Balance

The mass balance was done considering the stages previously described, as well as the chemical reactions, reactants, products and their stoichiometric values. Additionally, the information of the CO_2 generated in the DR plant and the EAF slag production of the steel plant was considered. Table 5-2 lists the main technical assumptions taken to elaborate the pilot plant mass balance.

From the assumptions it is concluded that a makeup of the NH_4Cl solution will be need because its recovery efficiency is not 100%. The coating target represents the amount of $CaCO_3$ that is expected to be part of the LWA composition, the remain 67% would be the

substrate. The adherence efficiency is the effectiveness with which the $CaCO_3$ produced is deposit on the substrate surface, since the value established is not 100% there is an amount of carbonate that will not be used as coating.

Table 5- 2 General assumptions made for mass balance of the LWA pilot plant.

Parameter	Assumption
LWA production rate	1 ton/h
H_2O present in CO_2 stream	4%
NH_4Cl solution recovery efficiency	99.99%
Coating target **	33 wt%
Adherence efficiency **	70%
Moisture**	20%

**Specifications by Tenova HYL design Team

Once the design basis (see Table 3-8) and assumptions for mass balance and simulation have been determined, the Process Flow Diagram (PFD) of the LWA pilot plant model was elaborated and it is displayed in Figure 5-3. The operating conditions for the model described in this section are based on literature review, the experimental work done in this investigation and the knowledge of the Tenova HYL design team.

A simple PFD was elaborated considering the main equipment and operations needed it produce LWA from EAF slag and CO_2. Figure 5-2 shows the equipment and streams in the LWA pilot plant proposed. It consists of 18 equipment that represents the main stages of the mineralization process. Table 5-3 shows the group of units used to model each one of the six stages and it also indicates the ones simulated in Aspen plus.

As seen in Table 5-3, 13 out of the 18 equipment were simulated and they correspond to the first 3 stages of the process and a part of the coating stage. The mass balances for the units simulated were obtained directly from he Aspen results and the balances for the rest of the units were further calculated.

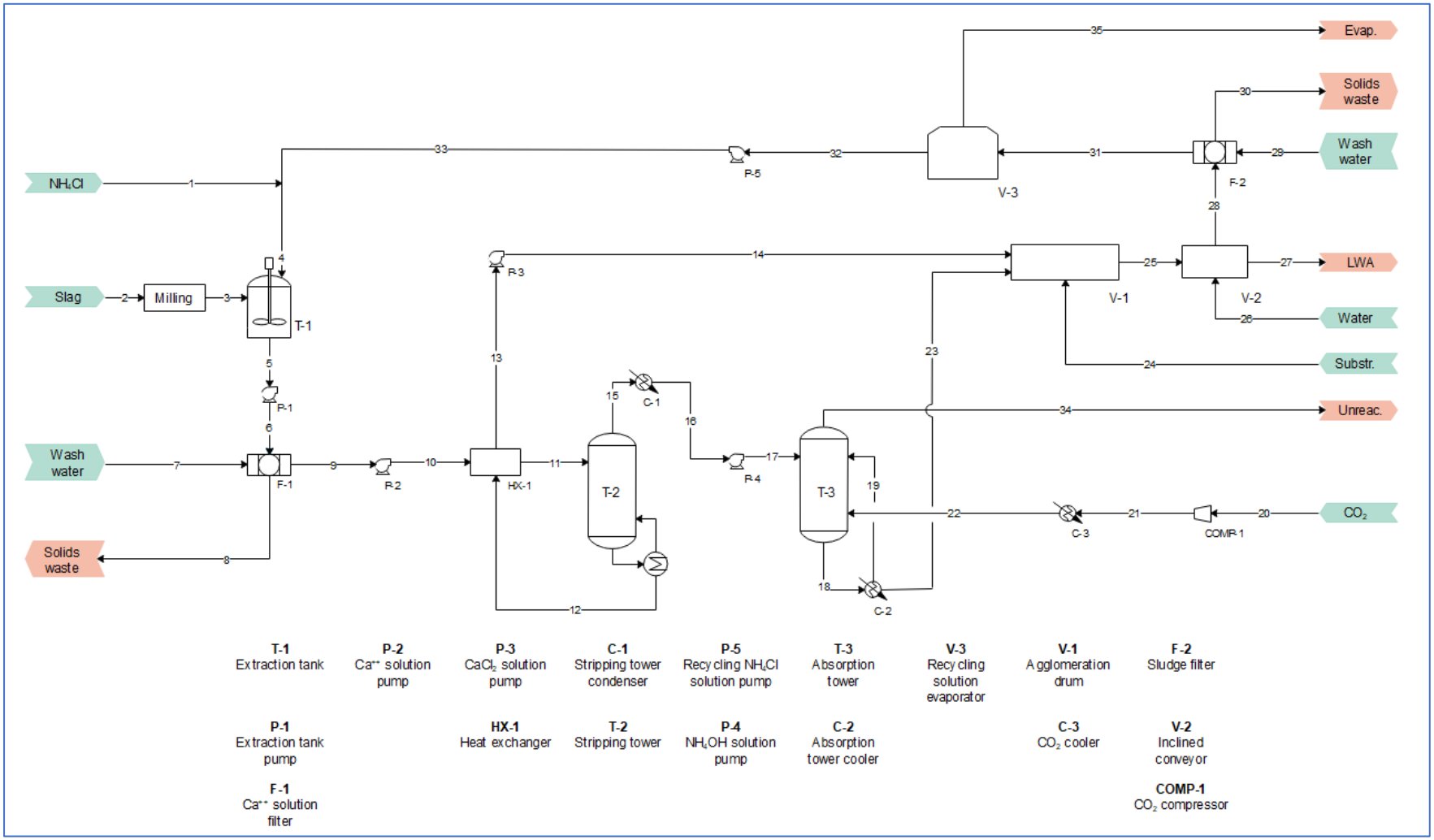

Figure 5- 2 Aspen model flowsheet for the LWA pilot plant simulation.

Table 5- 3 List of equipment considered in the design of the LWA pilot plant.

Tag	Name	Stage	Simulated in Aspen Plus
T-1	Extraction tank	E	**
P-1	Extraction tank pump	E	**
F-1	Ca^{++} solution filter	E	**
P-2	Ca^{++} solution pump	E	**
HX-1	Heat exchanger	S	**
T-2	Stripping tower	S	**
C-1	Stripping tower condenser	S	**
P-4	NH_4OH solution pump	S	**
T-3	Absorption tower	A	**
C-2	Absorption tower cooler	A	**
C-3	CO_2 cooler	A	**
COMP-1	CO_2 compressor	A	**
P-3	$CaCl_2$ solution pump	C	**
V-1	Agglomeration drum	C	
V-2	Inclined conveyor	W	
F-2	Sludge filter	W	
V-3	Recycling solution evaporator	R	
P-5	Recycling NH_4Cl solution pump	R	

E=Extraction, S=Separation, A=Absorption, C=Coating, W=Washing, R= Recovery of solvent.

There are 2 extra operations required to produce LWA, the milling of the EAF slag and the gas scrubbing system. These operations were not modeled nor simulated in this study. Since the purpose of the design was to conceptualize a process at a pilot plant level, the grinding of the raw material was not considered as a process stage but an external service (see Chapter 3). Regarding the gas scrubbing system, although it was not modeled, the mass balances calculated in this thesis give enough information to design the gas washer needed by the pilot plant.

The PFD was sectioned in 6 parts that represents the stages of the mineralization process. The next paragraphs describe the mass balances of each stage and present the discussion of the results obtained. These results are the combination from data obtained by the simulation of the pilot plant and stoichiometric calculations. The diagram of the stages simulated, as well as the description of all streams involved in the simulation are presented in Appendixes E and F respectively.

Extraction

After milling the EAF slag with <100 mesh, the solids and the NH_4Cl solution are fed to an extraction tank (T-1) as seen in Figure 5-3. The NH_4Cl solution (stream 4) represents the combination of the recovered solution recycled and the make-up needed. The extraction of Ca is specified by the input of Equation (-), in a stoichiometric reactor (RStoic) that operates at 25 °C and atmospheric pressure. The Aspen unit selected to model the extraction tank was a RStoic since the reaction kinetics were unknown, but the extent of reaction was already stablished as part of the design basis. Therefore, the conversion for the reaction was set as 0.4 of CaO present, to represent the Ca^{++} extraction efficiency. Additionally, temperature recordings during the experimental work, as well as revised literature, indicate that the Ca^{++} extraction reaction is exothermic, hence no external heating should be needed and T-1 was simulated with a specification of no duty.

After $CaCl_2$ and NH_4OH are generated in the extraction tank, the solution is pumped by P-1 to a press filter (F-1) to separate the undissolved slag efficiently from the solution containing the Ca^{++} ions. F-1 was modeled as a decanter by specifying the unreacted CaO as the key component in the solids waste outlet.

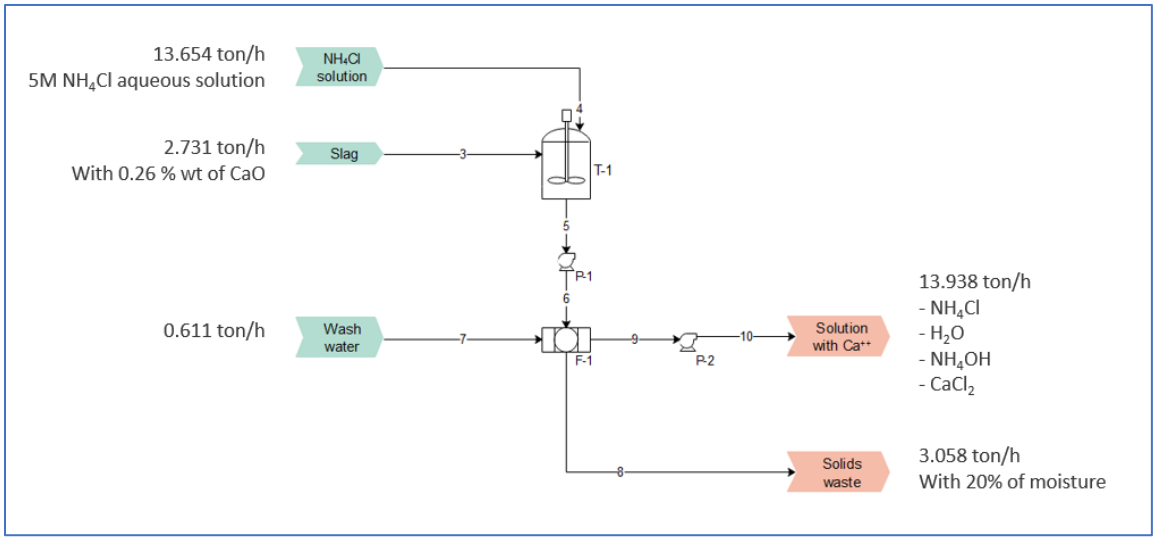

Figure 5- 3 Inlets and outlets of the extraction stage in LWA pilot plant design.

A total amount of 3,058 kg/h of solids waste exit the process in steam 8. This stream consists not only of undissolved slag but also the non-reacted CaO and water, that was required for the separation, as moisture on the solids. Table 5-4 displays each of the inlets and outlets for the extraction stage.

Table 5- 4 Mass balance of the extraction stage in LWA pilot plant design.

	Inlet			Outlet	
Flow (kg/h)	**3**	**4**	**7**	**8**	**10**
H_2O	0	10,244	611	611	10,336
CaO	710	0	0	426	0
Ca^{++}	0	0	0	0	203
H_3O^+	0	0.10	0	0	0
NH_4^+	0	1,150	0	0	967
HCl	0	0	0	0	0
Cl^-	0	2,260	0	0	2,260
NH_3	0	0.09	0	0	172
$CaOH^+$	0	0	0	0	0.02
OH^-	0	0	0	0	0
Solids	2,021	0	0	2021	0
Total	**2,731**	**13,654**	**611**	**3,058**	**13,938**
	16,996			**16,996**	

P-2 is used to pump the Ca^{++} containing solution to the next stage of the process. It is inferred by results shown in Table 5-4 that this solution mostly consists of the unreacted NH_4Cl solution. Nevertheless, 203 kg/h of Ca^{++} were generated in the extraction tank and will continue with the process flow.

Results from the experimental work showed that other elements might also dissolved when using a 5M MH_4Cl aqueous solution during the extraction. However, calcium had the more significant extraction efficacy between the elements analyzed and, since $CaCO_3$ is the product of interest in this mineralization process, is it assumed for the simulation of this stage that only calcium can be dissolved from CaO in the slag.

Separation

After extraction stage, the Ca^{++} solution is heated up to 100 °C in a heat exchanger (HX-1) as seen in Figure 5-4. Stream 11 enters a stripper tower (T-2) where the NH_4OH is separated from the $CaCl_2$ by operating the stripper at 130 °C and 4 bars. These conditions allow the NH_4OH to leave the stripper tower from the top, as vapor, and the $CaCl_2$ by the bottom (stream 13). T-1 was modeled with a distillation column (RadFrac) with two stages and a reboiler. This model allowed the specification for a distillate rate to assure the maximum separation of NH_4OH vapor from the solution.

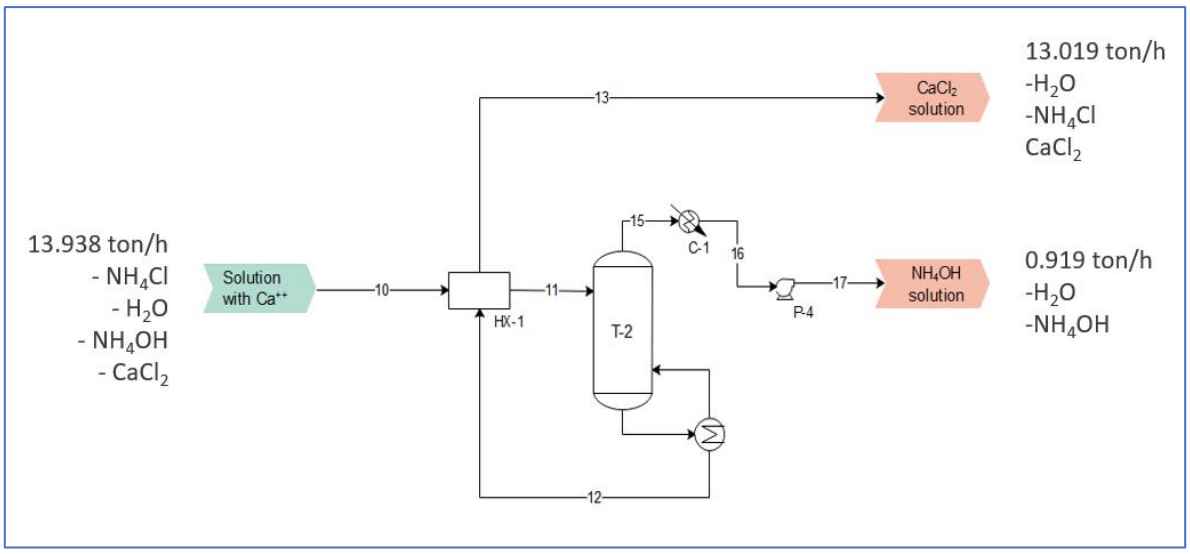

Figure 5- 4 Inlets and outlets of the separation stage in LWA pilot plant design.

The resulting mass balance for this stage is given by Table 5-5. All Ca^{++} and Cl^{-} ions that entered the stripping tower left in the form of $CaCl_2$ at the bottom (see Equation 5.15); it is assumed then, that $CaCl_2$, and unreacted NH_4Cl solution, has been successfully separated from the NH_4OH. The energy of this stream (12), is used in HX-1 to heat the Ca^{++} solution entering the tower and then continues the process flow.

The NH_4OH vapor condensates in C-1 in order to be pumped by P-4 to the next stage of the process, the CO_2 absorption. This solution contains almost all the NH4OH the initially entered the stripping tower; approximately 8% of the NH_3 could not be separated and remained in mixed with the $CaCl_2$ solution.

Table 5- 5 Mass balance of the separation stage in LWA pilot plant design.

	In (kg/h)	Out (kg/h)	
Stream	**10**	**13**	**17**
H_2O	10,336	9,574	762
Ca^{++}	203	203	0
H_3O^+	0	0	0
NH_4^+	967	967	0.04
HCl	0	0	0
Cl^-	2,260	2,260	0
NH_3	172	15	157
$CaOH^+$	0.02	0	0
OH^-	0	0	0.04
Total	**13,938**	**13,019**	**919**
	13,938	**13,938**	

Absorption

The inlets and outlets of the CO_2 absorption stage are displayed by Figure 5-5. Here, the NH_4OH containing solution is fed to an absorber tower (T-3) along with a CO_2 stream (20). The CO_2 comes from the DR process at 60 °C and atmospheric pressure. Since the main product of interest in this stage is the $(NH_4)_2CO_3$, which is stable under high pressure and low temperature, the CO_2 passes through a compressor (COMP-1) and a cooler (C-3) before entering the column to reach the conditions needed for the absorption.

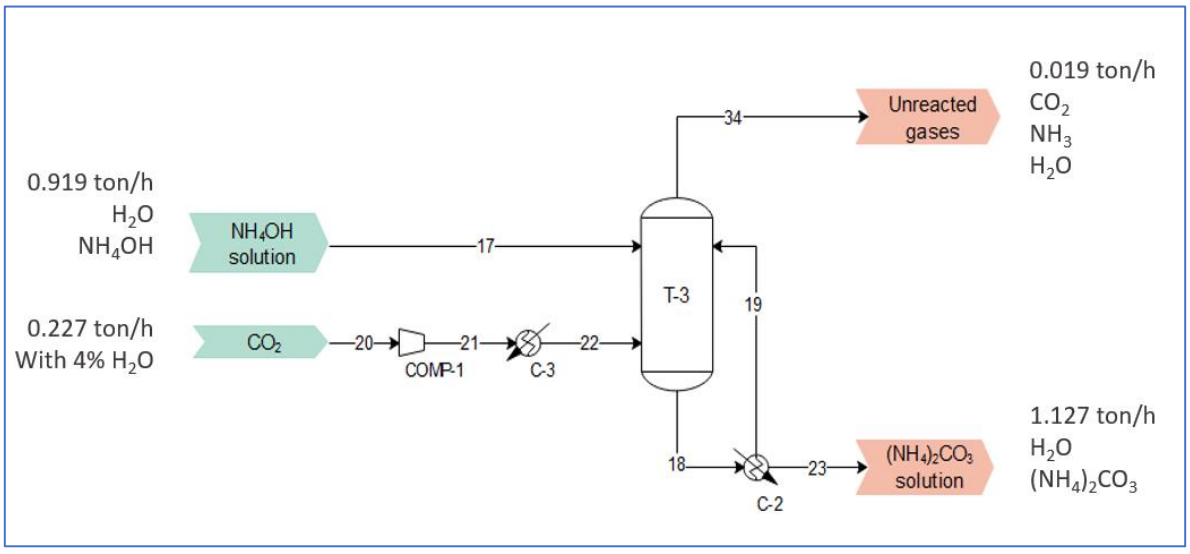

Figure 5- 5 Inlets and outlets of the absorption stage in LWA pilot plant design.

The absorption tower was also modeled as a RadFrac unit, this time without a reboiler and with operating conditions of 5.5 bar and 25 °C. A cooler (C-2) is placed at the bottom exit of T-3 to cooled it down to 25 °C since the heat released by the absorption reaction heated the solution. A 35% of this cooled stream is recirculated to the absorber to counter the effect of the exothermic reaction and avoid the $(NH_4)_2CO_3$ decomposition that occurs around 40 °C. Stream 19 absorbs part of the heat released by the reaction and then throws it out of the process through the cooler. With these measures, the emission of CO_2 and NH_3 are prevented and a greater amount of the ammonium carbonate is produced.

Table 5-6 shows the compositions of the in and out streams involved in this stage of the process. Some NH_3 leaves the absorber column at the top, as well as all the unreacted CO_2 (stream 34). The $(NH_4)_2CO_3$ solution exits the absorption tower by the bottoms (stream 23) in it dissociated form.

Table 5- 6 Mass balance of the absorption stage in LWA pilot plant design.

	In (kg/h)		Out (kg/h)	
Stream	**17**	**20**	**23**	**34**
H_2O	762	4	724	3
CO_2	0	223	0	11
NH_4^+	0.04	0	69	0
HCO_3^-	0	0	50	0
CO_3^{--}	0	0	12	0
NH_3	157	0	22	5
OH-	0.04	0	0	0
NH_2COO^-	0	0	158	0
NH_4HCO_3	0	0	92	0
Total	**919**	**227**	**1,127**	**19**
	1,146		**1,146**	

The 1,146 kg/h of $(NH_4)_2CO_3$ solution continues the flow of the process to form the $CaCO_3$ in the next stage.

Coating

In this stage, the $(NH)_4CO_3$ and the $CaCl_2$ react in an agglomeration drum (V-1), based on Equation 3.5, and form the expected $CaCO_3$. As Figure 5-6 shows, 670 kg/h of substrate is

also fed in V-1 to enable the deposit of the produced $CaCO_3$ on its surface. This leads to the generation of the LWA product.

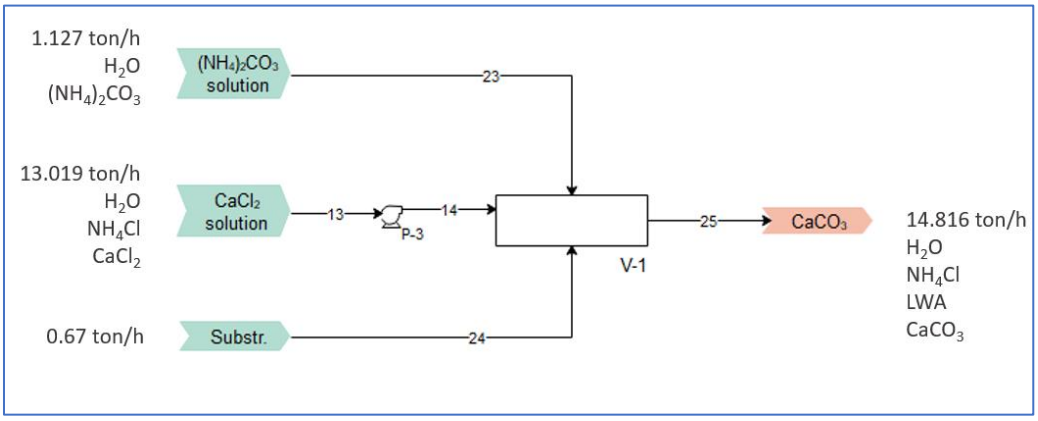

Figure 5- 6 Inlets and outlets of the coating stage in LWA pilot plant design.

Table 5-7 enlists the results from the simulation of this stage. The simulation made was limited to the production of the required amount of calcium carbonate to obtain a ton of LWA per hour. This means that, although the overall pilot plant final product is LWA, the final product for the simulation was $CaCO_3$.

Table 5- 7 Mass balance of the coating stage in LWA pilot plant design.

	In (kg/h)			Out (kg/h)
Stream	**13**	**23**	**24**	**25**
H_2O	9,574	724	0	10,251
Ca^{++}	203	0	0	14
CO_2	0	0	0	0.03
NH_4^+	967	69	0	1,139
HCO_3^-	0	50	0	5
CO_3^{--}	0	12	0	0.03
Cl^-	2,260	0	0	2,260
NH_3	15	22	0	6
OH-	0	0	0	0
NH_2COO^-	0	158	0	0.43
NH_4HCO_3	0	92	0	0
$CaCO_3$	0	0	0	471
Substrate	0	0	670	670
Total	**13,019**	**1,127**	**670**	**14,816**
	14,816			**14,816**

According to the results, there were 471 kg/h of $CaCO_3$ produced in this stage. Nevertheless, part of this carbonate is not used as coating in the LWA, since an adherence efficiency of 70% was stablished in the general assumptions of the design, hence, only 330 kg/h of $CaCO_3$ is part of the LWA. This amount added to the 670 kg/h of substrate fed to the agglomeration drum results in 1 ton/h of LWA produced.

Along with the $CaCO_3$ production, the interaction between the ammonium carbonate and the calcium chloride also leads to the regeneration of the NH_4Cl (see Equation). Therefore, the only outlet stream (25) of this stage is a solid-liquid solution that consists of the NH_4Cl aqueous solution, the LWA product and the $CaCO_3$ not used.

Washing

This stage was not simulated in Aspen plus, so the mass balance was calculated from the streams previously showed and the mains assumptions made for the technical analysis. Figure 5-7 shows the diagram of this stage, while Table 5-8 displays the compositions of the inlets and outlets of the stage.

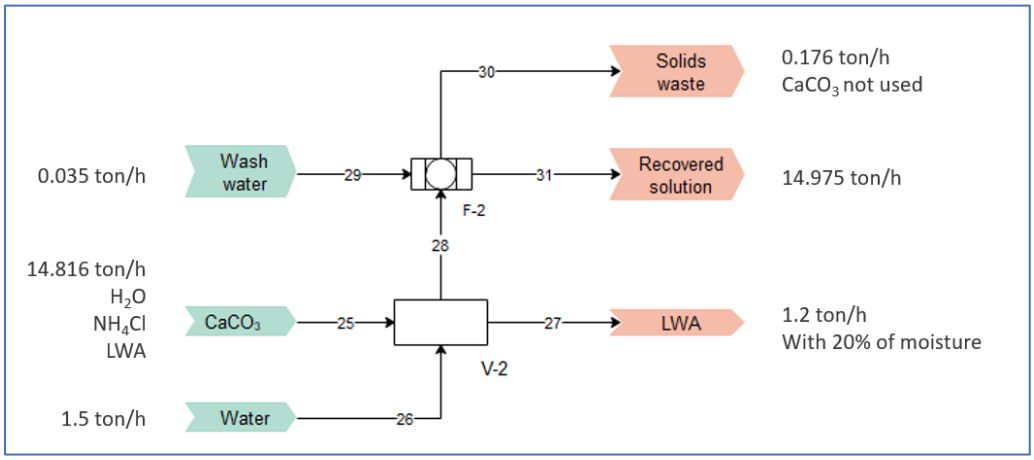

Figure 5- 7 Inlets and outlets of the washing stage in LWA pilot plant design.

When the carbonation and agglomeration is completed, the LWA is washed with water in an inclined conveyor (V-2) and exits the process with 20% of moisture and 33% of coating in

stream 27. The light weight aggregate leaves the mineralization process in stream 27 with a 20% of moisture; the target for 1 ton/h of LWA was achieved at this point.

Table 5- 8 Mass balance of the washing stage in LWA pilot plant design.

	In (kg/h)			Out (kg/h)		
Stream	**25**	**26**	**29**	**27**	**30**	**31**
H_2O	10,251	1,500	35	200	35	11,551
Ca^{++}	14	0	0	0	0	14
CO_2	0.03	0	0	0	0	0.03
NH_4^+	1,139	0	0	0	0	1,139
HCO_3^-	5	0	0	0	0	5
CO_3^{--}	0.03	0	0	0	0	0.03
Cl^-	2,260	0	0	0	0	2,260
NH_3	6	0	0	0	0	6
OH^-	0	0	0	0	0	0
NH_2COO^-	0.43	0	0	0	0	0.43
$CaCO_3$	471	0	0	330	141	0
Substrate	670	0	0	670	0	0
Total	**14,816**	**1,500**	**35**	**1,200**	**176**	**14,975**
	16,351			**16,352**		

The residual sludge from the inclined conveyor pass through another press filter (F-2) where the NH_4Cl solution regenerated is separated from the $CaCO_3$ not used. This separation step is considered to be developed by a press filter. Stream 30 consist of the 141 kg/h of CaCO3 that were not used as coating and it leaves the process with 20% of moisture. On the other hand, stream 31 contains mainly H_2O and NH_4Cl and continues the process flow to the final stage, the solvent recovery.

Solvent recovery

As established earlier, the recovered solution from the press filter contains mainly NH_4Cl and H_2O, nevertheless, there is an excess of liquid that needs to be evaporated from the solution in a partial evaporator (V-3) to obtain the NH_4Cl concentration required for the extraction stage. A representation of this stage is shown by Figure 5-8.

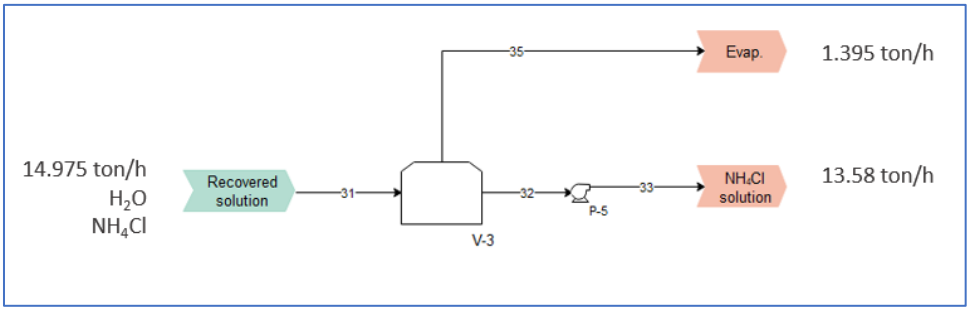

Figure 5- 8 Inlets and outlets of the solvent recovery stage in LWA pilot plant design.

According to the composition of stream 31, 1,358 kg/h of liquid needs t be separated from the recovered solution to satisfy the condition of a 5M NH_4Cl aqueous solution. After this condition is reached, the solvent is finally recycled through the pump P-5 and into the extraction tank.

Table 5- 9 Mass balance of the solvent recovery stage in LWA pilot plant design.

	In (kg/h)	Out (kg/h)	
Stream	**31**	**33**	**35**
H_2O	11,551	10,212	1,339
Ca^{++}	14	0	14
CO_2	0.03	0	0.03
NH_4^+	1,139	1139	0
HCO_3^-	5	0	5
CO_3^{--}	0.03	0	0.03
Cl^-	2,260	2260	0
NH_3	6	6	0
NH_2COO^-	0.43	0	0
Total	**14,975**	**13,617**	**1,358**
	14,975	**14,975**	

A total amount of 13,617 kg/h of recovered solution is now recycle to the first stage of the mineralization process. However, there is a requirement a solid-to-liquid ratio of 1:5 to enter the extraction tank so the need of a make-up of 37 kg/h of NH_4Cl solution. The initial assumption made for a solvent recycle efficiency of 99% was confirmed.

Figure 5-9 presents the global mass balance for the CO_2 mineralization pilot plant that produces 1 ton/h of LWA using EAF slag as raw material. The water needs of the process is mainly for the washing of the LWA product and a little amount for the make-up of the NH_4Cl solution. The outlet of the water consists of the unreacted water in the system and the humidity present in the solids that are separated in different parts of the process.

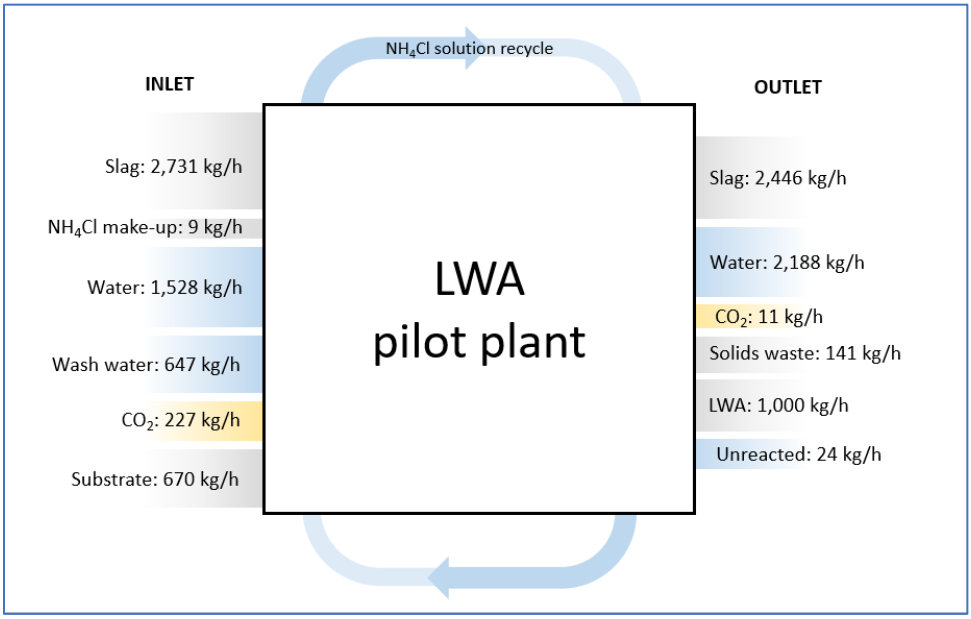

Figure 5- 9 Total mass balance for the LWA pilot plant design.

The amount of NH_4Cl entering the process is only in the form of a makeup for the solvent solution because of the existence of its recycle in the process. The unreacted solution, in the outlets, represents the amount of NH_4Cl that did not react during the extraction stage and the vapors released during the absorption stage. Now that the mass balance of the pilot plant has fullfed the technical requirements and the capacity assumed, the study continues with the calculation and analysis of the energy balance.

5.2.3 Energy balances

Through the pilot plants simulation, the optimal conditions for the production of 1 ton/h of LWA were found and used for the equipment's specifications. These conditions yielded the results of the mass balances presented in the previous section and are listed in Table 5-7.

Table 5- 10 Required input data for the LWA pilot plant simulation

Coolers/Heaters	**C-1**	**C-2**	**C-3**		
Pressure (bar)	2	5	5		
Temperature (°C)	25	25	25		
Type	V-L	V-L	V-L		
Heat duty (kcal/h)	-454,641	-40,315	-12,215		
Pumps/Compressors	**P-1**	**P-2**	**P-3**	**P-4**	**COMP-1**
Efficiency	0.5	0.5	0.5	0.5	0.72
ΔP (bar)	1	2	1.4	3.5	3.8
Power (kW)	0.82	1.42	1.02	0.34	10
Displacement(cum/h)					1,828
Reactors/Towers	**T-1**	**T-2**	**T-3**		
Temperature (°C)	25	140	105		
Pressure (bar)	1	4	5.5		
Heat duty (kcal/h)	0	570,127	0		
Distillate rate (kg/h)		919			
Stages		2	2		
Reboiler		Thermosiphon	NA		

The simulation of the LWA pilot plant also generated and confirmed the global energy balance for the equipment modeled. The heat duty for T-2 presented above represents the heat required for the stripper reboiler. The absorber column (T-3) on the other hand, resulted in a heat duty of o kcal/h because its cooler (C-2) does the work of releasing the heat of the CO_2 absorption reaction.

The heat, cool and work requirements for each unit is shown in Table 5-11. Also, it shows the utilities and services contemplated to fulfill these requirements, and the indirect CO_2 emissions for the power and thermal energy consumption.

Table 5- 11 Energy consumption from unit operations in LWA pilot plant simulation

Energy requirement			Utilities		
Equipment	Rate (kW)	CO_2 emission (kg/h)	Steam (kg/h)	Cooling water (kg/h)	Electricity (kWh)
Power (kW)					
P-1	0.82	0.37			0.82
P-2	1.43	0.65			1.43
P-3	1.02	0.47			1.02
P-4	0.34	0.16			0.34
P-5	3.59	1.64			3.59
COMP-1	10.01	4.57			10.01
V-1 *	32.40	14.78			32.40
V-2, F-2 *	6.20	2.83			6.20
**	61.78	28.18			61.78
Thermal energy (kcal/h)					
T-2	570,127	150	1,056		
C-1	-225,736			28,348	
C-2	-30,326			3,808	
C-3	-12,215			1,534	
V-3*	786,780.0	207	1,457		
	Total:	**410**	**2,513**	**33,690**	**118**

*Data provided by Tenova HYL design Team

**Data obtained in Aspen simulation for the auxiliaries needed to operate the equipment

The major requirement of electricity in this pilot plant comes from the CO_2 compressor. On the other hand, thermal energy needs of the process are mainly for the heating in the stripper tower, to separate the NH_4Cl prior CO_2 absorption, and the partial evaporator for concentrating the NH_4Cl recovered solution. The compressing and stripping steps, discussed earlier in this chapter, are essential to meet the target of I ton/h of LWA produced because of their direct impact in the amount of $CaCO_3$ that can be precipitated. Furthermore, the recycle of the solvent is fundamental for good economics of the pilot plant.

5.3 PRECIPITATED CALCIUM CARBONATE PILOT PLANT

Other CO_2 mineralization alternative for implementation in a DR-EAF plant is the production of Precipitated Calcium Carbonate (PCC). As part of this thesis, it was also developed the conceptual design of a PCC pilot plant. This work was similar to the LWA pilot plant design in order to have a fair comparison between both options. A block diagram of the CO_2 mineralization process with PCC as final product is shown in Figure 5-10. Deferring from the LWA pilot plant design, the process consists of only 3 stages, excluding the intermediate separation, the coating and washing stages. As seen in the block diagram, only extraction and carbonation stages were simulated in Aspen Plus.

The process is divided into three sections, namely, calcium extraction, carbonation and solid/liquid separation. A more detailed description of these stages is presented as follows.

Extraction

As in LWA production, the mineralization process begins with an extraction stage. The aqueous NH_4Cl solution is mixed with EAF slag to enable the CaO dissolution. NH_4OH and $CaCl_2$ are generated from this extraction reaction and the undissolved solids are separated from the Ca-rich solution that continues its way into the next stage.

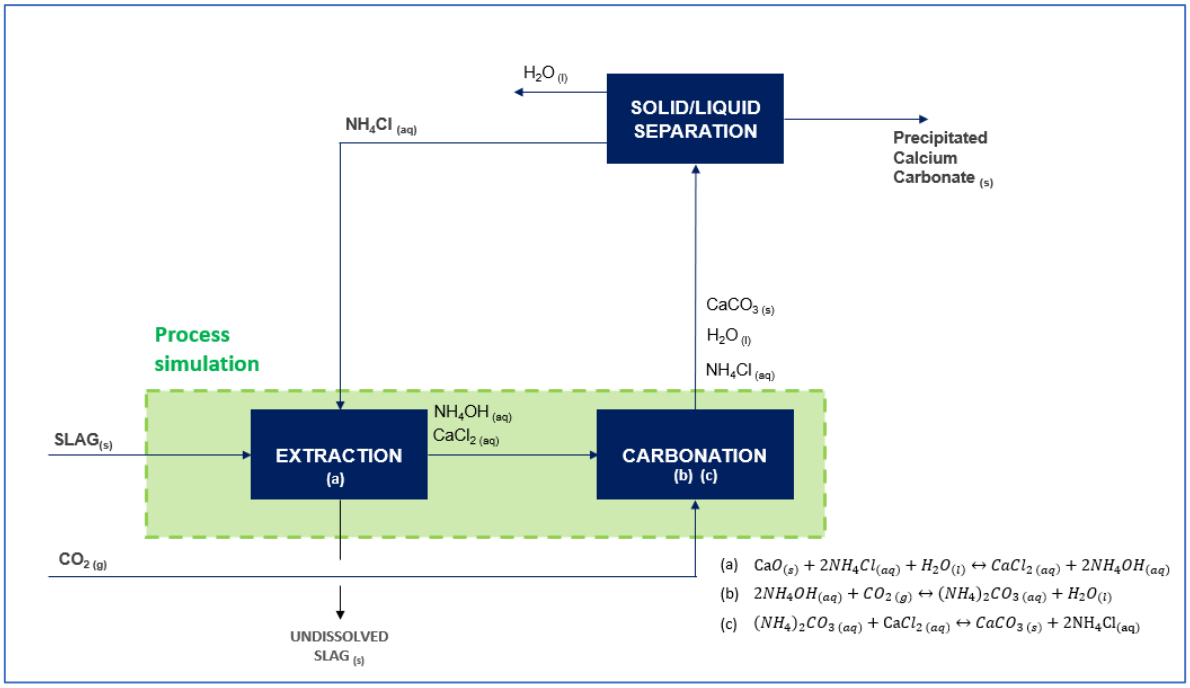

Figure 5- 10 Block Process Diagram of PCC pilot plant

Carbonation

This is the main difference between the two CO_2 mineralization processes presented in this study. In this stage the CO_2 absorption and the $CaCO_3$ precipitation take place simultaneously. The NH_4OH generated during the previous stage, reacts with CO_2 to produce $(NH_4)_2CO_3$ as in Equation 5.18. The instable ammonium carbonate instantly reacts with the $CaCl_2$ also present in the solution and produces $CaCO_3$ as (See Equations 3.4 and 3.5).

Solid/liquid separation

As in case of the LWA process, it is very important to recover the NH_4Cl that was regenerated during the carbonation reaction. This is essential not only for environmental reasons but also to make the process economically viable. Although this process is not simulated in Aspen Plus, it is assumed for the mass balances that a high percentage of the NH_4Cl solution firstly introduced is recovered and fed back to extraction stage. Therefore, a solid/liquid separation is needed to separate the PCC produced from the solvent solution.

5.3.1 Mass Balance

This section includes material balances of the stages considered for the pilot plant model as well a total mass balance for the whole PCC process. The design was made under similar conditions stablished for the LWA alternative. Table 5-12 Table 5-12 lists the main technical assumptions for the mass balances calculation in the PCC pilot plant.

Table 5- 12 General assumptions made for mass balance of the PCC pilot plant.

Parameter	Assumption
PCC production rate	1 ton/h
H_2O present in CO_2 stream	4%
NH_4Cl solution recovery efficiency	99.99%
Mineralization efficiency	100%
Moisture**	20%

**Specifications by Tenova HYL design Team

The production rate, CO_2 stream conditions and solvent recovery efficiency are the same as for the LWA pilot plant. Nevertheless, the mineralization efficiency in this case is 100%, which means that the target of the mass balance for this pilot plant is to produce 1,000 kg/h of $CaCO_3$. Additional to these technical assumptions, it was also established the same design basis (see Table 3-8) because the results obtained during the experimental work were suitable for both mineralization processes.

The Process Flow Diagram (PFD) of the PCC process design was elaborated and it is presented in Figure 5-11. The equipment and operations described by the PFD were considered as the main steps requires to PCC from EAF slag and CO_2.

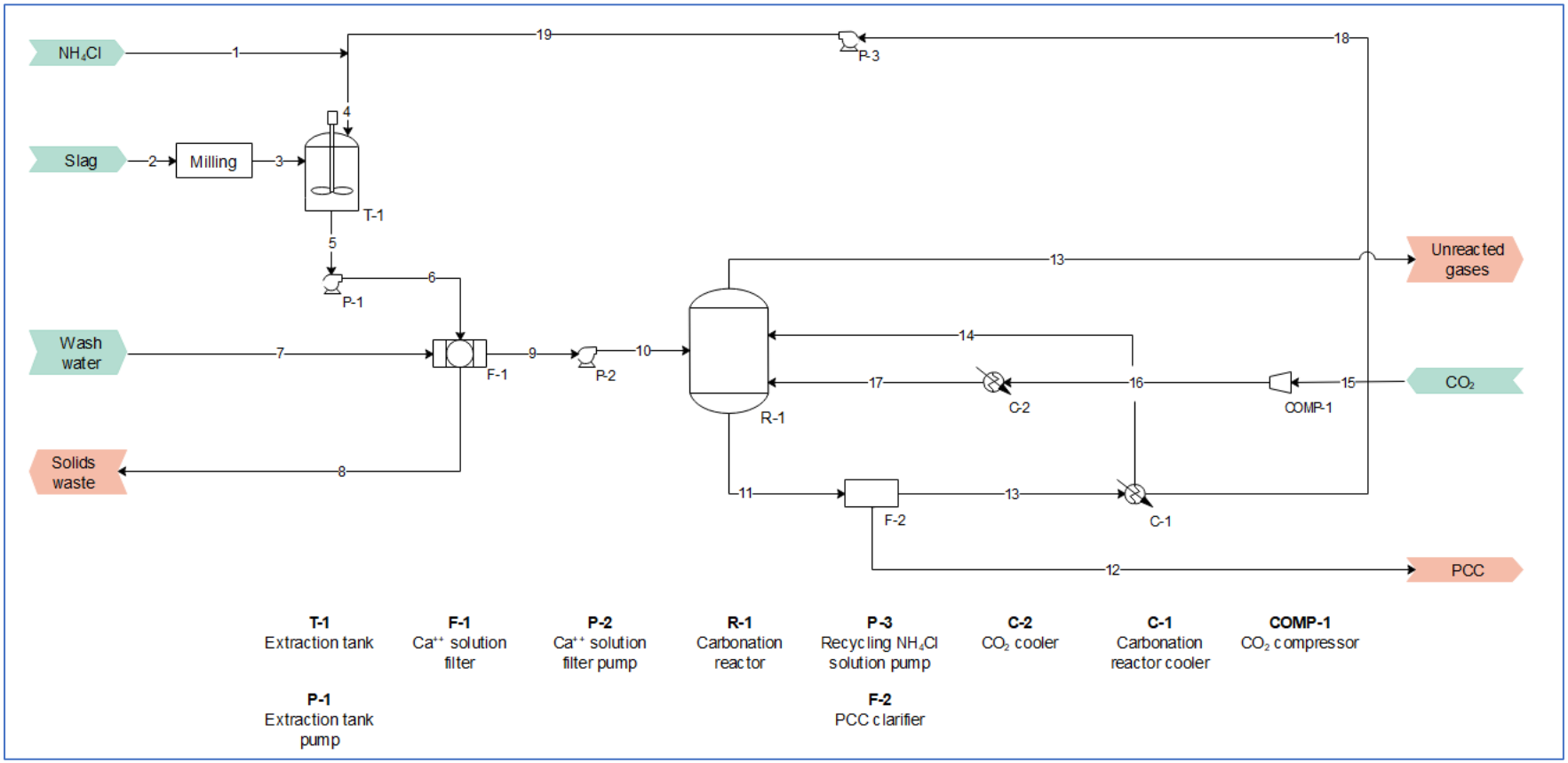

Figure 5- 11 Aspen model flowsheet for the PCC pilot plant.

The main components in the pilot plant design are the extraction tank and a carbonation reactor. There are 10 equipment considered to model the three stages of the mineralization process, as seen in Table T-13.

Table 5- 13 List of equipment considered in the design of the PCC pilot plant.

Tag	Name	Stage	Simulated in Aspen Plus
T-1	Extraction tank	E	**
P-1	Extraction tank pump	E	**
F-1	Ca^{++} solution filter	E	**
P-2	Ca^{++} solution pump	E	**
COMP-1	CO_2 compressor	C	**
C-2	CO_2 cooler	C	**
R-1	Carbonation reactor	C	**
F-2	PCC clarifier	S	**
C-1	Carbonation reactor cooler	S	**
P-3	Recycling NH_4Cl solution pump	S	**

E=Extraction, C=Carbonation, S=Solid/liquid separation.

Different from the LWA analysis, in this case all the equipment was simulated in Aspen Plus and the mass balances presented in the next paragraphs were calculated, in its majority, from the data obtain by the software.

There are 3 extra operations required in the PCC mineralization process that were not modeled nor simulated in this study: the milling of the EAF slag, the gas scrubbing system, and the washing of the final product. The implications and importance of the first two were discussed previously. As for the third one, it is assumed that the solid/liquid separation stage will have a similar effect as the PCC washing. In the LWA pilot plant, a washing stage is crucial to separate the final product from the $CaCO_3$ that could not be adhered to the substrates surface. The PCC pilot plant does not have that problem because all the $CaCO_3$ produced in this process is directly the final product.

The PFD was sectioned in 2 parts that represents the 3 main stages of pilot plant. The next paragraphs describe the mass balances of both sections and present the discussion of the results obtained by the simulation and stoichiometric calculations. The diagram of the PCC

pilot plant as well as the description of all streams involved in the simulation are presented in Appendixes G and H.

Extraction

The solid feedstock (EAF slag) is milled down to a particle size <100 mesh and then mixed with the NH_4Cl solution at a 1:5 SLR in the extraction tank (T-1) with same conditions and parameters as the one in the LWA pilot plant model. Here, the NH_4Cl solution (stream 4) similarly represents the combination of the solvent make-up needed and the recovered solution. The same Ca^{++} extraction reaction (See Equation 3.1) is loaded in the RStoic reactor and the heat duty is specified as zero. Figure 5-12 shows the main inlets and outlets of this stage.

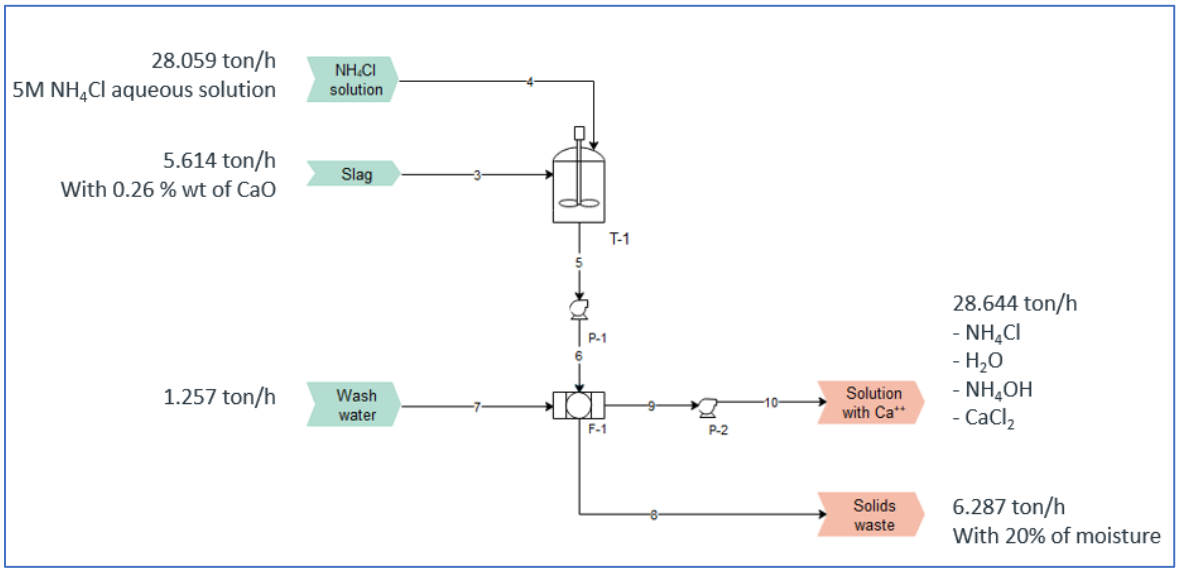

Figure 5- 12 Inlets and outlets of the extraction stage in PCC pilot plant design.

The exit solution from T-1 (stream 5) contains $CaCl_2$ and NH_4OH produced during the extraction, as well as undissolved slag and unreacted solvent. This solution is pumped by P-1 to a press filter (F-1) to separate the solids. As shown by Table 5-14 and the mass balance for this stage, 5029 kg/h of slag did not dissolve in T-1 and exit the PCC production process in stream 8 with 20% of moisture content.

The solution, free from solids, contains 417 kg/h of Ca^{++} and 4,644 kg/h of Cl^-, which confirms the calcium extraction from EAF slag in the form of $CaCl_2$. The chloride ions (Cl^-) present in stream 10, along with ammonium ions (NH_4^+), are also part of the NH4Cl solution that did not react in T-1.

Table 5- 14 Mass balance of the extraction stage in PCC pilot plant design.

	Inlet			Outlet	
Flow (kg/h)	**3**	**4**	**7**	**8**	**10**
H_2O	0	21,052	1,258	1,258	21,240
CaO	1460	0	0	875	0
Ca^{++}	0	0	0	0	417
H_3O^+	0	0.01	0	0	0
NH_4^+	0	2,363	0	0	1,988
HCl	0	0	0	0	0
Cl^-	0	4,644	0	0	4,644
NH_3	0	0.01	0	0	355
$CaOH^+$	0	0	0	0	0.04
OH^-	0	0	0	0	0.01
Solids	4,154	0	0	4,154	0
Total	**5,614**	**28,059**	**1,258**	**6,287**	**28,644**
	34,931			**34,931**	

It is also inferred by the results shown in Table 5-14, that stream 10 contains NH_4OH because of the presence of ammonia (NH_3) and the increase of H_2O in the flow. Once all the elements of interest are confirmed, the solution is pumped by P-2 into the carbonation stage.

Carbonation and solid/liquid separation

This section the last two stages of the PCC pilot plant, the carbonation and the solid/liquid separation. Both stages were simulated as one because of the implications of the process. Figure 5-13 shows the equipment and streams that represents these stages. Here, the CO_2 absorption (Equation__) and $CaCO_3$ precipitation (Equation __) is assumed to occur in a single step carbonation reactor (R-1). This equipment is simulated in aspen as a Flash model flooded by the $CaCl_2$-NH_4OH solution and with a CO_2 flow (stream 17) bubbled by its bottom. It operates at 25 °C and atmospheric pressure.

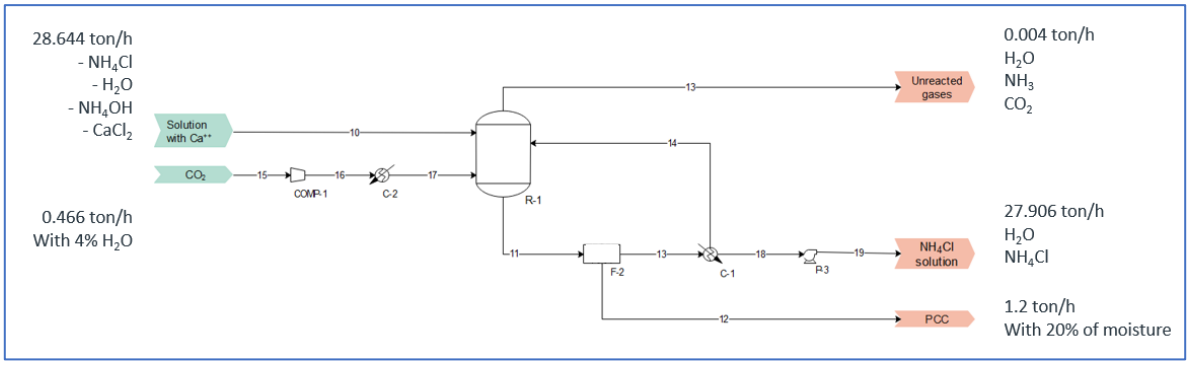

Figure 5- 13 Inlets and outlets of the carbonation stage in PCC pilot plant design.

Although R-1 is not pressurized as the absorption tower in the LWA pilot plant, the CO_2 still needs to be pressurized by a compressor (COMP-1) to overcome the volume of the solution in R-1 and assure as much contact as possible between the CO_2 and the solution. A cooler (C-2) is then needed to remove the heat generated during the compression and meet the operating temperature of the carbonation reactor. the absorber column (1.5 bar) and added to the slurry.

Similarly, to the LWA process, the reactions occurring in R-1 are overall exothermic so a cooler (C-1) is needed to recirculate part of the resulting solution at 25 °C and avoid the decompositions of $(NH_4)_2CO_3$ and volatilization of NH_3 and CO_2. The difference is that, in this case, is that stream 11 is not a diluted solution but a slurry and it cannot be cooled immediately for recirculation. To address this problem, the solid/liquid separation is placed between both operations (Carbonation and recirculation). After carbonation is complete in R-1, the slurry (stream 11) is filtered in a clarifier (F-2) to separate and collect the PCC produced. A clarifier is proposed for this operation because of the slurry temperature (See Appendix H). Once the solids have been removed, the solution is cooled and 85% of it is recycle to R-1 while the rest continues with the flow of the process.

Table 5-11 shows the mass balance obtain from the simulation of these stages. The process design objective is for most of the Ca^{++} solution to be carbonated in, with a small amount of unreacted Ca^{++} ions kept aside in stream 19. The results obtained by the simulation show that 96% of the calcium extracted from the EAF slag was successfully carbonated.

Table 5- 15 Mass balance of the carbonation stage in PCC pilot plant design.

	In (kg/h)		Out (kg/h)		
Stream	**10**	**15**	**12**	**13**	**19**
H_2O	21,240	8	200	3	20,859
Ca^{++}	417	0	16	0	0
CO_2	0	458	0.06	0	0
NH_4^+	1,988	0	0	0	2,358
HCO_3^-	0	0	0	0	22
CO_3^{--}	0	0	0.08	0	0
Cl^-	4,644	0	0	0	4,644
NH_3	355	0	6	1	0
OH^-	0.01	0	0	0	0
NH_2COO^-	0	0	1	0	0
NH_4HCO_3	0	0	0	0	0
$CaOH^+$	0.04	0	0	0	0
$CaCO_3$	0	0	1000	0	0
Total	**28,644**	**466**	**1,223**	**4**	**27,883**
	29,110		**29,110**		

Stream 19 contains mainly NH_4^+, Cl^- ions and H_2O which is inferred as the regeneration of the solvent solution, therefore, this solution is pumped by P-3 for its recirculation into the initial stage of the process, the calcium extraction. Although the solvent recycle was not simulated, the results from the mass balance of these stages give enough information to calculate the NH_4Cl make up and the gas washer needed, is any.

Finally, 1,000 kg/h of PCC is produced and leaves the process in stream 12 with a 20% of moisture. This humidity in the sludge is intended to be removed naturally in a pit. It is important to mentioned that another filtration after the clarifier might be required in order to remove the NH_3 and other unreacted compounds present in the final sludge, nevertheless, in the results shown above, only a 0.25% of the sludge would have to be separated so this process was not modeled nor considered in the pilot plant design.

Figure 5-14 presents the global mass balance for the pilot plant designed that produces 1 ton/h of PCC. The mass balance considered all process stages described and the results previously obtained.

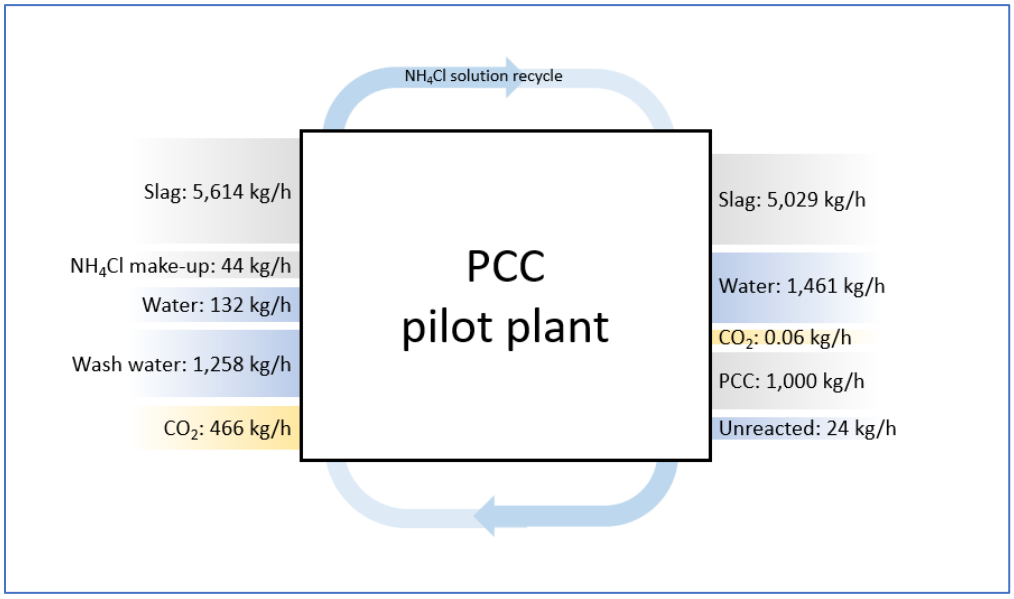

Figure 5- 14 Total mass balance for the LWA pilot plant design.

In this study, it was found that 99.99% of the inlet CO_2 flow reacts and transform into the final product. On the other hand, there are 24 kg/h of unreacted compounds that exit the process. This amount consists mainly from the $(NH_4)_2CO_3$ that din not react during the carbonation.

To produce 1000 kg/hr of PCC, 5,614 kg/h of EAF slag is needed, assuming a Ca^{++} extraction efficiency of 40%. The amount of slag required to accomplished this is quite significant and greater than the required by the LWA pilot plant. The comparisons between the technical parameters and implications of both pilot plants is discussed in Chapter 7.

5.3.3 Energy balances

The simulation of the pilot plant also provide data from the energy balance of the process. The results and their discussion are presented in this section. First, a summary of the units modeled is shown in Table 5-16, with the equipment's conditions that were stablished for the simulation.

Table 5- 16 Required input data for the PCC pilot plant simulation

Condensers/Heat Exchangers	**C-1**	**C-2**		
Pressure (bar)	1	1		
Temperature (°C)	25	25		
Type	V-L	V-L		
Heat duty (kcal/h)	-9,073	-11,410		
Pumps/Compressors	**P-1**	**P-2**	**P-3**	**COMP-1**
Efficiency	0.5	0.5	0.5	0.72
ΔP (bar)	1	1	1	1.5
Power (kW)	1.4	1.32	0.65	8.46
Reactors/Towers	**T-1**	**R-1**		
Temperature (°C)	25	25		
Pressure (bar)	1	1.5		
Heat duty (kcal/h)	0	-429,120		

Basically, all the equipment operates at atmospheric pressure and ambient temperature. There is no heat required for any of the units in this process and the major electricity demand comes from the power required to compress the CO_2 flow from the DR pilot plant in COMP-1.

The energy consumption of the pilot plant was calculated considering 1000 kg/h of PCC produced. Table 5-17 shows the energy balance of each operational unit in terms of power, heat or cooling requirements for the overall pilot plant. This table shows all the steps of the process, including stages outside the limitations of the simulation.

The table also shows the amount of CO_2 emitted indirectly by the energy consumption of the process. A total of 25 kg/h of CO_2 is emitted per ton of PCC produced. This value is lower than the one obtained in the LWA pilot plant (410 kg/h per ton of LWA produced).

The CO_2 attractive sequestration capacity of 99.99% (0.46 tCO_2 per tPCC produced) was achieved in the process with a total electricity consumption of 55 kWh and without heat requirement. This consumption is lower than both electricity and heat consumption to produce LWA.

Table 5- 17 Energy consumption from unit operations in PCC pilot plant simulation

Energy requirement			Utilities		
Equipment	Rate (kW)	CO_2 emission (kg/h)	Steam (kg/h)	Cooling water (kg/h)	Electricity (kWh)
Power (kW)					
P-1	1.4	0.64			1.4
P-2	1.32	0.60			1.32
P-3	0.65	0.30			0.65
COMP-1	8.47	3.86			8.47
**	42.49	19.38			42.49
Thermal energy (kcal/h)					
C-1	-12,974			1,629	
C-2	-23,433			2,943	
	Total:	**24.78**	**0**	**4,572**	**54.32**

**Data obtained in Aspen simulation for the auxiliaries needed to operate the equipment

After this analysis it is inferred that the PCC pilot plant represents a better option for implementation in a DR-EAF facility due to its lower energy requirements. Nevertheless, a deeper comparison between both process was made and is presented in the next chapters.

CHAPTER 6 ECONOMIC ANALYSIS

It is crucial for the feasibility implementation of a pilot plant that it be economically viable. Work until now has focused on the technical aspects of both CO_2 mineralization processes. Hence, this chapter presents an economic assessment of the two pilot plants alternatives by estimating the NPV, IRR and payback period of both pilot plants design.

The objective of this exercise is to evaluate the economics of the pilot plants, estimating the costs of implementation and production of 1 ton/h of LWA or PCC to obtain another tool for a successful comparison between both CO_2 mineralization processes. This was done considering the technical assumptions made, mass and energy results, pilot plants simulation's data about equipment costs estimation. Some key considerations for the economic analysis were provided by the Tenova HYL design team.

6.1 PRODUCTION COSTS

In the present work, the production cost consists of the sum of the expenses related to raw materials, services and operation of the pilot plants.

6.1.2 Raw material costs

The prices of the raw material needed in both pilot plants are presented in Table 6-1. The unit cost information of each material was mainly obtained from literature (see Chapter 3) and was used to calculate the costs for the inlet flows of each process.

As mentioned before, the pilot plants were designed considering they would be located in a DR-EAF where both CO_2 and EAF slag are available, as an unwanted residue, at zero cost in the same site. As for the price for substrate, it is just applicable only in the LWA pilot plant.

It was also assumed for this part that the slag is always available in the required amount to satisfy the production rate.

Table 6- 1 Raw material costs for LWA and PCC pilot plants.

		LWA pilot plant		PCC pilot plant	
Material	Unit cost (USD/kg)	Flow (kg/h)	Cost per year (USD/year)	Flow (kg/h)	Cost per year (USD/year)
Slag	NA	2,731	$0	5,614	$0
CO_2	NA	227	$0	466	$0
Water	$0.002	1,528	$26,833	1,258	$22,091
Substrate	$0.026	670	$139,360	NA	$0
		Total:	**$166,193**	**Total:**	**$22,091**

The raw material cost for the production of LWA is seven times greater than in the case of the PCC production. As already mentioned, there is no require for substrate to produce precipitated calcium carbonate, so that expense only exists in the LWA pilot plant. The second reason, that does not impact the result as much as the first one, is that the LWA pilot plant also requires a greater amount of water in its process because of the product washing stage.

6.1.2 Services costs

The services costs refer to the expenses on energy needs and other activities required for the process. The energy requirements for both pilot plants were obtained from electricity, heat and cooling consumption obtained from the balances and simulation of the processes using Aspen Plus. Additionally, the NH_4Cl make-up and the grinding of the slag are considered as services because both activities, although were not modeled, are essential for both processes. A summary of the total services cost for the LWA and PCC pilot plants are presented in Table 6-2.

The Total Services Cost (TSC)of both pilot pants was calculated considering the unit costs presented. The unit costs of electricity, cooling water and steam were obtained from Aspen Plus User's Manual [47]. The cost of the pre-treatment of the slag was provided as an

estimation by an external supplier of Tenova HYL. Finally, the cost of NH4Cl was stablished based on bibliography consulted (See Chapter 3).

Table 6- 2 Services costs for LWA and PCC pilot plants.

			LWA pilot plant		PCC pilot plant	
Service	Unit	Unit cost (USD/unit)	Rate	Cost per year (USD/year)	Rate	Cost per year (USD/year)
Electricity	kW	$0.05	118	$50,646	54	$23,314
Cooling water	kg	$0.0003	33,690	$70,857	4,572	$9,616
Steam @100PSI	kg	**	2,513	$107,697	NA	$0
Slag pre-treatment	kg	$0.02	2,731	$327,710	5,614	$673,638
Solvent make-up	kg	$1.63	9	$122,526	24	$312,832
			Total:	**$679,436**	**Total:**	**$1,019,400**

**Natural gas considered to produce the steam requirements. Unit cost: 2.5 USD/MMBtu

Although the overall LWA production process resulted in an energy consumption far greater than PCC pilot plant, its total service cost is lower. This is because the implication of the slag grinding as a service. The PCC pilot plant requires a greater flow of slag per hour than the LWA production, hence the higher cost. Figure 6-1 shows the distribution of the TSC for the two pilot plants design where it is showed that in both processes, the milling of the slag represents the highest expense out of the other services contemplated.

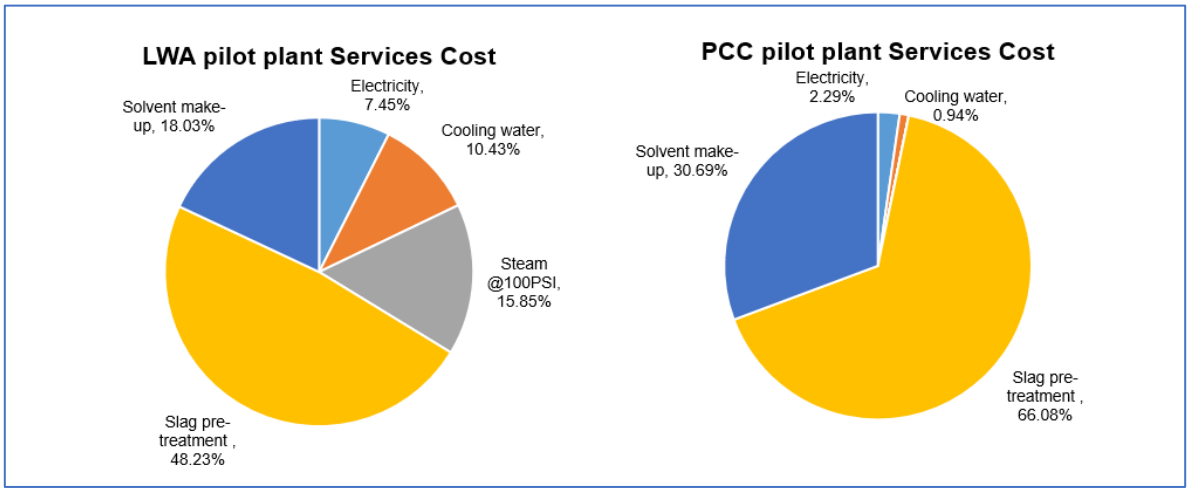

Figure 6- 1 Distribution of the total Services cost for LWA and PCC pilot plants.

As for the NH_4Cl, that had the highest unit cost listed in Table 6-2, it was neglected from raw materials costs due to the recovery system proposed in both pilot plants and it high recycle efficiency. Therefore, the flow of NH_4Cl needed as make-up is contemplated as another service cost. The PCC pilot plant requires more NH4Cl than the LWA process because of the losses that present during the carbonation reactor and the solid/liquid separation. The cost of solvent make-up along with the cost of slag pretreatment are directly reflected un the difference between the TSC of the two pilot plants.

6.1.3 Operating costs

The operating costs consist of the expenditures that the pilot plants incur to engage in any activities that are not directly associated with the production of the LWA or PCC. In this economic exercise, the operating cost for the process is considered as the sum of the labor cos and operating charges. Table 6-3 shows the work scheme considered to calculate the labor cost. The values presented were established based on industrial experience.

Table 6- 3 Work scheme considered for both pilot plants operation.

Personnel	People per shift	Salary (USD/h)
Operator	2	$6
Laboratory technician	1	$8
Supervisor	1	$18

For this economic exercise, 8-hour shifts were assumed. It was also considered 3 shifts per day for plant operators and the laboratory technician and only 2 shifts/day for the supervisor. After setting up the work scheme, the Total Operating Cost (TOC) was calculated and it is shown in Table 6-4.

Table 6- 4 Total Operating Costs for LWA and PCC pilot plants

Category	USD/year
Operating Labor Cost	$720,000
Operating charges	$72,200
Total:	**$792,000**

The TOC obtained was stablished for both pilot plants. The operating charges was calculated as the 15% of the operating labor cost. This percentage is assumed to cover the operational fees and supplies that might be required by the manpower involved in the processes.

The Total Production Costs (TPC) needed to produce 1 ton/h of LWA and PCC were calculated from the results of material, services and operating charges. Table 6-5 display the summary of these costs and the TPC for each pilot plant

Table 6- 5 Estimated Total Production Costs for LWA and PCC pilot plants

	LWA pilot plant	PCC pilot plant
Total Operating Cost	$792,000	$792,000
Total Raw materials cost	$166,192	$22,091
Total Services Cost	$679,436	$1,019,340
Total:	**$1,637,629**	**$1,833,491**

The total production cost for the LWA pilot plant with a capacity of 8 ton/year was calculated in $1.637 million USD per year while the PCC production cost was 1.833. The similarity of the estimated cost was due to the singularities of each pilot plant. While, mentioned before, LWA pilot plant has a lower service cost, the PCC process compensates this by the minor Raw material cost because of its lack of substrate need.

With these results it is inferred that the annual cost of producing LWA or PCC products does not give enough information to select the better option (economically) to implement in the DR-EAF plant. Therefore, the economic analysis continues with the estimation of the investment cost in the next section.

6.2 INVESTMENT COST

The development of any industrial process requires a strong investment in assets to start the manufacture. The investment costs of the pilot plants designed in this thesis were estimated only for the main equipment of the process using the estimation costs obtained by the simulation and from Tenova HYL design team.

6.2.1 Equipment costs

The costs of core processing equipment were calculated using the Aspen Plus: Process Economic Analizer (PEA) while the costs the not-simulated units were separately estimated and handled by Tenova HYL engineering design team. Aspen PEA does the equipment sizing according to its data base and the information loaded during the simulation (slows, temperature, pressure, heat duties, stages, etc.). It is important to mention that this database is not able to make a rigorous sizing and does not select the equipment material, leaving carbon steel as the predeterminate material. Nevertheless, using only, the Aspen PEA database is enough for the estimation of equipment costs. Tables 6 and 7 show the total equipment costs for the LWA and PCC pilot plants, respectively,

Table 6- 6 Total equipment cost for LWA pilot plant

Unit tag	Equipment Cost (USD)	% of total
C-1	$11,400	1
C-2	$10,000	0.83
C-3	$9,400	0.78
P-1	$6,700	0.55
P-2	$7,800	0.64
P-3	$6,700	0.55
P-4	$8,500	0.70
P-5	$6,000	0.50
P-6**	$6,700	0.55
COMP-1	$473,000	39
HX-1	$35,100	2.90
F-1	$18,800	1.55
F-2	$12,500	1
T-1	$98,400	8.13
T-2 reboiler	$24,300	2
T-2	$18,200	1.50
T-3	$26,200	2.16
V-1**	$230,600.00	19
V-2**	$99,800.00	8.24
V-3**	$100,500.00	8.30
Total	**$1,210,600.00**	**100%**

** Costs of these units were given by Tenova HYL Engineering Design team.

As the previous tables show, in the LWA pilot plant the most expensive unit is the CO_2 compressor, which represents 39% of the total equipment cost. On the other hand, in the PCC pilot plant, is the extraction tank, accounting for 34.6% of the total. After this one, the agglomeration drum is the second most expensive equipment, with a cost of 19% of the total.

Table 6- 7 Total equipment cost for PCC pilot plant

Unit tag	Equipment Cost (USD)	% of total
C-1	$10,800	2.48
C-2	$12,000	2.75
P-1	$6,700	1.54
P-2	$6,400	1.47
P-3	$6,500	1.49
COMP-1	$120,300	27.59
F-1	$23,400	5.37
F-2**	$100,600	23.07
T-1	$98,900	22.68
R-1	$50,400	11.56
Total	**$436,000**	**100%**

At the end, there is a significant difference between the equipment cost for both pilot plants, where the LWA equipment cost almost three times the cost of PCC equipment. Despite this difference, the most expensive unit in the PCC pilot plant is also de CO_2 compressor. This is due because of the conditions of the CO_2 stream that comes from the DR process. The CO_2 leaves the DR plant at nearly atmospheric pressure. The ΔP required in both process, along with the gas volume, reflects directly in the power required by the CO_2 compression and its cost.

The Total Capital Cost (TCC) is then calculated as the sum of the units cost and their installation. Table 6-8 displays all the expenses contemplated for the equipment installation and the TCC of both pilot plants. It also shows some other charges as the General and Administrative (G and A) and contingencies-related expenses. The G and A costs involve some general and administrative costs as office building, heating and air conditioning (HVAC), and their maintenance. The charge for contingencies is assumed as 15% of the TCC

and represents a provision for unforeseeable elements that might occur regarding these costs once the implementation of the pilot plant begins.

Table 6- 8 Fixed Capital investment Cost for LWA and PCC pilot plants

Category	Cost (USD)	
	LWA pilot plant	PCC pilot plant
Purchased Equipment	$1,210,600	$436,000
Equipment Setting	$23,432	$17,513
Piping	$354,971	$252,774
Steel	$39,418	$42,101
Instrumentation	$976,205	$629,446
Electrical	$538,932	$511,528
Insulation	$101,744	$35,627
G and A Overheads	$113,756	$77,253
Contingencies	$547,278	$338,698
Total Investment Cost	**$3,906,336**	**$2,340,939**
Working capital	$585,950	$351,141
Fixed Capital Investment	**$4,492,287**	**$2,692,080**

The cost specified as piping, steel, instrumentation, electrical and insulation corresponds to the equipment installation requirements it is included to cover further facilities such as pumps, pipe lines, cooling towers, control equipment, auxiliary equipment and electrical installations.

The table above also shows the Fixed Capital Investment (FCI) calculated as the sum of TCC and the working capital. The working capital requirements include the money needed to maintain inventories and cover accounts payable. It is charged at the beginning of plant operation but is never actually consumed. In this study, the working capital is assumed as 5% of the FCI.

The costs obtained in this analysis showed a FCI of 4.5 million USD for the LWA pilot plant and 2.7 million USD for PCC pilot plant. This difference was mainly due to the higher equipment cost required by the first one which also resulted in higher installation cost.

6.3 CASH FLOWS

Cash flow is the movement of money in or out of the project. The analysis of cash flow determined the increasing earnings that might be generated by the execution of implementing the pilot plans; it was used in this investigation to evaluate and compare both alternatives by the calculation of the economic Key Parameter Indicators (KPI) established in the methodology: The Net Present Value (NPV), Internal Rate of Return (IRR), Payback period (PP) and Benefit/Cost Ratio (BCR).

The costs for implementing the pilot plants (Investment costs) and their further operation (Operating costs) have been previously calculated, so the purpose of this section was to determine the project feasibility contouring these expenses with the earnings of the mineralization processes. Basically, the incomes are due to sales generated by the pilot plants (LWA and PCC sales) and its indirect effects on sales of other products of the processes, if any (unreacted Slag and CO_2). In this case just sales generated from the residual slag were considered. Table 6-9 shows the prices for these products.

Table 6- 9 Product prices consider for the economic assessment of both LWA and PCC pilot plants.

		LWA pilot plant		PCC pilot plant	
Product	**Selling price (USD/kg)**	**Flow (kg/h)**	**Earnings (USD/year)**	**Flow (kg/h)**	**Earnings (USD/year)**
LWA	0.23	1,000	$1,840,000	0	$0
PCC	0.14	0	$0	1,000	$1,120,000
Treated slag	0.04	2,447	$783,040	5,029	$1,609,280
		Total:	**$2,623,040**	**Total:**	**$2,729,280**

Although the selling price of LWA is significantly higher than PCC, the total incomes for the pilot plants are very similar. This is because the earnings by selling 8,000 ton/year of LWA is offset by the greater amount of residual slag that can be sold during the PCC production process. The values considered for the LWA, PCC and treated slag were specified based on literature review (see Chapter 2).

Regarding the pilot plants, for economic assessment of potential investment, the projected cash flow for each one was built incorporating all expected positive and negative incomes

and outcomes. Cash flow for both investment projects (See Figures 6-1 and 6-2) were compared, and the viability of both processes is further discussed.

Starting from year 0, for the pilot plant installation, just the FCI was considered; there were neither sales nor production. The operation of the plant was set to 91% (8000 h/y) in year 1 and subsequent years, without considering increase of sales or production capacity in the horizon of the project. In other words, there were not variable costs considered for the elaboration of both cash flows.

Cash flows were calculated in a separate Excel spreadsheet. The numbers in red represents the negative incomes of the projects. The economic KPI´s shown in Table 6-10 were calculated applying equations enlisted in the methodology and the data obtained by the cash flows.

Table 6- 10 Economic Key Parameters Indicators (KPI) of LWA and PCC pilot plants.

KPIs	LWA pilot plant	PCC pilot plant
Net Present Value (USD)	$175,186	$2,202,974
Payback period (years)	12	8
Internal rate of return (%)	8.42%	16.28%
Benefit Cost Ratio	1.6	1.5

As presented above, the NPVs obtained was positive in both cases. These results indicate that the projected earnings generated by the two pilot plants (in present USD) exceeds the anticipated costs (also in USD). It is inferred then that both implementation projects will be profitable and PCC pilot plant represents a better option because of its higher NPV. As for the payback period, the PCC pilot plant project also turned out to be more attractive than LWA project because it generates net positive incomes 4 year before the latter.

The IRR for both pilot plants is higher than the interest rate assumed for the economic analysis (8%), which indicates the rentability of the two projects. This result represented a complementation for the NPVs obtained. The IRR calculated confirm the anticipated profitability of the pilot plant investment regarding its duration.

	YEAR																						
	-2	-1	0	1	2	3	4	5	6	7	8	9	10	11	12	13	14	15	16	17	18	19	20
LOAN PAYMENT NA				$0	$0	$0	$0	$0	$0	$0	$0	$0	$0										
Loan interest payment				$0	$0.00	$0	$0	$0	$0	$0	$0	$0	$0										
Loan Principal				$0	$0	$0	$0	$0	$0	$0	$0	$0	$0										
LWA SALES				$1,840,000	$1,840,000	$1,840,000	$1,840,000	$1,840,000	$1,840,000	$1,840,000	$1,840,000	$1,840,000	$1,840,000	$1,840,000	$1,840,000	$1,840,000	$1,840,000	$1,840,000	$1,840,000	$1,840,000	$1,840,000	$1,840,000	$1,840,000
Other (reformed slag & CO_2 unreacted)				$783,040.00	$783,040.00	$783,040.00	$783,040.00	$783,040.00	$783,040.00	$783,040.00	$783,040.00	$783,040.00	$783,040.00	$783,040.00	$783,040.00	$783,040.00	$783,040.00	$783,040.00	$783,040.00	$783,040.00	$783,040.00	$783,040.00	$783,040.00
Total Annual Sales				$2,623,040	$2,623,040	$2,623,040	$2,623,040	$2,623,040	$2,623,040	$2,623,040	$2,623,040	$2,623,040	$2,623,040	$2,623,040	$2,623,040	$2,623,040	$2,623,040	$2,623,040	$2,623,040	$2,623,040	$2,623,040	$2,623,040	$2,623,040
ANNUAL MANUFACTURING COST																							
Raw materials				$166,193	$166,193	$166,193	$166,193	$166,193	$166,193	$166,193	$166,193	$166,193	$166,193	$166,193	$166,193	$166,193	$166,193	$166,193	$166,193	$166,193	$166,193	$166,193	$166,193
Fixed Operating Costs				$1,471,436	$1,471,436	$1,471,436	$1,471,436	$1,471,436	$1,471,436	$1,471,436	$1,471,436	$1,471,436	$1,471,436	$1,471,436	$1,471,436	$1,471,436	$1,471,436	$1,471,436	$1,471,436	$1,471,436	$1,471,436	$1,471,436	$1,471,436
Total Product cost				$1,637,629	$1,637,629	$1,637,629	$1,637,629	$1,637,629	$1,637,629	$1,637,629	$1,637,629	$1,637,629	$1,637,629	$1,637,629	$1,637,629	$1,637,629	$1,637,629	$1,637,629	$1,637,629	$1,637,629	$1,637,629	$1,637,629	$1,637,629
ANNUAL DEPRECIATION																							
Depreciation				$577,579.74	$577,579.74	$577,579.74	$577,579.74	$577,579.74	$577,579.74	$577,579.74													
Remaining Value			$4,043,058	$3,465,478	$2,887,899	$2,310,319	$1,732,739	$1,155,159	$577,580	$0													
NET REVENUE			($4,492,287)	$407,831	$407,831	$407,831	$407,831	$407,831	$407,831	$407,831	$985,411	$985,411	$985,411	$985,411	$985,411	$985,411	$985,411	$985,411	$985,411	$985,411	$985,411	$985,411	$985,411
Taxable Income				$407,831	$407,831	$407,831	$407,831	$407,831	$407,831	$407,831	$985,411	$985,411	$985,411	$985,411	$985,411	$985,411	$985,411	$985,411	$985,411	$985,411	$985,411	$985,411	$985,411
Income Tax				$122,349	$122,349	$122,349	$122,349	$122,349	$122,349	$122,349	$295,623	$295,623	$295,623	$295,623	$295,623	$295,623	$295,623	$295,623	$295,623	$295,623	$295,623	$295,623	$295,623
ANNUAL CASH INCOME				$863,062	$863,062	$863,062	$863,062	$863,062	$863,062	$863,062	$689,788	$689,788	$689,788	$689,788	$689,788	$689,788	$689,788	$689,788	$689,788	$689,788	$689,788	$689,788	$689,788
Net Cash flow			($4,492,287)	$285,482	$285,482	$285,482	$285,482	$285,482	$285,482	$285,482	$689,788	$689,788	$689,788	$689,788	$689,788	$689,788	$689,788	$689,788	$689,788	$689,788	$689,788	$689,788	$689,788
Cumulative cash flow				($4,206,805)	($3,921,323)	($3,635,841)	($3,350,359)	($3,064,877)	($2,779,395)	($2,493,913)	($1,804,125)	($1,114,337)	($424,549)	$265,239	$955,026	$1,644,814	$2,334,602	$3,024,390	$3,714,178	$4,403,966	$5,093,753	$5,783,541	$6,473,329
Discount Factor NA			1	0.925925926	0.85733882	0.793832241	0.735029853	0.680583197	0.630169627	0.583490395	0.540268885	0.500248967	0.463193488	0.428882859	0.397113759	0.367697925	0.340461041	0.315241705	0.291890468	0.270268951	0.250249029	0.231712064	0.214548207
Discounted Cash			($4,492,287)	$264,335.20	$244,754.81	$226,624.83	$209,837.80	$194,294.26	$179,902.09	$166,576.01	$372,670.90	$345,065.65	$319,505.23	$295,838.18	$273,924.24	$253,633.55	$234,845.88	$217,449.89	$201,342.49	$186,428.23	$172,618.73	$159,832.16	$147,992.74
Cummulative Discounted Cash flow				($4,227,952)	($3,983,197)	($3,756,572)	($3,546,734)	($3,352,440)	($3,172,538)	($3,005,962)	($2,633,291)	($2,288,225)	($1,968,720)	($1,672,882)	($1,398,958)	($1,145,324)	($910,478)	($693,028)	($491,686)	($305,258)	($132,639)	$27,193	$175,186

Figure 6- 2 Cash Flow at 20 years for the project of LWA pilot plant implementation.

	YEAR																						
	-2	-1	0	1	2	3	4	5	6	7	8	9	10	11	12	13	14	15	16	17	18	19	20
LOAN PAYMENT NA				$0	$0	$0	$0	$0	$0	$0	$0	$0	$0										
Loan interest payment				$0	$0.00	$0	$0	$0	$0	$0	$0	$0	$0										
Loan Principal			$0	$0	$0	$0	$0	$0	$0	$0	$0	$0	$0										
PCC SALES				$1,120,000	$1,120,000	$1,120,000	$1,120,000	$1,120,000	$1,120,000	$1,120,000	$1,120,000	$1,120,000	$1,120,000	$1,120,000	$1,120,000	$1,120,000	$1,120,000	$1,120,000	$1,120,000	$1,120,000	$1,120,000	$1,120,000	$1,120,000
Other (reformed slag & CO_2 unreacted)				$1,609,280	$1,609,280.00	$1,609,280.00	$1,609,280.00	$1,609,280.00	$1,609,280.00	$1,609,280.00	$1,609,280.00	$1,609,280.00	$1,609,280.00	$1,609,280.00	$1,609,280.00	$1,609,280.00	$1,609,280.00	$1,609,280.00	$1,609,280.00	$1,609,280.00	$1,609,280.00	$1,609,280.00	$1,609,280.00
Total Annual Sales				$2,729,280	$2,729,280	$2,729,280	$2,729,280	$2,729,280	$2,729,280	$2,729,280	$2,729,280	$2,729,280	$2,729,280	$2,729,280	$2,729,280	$2,729,280	$2,729,280	$2,729,280	$2,729,280	$2,729,280	$2,729,280	$2,729,280	$2,729,280
ANNUAL MANUFACTURING COST																							
Raw materials				$22,091	$22,091	$22,091	$22,091	$22,091	$22,091	$22,091	$22,091	$22,091	$22,091	$22,091	$22,091	$22,091	$22,091	$22,091	$22,091	$22,091	$22,091	$22,091	$22,091
Fixed Operating Costs				$1,811,400	$1,811,400	$1,811,400	$1,811,400	$1,811,400	$1,811,400	$1,811,400	$1,811,400	$1,811,400	$1,811,400	$1,811,400	$1,811,400	$1,811,400	$1,811,400	$1,811,400	$1,811,400	$1,811,400	$1,811,400	$1,811,400	$1,811,400
Total Product cost				$1,833,491	$1,833,491	$1,833,491	$1,833,491	$1,833,491	$1,833,491	$1,833,491	$1,833,491	$1,833,491	$1,833,491	$1,833,491	$1,833,491	$1,833,491	$1,833,491	$1,833,491	$1,833,491	$1,833,491	$1,833,491	$1,833,491	$1,833,491
ANNUAL DEPRECIATION																							
Depreciation				$346,124.58	$346,124.58	$346,124.58	$346,124.58	$346,124.58	$346,124.58	$346,124.58													
Remaining Value			$2,422,872	$2,076,747	$1,730,623	$1,384,498	$1,038,374	$692,249	$346,125	$0													
NET REVENUE			($2,692,080)	$549,664	549664.218	$549,664	$549,664	$549,664	$549,664	$549,664	$895,789	$895,789	$895,789	$895,789	$895,789	$895,789	$895,789	$895,789	$895,789	$895,789	$895,789	$895,789	$895,789
Taxable Income				$549,664	$549,664	$549,664	$549,664	$549,664	$549,664	$549,664	$895,789	$895,789	$895,789	$895,789	$895,789	$895,789	$895,789	$895,789	$895,789	$895,789	$895,789	$895,789	$895,789
Income Tax				$164,899	$164,899	$164,899	$164,899	$164,899	$164,899	$164,899	$268,737	$268,737	$268,737	$268,737	$268,737	$268,737	$268,737	$268,737	$268,737	$268,737	$268,737	$268,737	$268,737
ANNUAL CASH INCOME				$730,890	$730,890	$730,890	$730,890	$730,890	$730,890	$730,890	$627,052	$627,052	$627,052	$627,052	$627,052	$627,052	$627,052	$627,052	$627,052	$627,052	$627,052	$627,052	$627,052
Net Cash flow			($2,692,080)	$384,765	$384,765	$384,765	$384,765	$384,765	$384,765	$384,765	$627,052	$627,052	$627,052	$627,052	$627,052	$627,052	$627,052	$627,052	$627,052	$627,052	$627,052	$627,052	$627,052
Cumulative cash flow				($2,307,315)	($1,922,550)	($1,537,785)	($1,153,020)	($768,255)	($383,490)	$1,275	$628,327	$1,255,379	$1,882,431	$2,509,483	$3,136,535	$3,763,588	$4,390,640	$5,017,692	$5,644,744	$6,271,796	$6,898,848	$7,525,901	$8,152,953
Discount Factor NA			1	0.925925926	0.8573882	0.793832241	0.735029853	0.680583197	0.630169627	0.583490395	0.540268885	0.500248967	0.463193488	0.428882859	0.397113759	0.367697925	0.340461041	0.315241705	0.291890468	0.270268951	0.250249029	0.231712064	0.214548207
Discounted Cash			($2,692,080)	$356,263.84	$329,873.93	$305,438.82	$282,813.73	$261,864.56	$242,467.19	$224,506.65	$338,776.77	$313,682.19	$290,446.48	$268,931.92	$249,011.04	$230,565.78	$213,486.83	$197,672.99	$183,030.55	$169,472.73	$156,919.19	$145,295.55	$134,532.92
Cummulative Discounted Cash flow				($2,335,816)	($2,005,942)	($1,700,503)	($1,417,690)	($1,155,825)	($913,358)	($688,851)	($350,075)	($36,392)	$254,054	$522,986	$771,997	$1,002,563	$1,216,050	$1,413,723	$1,596,753	$1,766,226	$1,923,145	$2,068,441	$2,202,974

Figure 6- 3 Cash Flow at 20 years for the project of PCC pilot plant implementation.

Finally, the benefit/cost ratio (BCR) is defined as the ratio between the unitary benefit and the unitary cost, (see Chapter 3). This metric reflects how much of the cost to manufacture a product is covered by the benefit of selling it. Since both ratios are greater than 1, they indicate that the NPV of the project benefits outweigh the NPV of the costs. Nevertheless, there is a slight difference between the BCRs of both processes. The LWA has a higher ratio, which means greater benefits relative to its costs. Nevertheless, when including the investment cost for implementing the pilot plants, this ratio is offset for the LWA alternative and that is why the PCC project obtained value of NPV, PP and IRR more attractive.

Due to the low NPV obtained for the LWA pilot plant implementation project, a sensitivity exercise was developed in order to visualize the NPV behavior when varying both LWA and PCC selling prices. Table 6-11 displays the selling prices analyzed for each pilot plant. The prices were selected in a range that include the value assumed (from literature review) during this economic evaluation.

Table 6- 11 Results of sensitivity analysis of LWA and PCC selling prices

LWA pilot plant		PCC pilot plant	
Selling price (USD/kg)	Net Present Value (USD)	Selling price (USD/kg)	Net Present Value (USD)
0.2	-1,474,263	0.11	553,525
0.21	-924,446	0.12	1,103,341
0.22	-374,630	0.13	1,653,157
0.23**	175,186	0.14**	2,202,974
0.24	725,002	0.15	2,752,790
0.25	1,274,819	0.16	3,302,606
0.26	1,824,635	0.17	3,852,422

** Values used in the original economic analysis

Figure 6-4 complements these results. In the graphic it both projects are similarly dependent on the selling price of their respective final product. The slope of both lines is alike, so it cannot be concluded that one of the project is more sensitive than the other. However, this

exercise did show how the rentability of the LWA pilot plant changes when decreasing the LWA selling price.

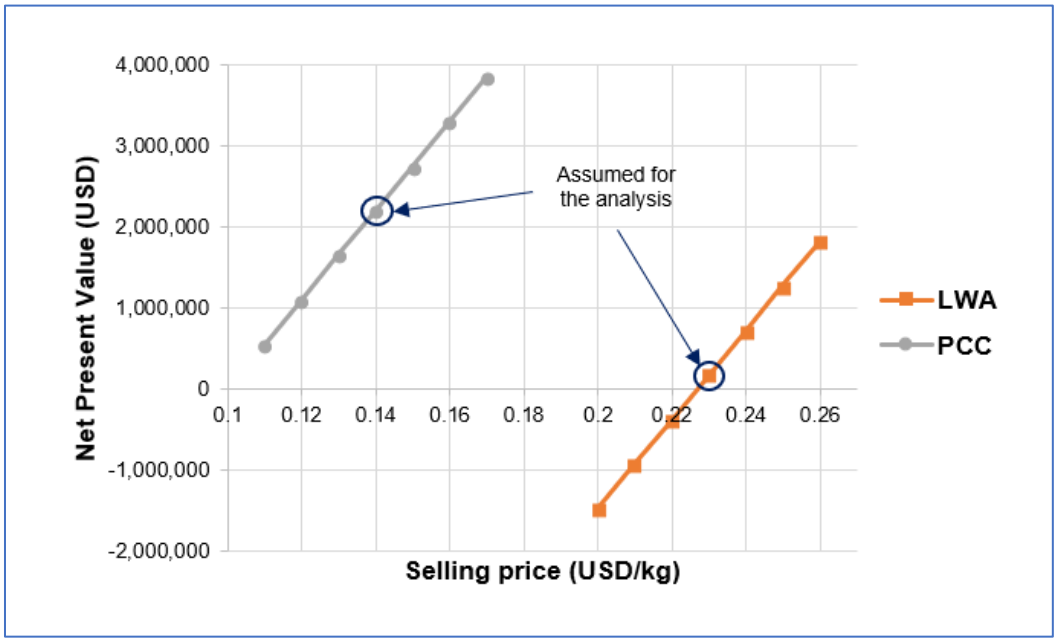

Figure 6- 4 Sensitivity analysis of LWA and PCC selling prices

If the produced light weight aggregate were sold to a price lower than 0.23 USD/kg the project of is not economically viable. This result gives a great advantage for the PCC pilot plant since all seven selling prices tested resulted in positive NPV for the project. Even the lowest values tested for PCC price (0.11 USD/kg) resulted in a higher NPV than the originally assumed LWA selling price (0.23 USD/kg).

Another economic scenario was tested, this time juts for the LWA pilot plant. As the previous chapter had shown, the difference in the overall energy consumption of both processes falls in the steam required by the production of LWA. So, the scenario considered consisted in having heat waste in the steel plant and/or the DR process. This would allow to satisfy the heating requirements of the LWA pilot plant without burning Natural Gas. Table 6-12 shows the result of this economic test.

Table 6- 12 Economic Key Parameters Indicators (KPI) for different scenarios in LWA pilot plant.

KPIs	Scenario 1	Scenario 2
Net Present Value (USD)	$175,186	$915,358
Payback period (years)	12	10
Internal rate of return (%)	8.42%	10%
Benefit Cost Ratio	1.6	1.7

Scenario 1: Where heat waste is not available for the mineralization process.
Scenario 2: Where heat waste is available either in the steel plant or DR plant or both.

There is an improvement in the economics of the LWA pilot plant when the cost of generating 2513 kg/h of steam is neglected. However, the increase of the economic KPIs is not very significant and it is inferred that the LWA selling price should still be set around 0.23 USD/kg for the pilot plant to be economically viable. This might be because the cost of generating steam only accounts for 15% of the total services costs.

CHAPTER 7 COMPARATIVE EVALUATION

Overall, this chapter combines the modelling; technical and economic metrics evaluation and the comparison between the two CO_2 mineralization processes.

The simulation results were correlated with an economic evaluation to select the more feasible process, and to proceed accordingly to develop a conceptual design for the plant facilities. The decision about feasibility of the pilot plants was based on projection of income statements, cash flow and determination of some indicators, previously mentioned. Based on the goals and objectives for this comparison, various key performance indicators (KPIs) were selected for evaluating the entire processes. In this study, the relevant the KPIs are categorized into technical and economic parameters.

Besides that, a single environmental KPS was also selected for the pilot plants comparison. The net CO_2 emissions from both mineralization process was calculated, and the results are shown in Table 7-1.

Table 7- 1 Net CO_2 emissions by the LWA and PCC pilot plants.

Pilot plant	Unreacted CO_2 ($kg/t_{produced}$)	CO_2 by energy consumption ($kg/t_{produced}$)	Net CO_2 emitted ($kg/t_{produced}$)
LWA	11	410	421
PCC	0.06	25	25.06

The table displayed above whose 2 ways in which CO_2 is released to the atmosphere in the mineralization processes. First, the CO_2 that did not react during the absorption and carbonation stages and second, the CO_2 that is indirectly emitted for the energy consumption of the pilot plants. The LWA design accounted for a total 421 kg of CO_2 emitted per ton of LWA produced. The alternative mineralization process binds only 25 kg of CO_2 per ton of PCC produced. These results reveal that the LWA pilot plant, with the conditions a design basis proposed in this thesis, is less environmentally friendly than the PCC pilot plant.

Table 7-2 summarizes LWA and PCC pilot plant technical, economic and environmental KPIs. The CO_2 change corresponds to the relation between the CO_2 processed and the net CO_2 emitted. The two scenarios tested in the economic evaluation of the LWA pilot plant were also considered to represent the environmental KPI.

Table 7- 2 KPIs results for the LWA and PCC pilot plant designs.

KPIS	LWA pilot plant	PCC pilot plant
Technical		
Mass balance		
CO_2 processed (kg/tproduced)	212	458
Slag processed (kg/tproduced)	284	584
Energy balance		
Cooling needs (kgCoolwater/tproduced)	71,132	2,967
Heating needs (kgSteam/tproduced)	2,513	0
Heating needs (kW/tproduced)	1,578	0
Electricity consumption (kWh/tproduced)	118	55
Environmental		
CO_2 emited$_1$ (kg/tproduced)	421	25
CO_2 emited$_2$ (kg/tproduced)	65	25
CO_2 change$_1$ (%)	1.99	0.05
CO_2 change$_2$ (%)	0.31	0.05
Economic		
Fixed Capital Investment (USD)	$4,492,287	$2,692,080
Total Production Cost (USD/year)	$1,637,629	$1,833,491
Total Incomes (USD/year)	$2,623,040	$2,729,280
Net present Value (USD)	$175,186	$2,202,974
Payback period (years)	12	8

Subscript 1: Scenario where here heat waste is not available for the mineralization process.
Subscript 1: Scenario where heat waste is available either in the steel plant or DR plant or both.

The CO_2 change indicator denotes how significant the net CO_2 emissions reduction could be at a pilot plant level, if the CDU processes were implemented. At these evaluation conditions, PCC has a higher CO_2 sequestration performance and CO_2 emission reduction than LWA pilot plant. As for the LWA pilot plant, jus the scenario where heat waste is available in the steel and/or DR plant represents an overall reduction in CO_2 emissions. Otherwise, if heat waste is not available, the LWA pilot plant would emit more CO_2 than the captured.

Technical KPIs showed that PCC pilot plant can sequestered a greater amount of CO_2, more than twice than LWA pilot plant. On the other hand, the great amount required by the PCC process represents a disadvantage because of the cost of grinding the solid and the energy and equipment specification needed to move this flow through the process. In terms of energy consumption, the LWA pilot plant is in a disadvantage position generated by the greater number of equipment and their heating, cooling and electricity needs.

Economic KPIs showed that the PCC pilot plant could meet the payback period in fewer years than LWA. In addition, the leading advantage of PCC pilot plant is the significantly lower Fixed Capital Investment (FCI), while the productions costs remain very similar between both process, hence the attractiveness for this pilot plant than for LWA one.

CHAPTER 8 Conclusions

The research presented in this thesis consisted of literature study, experimental work, model calculations, process simulations, and economic analyses of two CO_2 mineralization pilot plants for their proper comparison and evaluation to implement in a Direct Reduction-Electric Arc Furnace (DR-EAF) facility. The pilot plants designs presented accurately modeled the CO_2 mineralization processes and obtained representative results. These results confirmed the CO_2 mineralization using EAF slag and provided boundary conditions for their implementation in a steel plant with a direct reduction process.

It is possible to extract calcium ions from electric arc furnace slag using aqueous solution of ammonium chloride as solvent and form a precipitate with the bubbling of CO_2. The methods were proven to work well and effectively in laboratory scale. The conceptualization and designing of the processes at a pilot plant level was a necessary step in order to find out in what form the processes were best suitable for industrial scalation, and for the final step it they were economically viable to implement

It has been shown that the parameters solid-to-liquid ratio and the particle size has the largest effect during the extraction stage; directly influencing the Ca extraction from the slag. The solvent concentration affects directly on the dissolution of other elements present in the EAF slag, hence it might be required the separation of unwanted elements from the resulting solution containing Ca^{++} ions, although this separation was not modeled nor simulated during the technical analysis.

The selective calcium extraction efficiency is the most important factor for CO2 mineralization technologies to be feasibly, since it determines the quantity of materials needed for the production of carbonated materials as Light Weight Aggregates (LWA) or Precipitated Calcium Carbonate (PCC).

The amount of CO_2 processed by the LWA pilot plant is offset by the heat requirements of the overall process (stripper tower and evaporator) as seen in scenario 1. Nevertheless, when applying scenario 2 conditions, this pilot plant turns into and environmental friendly process, which means that it is necessary that waste heat is available in the steel plant in order to implement this LWA production process.

A disadvantage found in the PCC process was that large amounts of Ca-containing slag is required to sequester a significant fraction of the CO_2 emitted from the DR process, therefore, greater flows (including sludges) exist in the process and impact in the equipment designs. Additionally, there is the need for the steel plant to have this amount of EAF slag available.

Although the ammonium chloride spent in extraction stage is regenerated after the carbonation takes place (in both pilot plants), vaporization losses of ammonia as well as contamination must be minimized to minimize the solvent make-up needed during continuous operation.

The PCC product needs to be filtered and subsequently washed to remove the remnants of ammonium chloride from the calcium carbonate product. The washing requirements and filterability of calcium carbonates produced with the pilot facility was recently tested [27]. The results showed that the tested calcium carbonate slurries are easy to filter with both pressure filtration and vacuum filtration.

First, the processes were simulated to determine the properties of streams as well as the power and heat consumption of the processes equipment. Second, total investment costs were estimated with the help of available literature and known estimation method. For LWA, major costs are associated with the equipment cost and the extra feedstock required (substrate). As for the PCC pilot plant, the major costs rely in the Total Services Cost (TSC) because of the grinding of slag. In general, the PCC pilot plant process is cheaper than the LWA process. On top of this, the prices range at which LWA can be sold is very limited and this represents a disadvantage in the economics of the LWA pilot plant.

Both pilot plants result in a positive NPVs which is translated as the economic feasibility of the process, although the Net Present Value (NPV) of PCC pilot plant is significantly higher than the NPV of LWA pilot plant, even when scenario 2 is considered. As it was shown earlier, the total production costs as well as the production sales are very similar for both pilot plants and this can lead to the conclusion that they both are equally feasible. Nevertheless, there is a significant difference between their economics in the investment cost, mainly represented by the equipment's purchasing and installation and this is reflected in the NPVs and payback periods of the projects.

Taking all the considerations mentioned above, it is acceptable to conclude that PCC pilot plant represents a more attractive process to couple with a DR-EAF plant. For this conclusion, it was considered the technical limitations of both processes as well as the economics of the projects. PCC pilot plant resulted in a lower investment cost comparing to the LWA process and a simpler conceptual design.

Finally, although the amounts of CO_2 handled by this CDU technology may never become significant for CO_2 emissions reduction on a global scale, for a steel plant the process could still be beneficial with respect to minimizing the amount of waste materials generated to produce a marketable product.

It is important to mention that the experimental work and mass balances allowed the design and estimation cost of the mineralization processes. Once the pilot plants are started-up, the real efficiency of Ca^{++} extraction from EAF slag will be obtained and, with this, the amount of the carbonated product that can be produced.

8.1 RECOMMENDATIONS FOR FUTURE WORK

To overcome the challenges mentioned earlier, a few solutions paths are proposed and discussed in this section.

The selective Ca^{++} extraction efficiency must be further investigated in order to prevent that other elements, such as heavy metals, may also leach out during the extraction stage, thus this leads to impure carbonate precipitate and affects directly the economics of the process.

It is recommended to analyze the carbonate product formed in the CO_2 mineralization technology via XRD (X-ray powder diffraction), TC (Total Carbon), and/or SEM analysis to confirm that the final product consists primarily of calcium carbonate and, if necessary, try out the pH raising or other methods in the selective extraction of CaO from EAF slag. Also, the study on the carbonation kinetics is important in order to enable the control of the PCC quality, for example, morphology, agglomeration, and PSD.

The temperature influence in the extraction testes should be further investigated as it may lead to a different conclusion and operating conditions for the pilot plant. No examples in the literature could be found of such tests when using EAF slag as raw material.

It is recommended to run new simulations of both mineralization processes, this time using a 2M NH_4Cl solution to confirm that the same extraction efficiency (40%) can be achieved with a lower flow of the solvent. This would directly benefit the economics of the process since both the energy and raw material flow would decrease.

To address the problem of the overall net CO_2 emissions of the CDU technology, an entire waste-to-supply chain should be critically evaluated by a life cycle assessment (LCA). Also, a proposed CDU process in combination with renewable energy sources could be analyzed in order to overcome the CO_2 energy equivalent required.

The carbonation reactor design in the PCC pilot plant needs to be heavily investigated as well as the alternative of using 2 carbonation steps instead of 1. The gas feed to the process stage

is larger than what is usual for conventional reactors. The size and type of the carbonator depends on the CO_2 conversion kinetics. A model of the physical and chemical phenomena in this type of bubbling reactor needs to be studied.

References

[1] M. K. a. L. Lazi, "CO2 Emissions in the Steel Industry," *Metalurgija,* 2009.

[2] G. a. M. M. M.-V. Dennis Y.C. Leung, "An overview of current status of carbon dioxide capture and storage technologies," *Renewable and Sustainable Energy Reviews,* vol. 39, pp. 426-443, 2014.

[3] W. K. a. J.-F. Hake, Carbon Capture, Storage and Use, 2015: Springer.

[4] M. A. a. A. Dibenedetto, "Utilisation of CO2 as a chemical feedstock: opportunities and challenges," *," Dalton Trans., vol. 28, pp. 2975– 2992, 2007..,* Vols. 2975-2992, p. 28, 2007.

[5] H.-P. M. a. R. Zevenhoven, "Design of a Continuous Process Setup for Precipitated Calcium Carbonate Production from Steel Converter Slag," *ChemSusChem,* vol. 7, p. 903 – 913, 2014.

[6] G. C. a. S. Perathoner, Green Carbon Dioxide: Advances in CO2 Utilization, Wiley, 2014.

[7] A. A.-D. A. C.-C. Y. K. a. L. R. J. Patricio, "Region prioritization for the development of carbon capture and utilization technologies," *Journal of CO2 Utilization,* vol. 17, pp. 50-59, 2017.

[8] A. B.-D. a. E. T. M. Prez-Fortes, "CO2 utilization pathways: Techno-economic assessment and market opportunities," *Energy Procedia,* vol. 63, pp. 7968-7975, 2014.

[9] E. A. Q. a. K. A. Peter Styring, Carbon Dioxide Utilisation: Closing the Carbon Cycle, Elsevier, 2014.

[10] L. K. S., "Carbonate Chemistry for Sequestering Fossil Carbon," *Annual Review of Energy and the Environment,* vol. 27, pp. 193-232, 2002.

[11] "Industrial Efficiency Technology Database," [Online]. Available: http://ietd.iipnetwork.org/content/hyl-iii-process. [Accessed December 2017].

[12] "Tenova," [Online]. Available: https://www.tenova.com. [Accessed December 2017].

[13] V. Shatokha, "Environmental Sustainability of the Iron and Steel Industry: Towards Reaching the Climate Goals," *European Journal of Sustainable Development,* vol. 5, pp. 289-300, 2016.

[14] T.-C. C. C.-C. H. C.-J. H. Y.-H. C. a. P.-C. C. Shu-Yuan Pan, "CO2 Mineralization and Utilization using Steel Slag for Establishing a Waste-to-Resource Supply Chain," *Scientific Reports ,* vol. 7, 2017.

[15] R. C. J. A. V. O. M. M. a. A. M. C. Gustavo León, "Treatment of Hazardous Waste by Carbon Dioxide Capture from an Electric Arc Furnace," *ISIJ International,* vol. 55, no. 3, p. 559–563, 2015.

[16] H.-P. a. Forsman, "Reduction of CO2 Emissions from Steel Plants by Using Steelmaking Slags for Production of Marketable Calcium Carbonate," *Steel Research International,* vol. 80, pp. 415 - 421, 2009.

[17] J. R. Centre, "Carbon Capture and Utilisation Workshop. Background and proceedings," 2013.

[18] K. L. S. S. H. R. N. P. a. M. M. Bonenfant D, "Carbon capture and storage using alkaline industrial wastes," *Engineering Chemistry Research,* vol. 47, pp. 7610-7616, 2008.

[19] N. T. Y. N. Y. K. a. Y. K. Kodama S, "Development of a new pH-swing CO2 mineralization process with a recyclable reaction solution," *Energy,* vol. 33, pp. 776-84, 2008.

[20] C. Y. T., Effects of process variables on the conversion of BOF slag to carbonate, 2008.

[21] S.-W. L. C. J. S. P. K. S. W. J. J. a. S. C. Jun-Hwan Bang, "Leaching of Metal Ions from Blast Furnace Slag by Using Aqua Regia for CO2 Mineralization," *Energies,* vol. 9, pp. 993-13, 2016.

[22] S.-Y. S. P. a. P.-C. Chiang, "CO2 Capture by Accelerated Carbonation of Alkaline Wastes: A Review on Its Principles and Applications," *Aerosol and Air Quality Research,* vol. 12, pp. 770-791, 2012.

[23] H. Z. H. L. S. L. a. W. L. Weijun Bao, "Process simulation of mineral carbonation of phosphogypsum with ammonia under increased CO2 pressure," *Journal of CO2 Utilization,* vol. 17, p. 125–136, 2017.

[24] M. U. G. C. R. K. a. M. M. M.-V. A. Sanna, "A review of mineral carbonation technologies to sequester CO2," *Chem. Soc. Rev.,* vol. 43, pp. 8049-8080, 2014.

[25] M. A. a. H. H. Amin Azdarpour, "A Review on Carbon Dioxide Mineral Carbonation Through pH-swing Process," *Chemical Engineering Journal,* pp. 615-630, 2015.

[26] A. W. S. E. G. V. M. a. H. B. Ron Z., "Carbonation of calcium-containing mineral and industrial by-products," *Frontiers of Chemical Engineering,* vol. 4, pp. 110-119, 2010.

[27] "Carbon utilization to meet california's climate change goals," *Energy Procedia,* vol. 37, pp. 6979-6986, 2013.

[28] I. Omae, "Recent developments in carbon dioxide utilization for the production of organic chemicals," *Coordination Chemistry Reviews,* vol. 256, p. 1384 – 1405, 2012.

[29] E. A. a. O. Y. Orhan, "CO2 utilization: Developments in conversion processes," *Petroleum,* 2016.

[30] G. K. H. K. a. H. L. J. Jang, "Review on recent advances in CO2 utilization and sequestration technologies in cement-based materials," *Construction and Building Materials,* vol. 127, pp. 762-773, 2016.

[31] G. C. J.-L. D. a. S. P. E. A. Quadrelli, "Carbon dioxide recycling: Emerging large-scale technologies with industrial potential," *ChemSusChem,* vol. 4, p. 1194–1215, 2011.

[32] C. Song, "Global challenges and strategies for control, conversion and utilization of CO2 for sustainable development involving energy, catalysis, adsorption and chemical processig," *Catalysis Today,* vol. 115, p. 2 – 32, 2006.

[33] G. I. a. G. C. Marcello De Falco, CO2: A Valuable Source of Carbon, Springer.

[34] S. V. d. Z. a. F. Zeman, "Production of Carbon Negative Precipitated Calcium Carbonate from Waste Concrete," *The Canadian Journal of Chemical Engineering,* 2017.

[35] S. E. a. R. Z. Sebastian Teir, "Production of precipitated calcium carbonate from calcium silicates and carbon dioxide," *Energy Conversion and Management ,* vol. 46, p. 2954–2979, 2005.

[36] a. R. Z. Hannu-Petteri Mattila, "Production of Precipitated Calcium Carbonate from Steel Converter Slag and Other Calcium-Containing Industrial Wastes and Residues," in *Advances in Inorganic Chemistry*, Elsevier Inc., 2014, pp. 347-384.

[37] T. K. J. P. a. H.-P. Sebastian Teir, "Case study for production of calcium carbonate from carbon dioxide in flue gases and steelmaking slag," *Journal of CO2 Utilization,* vol. 14, pp. 37-46, 2016.

[38] H. Y. J. Z. B. L. C. L. Y. W. L. X. a. X. Z. H. Xie, "Scientific and engineering progress in CO2 mineralization using industrial waste and natural minerals," *Engineering,* vol. 1, pp. 150-157, 2015.

[39] A. Tech, Modeling Processes with Electrolytes-Aspen Plus Users Manual, 1999.

[40] "Comisión Federal de Electricidad," [Online]. Available: www.cfe.gob.mx. [Accessed 2018].

[41] I. N. d. E. y. C. Climático, "Gobierno de la República Mexicana," 2014. [Online]. Available: https://www.gob.mx/.

[42] G. a. S. R. Towler, "Economic evaluation of projects," in *Chemical engineering design: principles, practice, and economics of plant and process design*, Waltham, USA, Elsevier Ltd, 2013.

[43] G. B. Urbina, Evalaución de proyectos, McGraw-Hill, 2016.

[44] A. S. C.-J. F. a. R. Z. Sanni Eloneva, "Preliminary assessment of a method utilizing carbon dioxide and steelmaking slags to produce precipitated calcium carbonate," *Applied Energy,* vol. 90, p. 329–334, 2012.

[45] I. G. 1. a. R. Z. Hannu-Petteri Mattila, "Chemical kinetics modeling and process parameter sensitivity for precipitated calcium carbonate production from steelmaking slags," *Chemical Engineering Journal,* vol. 192, pp. 77-89, 2012.

[46] P. A. a. F. LS., "CO2 mineral sequestration: physically activated dissolution of serpentine and pH swing process," *Chemical Engineering Science,* vol. 59, p. 5241–5248, 2004.

[47] J. M. N. a. B. S. D. Gómez-Días, "Analysis of mass transfer in the precipitation process of calcium carbonate using gas/liquid reaction," *Chemical Engineering Journal,* pp. 203-209, 2006.

[48] W. C. R. B. N. M. a. M. M. X. Wang, "Comprehensive Study of the Hydration and Dehydration Reactions of Carbon Dioxide in Aqueous Solution," *Journal of Physics and Chemistry ,* vol. 114, p. 1734–1740, 2010.

[49] A. Tech, Aspen Plus: Aspen Process Economic Analyzer (APEA), 2000.

[50] sdvf, "dsvsc," *c as ,* vol. sdvfs, no. sfbvbsfab, p. fvfb, dsvcsd.

[51] L. KS, "A guide to CO2 sequestration 2003;300(5626):1677–8.," *Science,* 2003.

[52] A. B. S. K. V. P. a. J. W. Abby Kirchofer, "Impact of alkalinity sources on the life-cycle energy efficiency of mineral carbonation technologies," *Energy Environ. Sci.,* vol. 5, p. 8631–8641, 2012.

[53] M. a. L. L. Kundak, "CO2 Emissions in the Steel Industry", Metalurgija, 2009.".

[54] I. Omae, "Aspects of carbon dioxide utilization," *Catalysis Today,* vol. 115, no. 14, pp. 33-52, 2003.

[55] P.-C. a. S.-Y. Pan, "Carbon Dioxide Mineralization and Utilization," *National Taiwan University,* 2017.

[56] E. P. J. K. A. E. R. Z. a. C. F. Sanni Eloneva, "Coutilisation of CO2 and steelmaking slags for production of pure CaCO3 – legislative issues," *Journal of Cleaner Production,* vol. 18, pp. 1833-1839, 2010.

[57] L. Xiaozhi, "How to make the most of carbon dioxide," *Nature,* vol. 526, pp. 628-630, 2015.

[58] W. S. Association, "World Steel in Figures," 2017.

[59] M. J. a. F. K. M. Mikkelsen, "The teraton challenge: a review of fixation and transformation of carbon dioxide," *Energy Environ. Sci. ,* vol. 3, pp. 43-81, 2010.

[60] G.-J. W. a. R. N. C. Wouter J. Huijgen, "Minerak CO2 Sequestration by Steel Slag Carbonation," *Environ. Sci. Technol.,* vol. 39, pp. 9676-9682, 2006.

[61] W. C. H. B. D. P. J. E. L. a. S. D. H. Lackner K. s., "Carbon dioxide disposal in carbonate minerals," *Eenrgy,* vol. 20, pp. 1153-1170, 1998.

[62] A. B.-D. a. E. T. M. Prez-Fortes, "CO2 utilization pathways: Techno-economic assessment and market opportunities," *Energy Procedia,* vol. 63, pp. 7968-7975, 2014.

Appendixes

Appendix A- Description of the Technology Readiness Levels (TRL)

TRL	Assumption
1	Basic principles observed
2	Technology concept formulated
3	Experimental proof of concept
4	Technology validated in lab
5	Technology validated in relevant environment (industrially relevant environment in the case of key enabling technologies)
6	Technology demonstrated in relevant environment (industrially relevant environment in the case of key enabling technologies)
7	System prototype demonstration in operational environment
8	System complete and qualified
9	Actual system proven in operational environment (competitive manufacturing in the case of key enabling technologies; or in space)

Appendix B- Description of the main CDU technologies implemented around the world.

CDU Category	Description	CDU Technology
Enhanced commodity production	This group of technologies involve using CO_2 to boost production of certain goods, typically where CO_2 is already used but could be modified. It also includes the use of CO_2 as a substitute in existing technologies. They generally involve applying new methods to techniques which are in commercial practice today but could be modified to use CO_2.	Power cycles (using super critic CO_2)
		Urea yield boosting
Enhanced hydrocarbon recovery	It involves the use of CO_2 as a working fluid to increase recovery of hydrocarbons from the subsurface. They range in maturity from commercially viable under certain conditions through to pilot phase.	CO_2-EOR
		CO_2-EGR
		ECBM
CO_2 to fuel	Technologies that can provide a means for new types of energy vectors. They partly consist of commercially established technologies liked to more novel use and more embryonic forms of energy carrier development.	Renewable methanol
		Formic acid
		Algae
		Photocatalytic proceses
CO_2 mineralization	These technologies rely on the accelerated chemical weathering of certain minerals using CO_2. It can be used un a range of applications, typically involving construction materials or in niche circumstances such as for mine tailing stabilization.	Cement production
		CO_2 concrete curing
		Carbonate mineralization
Chemicals production	CO_2 can be used in the synthesis of a range of intermediates for use in chemical and pharmaceuticals production, including carbamates, carboxylation, insertion reactions, inorganic complexes and polymer production. Conversion methods require the use of catalysts, heat and/or pressure to break the stable CO_2 structure, ad include photocatalysis or electrochemical reduction.	Sodium carbonate
		Polymers
		Acetic acid
		Algae

Appendix C- Protocol description for Extraction tests developed during Experimental Work

Step	Description
1	Preparation of Filter Crucibles. Crucibles were dried in the oven at 100-110 °C for one hour, cooled in a desiccator for 20 minutes and weighed. These steps were repeated 3 times until the mass of each crucible agrees to within 0.0005 g between the weightings.
2	Preparation of 5M NH_4Cl aqueous solution. 133.7275 g of NH_4Cl were added to the volumetric flask, adjusted to the final volume of 500 ml with deionized water and mixed thoroughly.
3	In total, 4 samples of 20 g slag and steel dust were weighed (2 samples of each). The geomass was preciously dried in the oven at 104 °C to remove humidity.
4	100 ml of the NH_4Cl aqueous solution were slowly added to the first slag sample at ambient temperature (20 °C) and the mixture was stirred constantly with a glass stirring rod for 10 minutes.
5	Mixture was left (covered) for at least 20 hours to fully precipitate.
6	Steps 4 and 5 were reproduced for the first steel dust sample.
7	100 ml of the NH_4Cl aqueous solution preheated at 75 °C were slowly added to the second slag sample and the mixture was stirred constantly with a glass stirring rod for 10 minutes at the same temperature (75 °C).
8	Mixture was left (covered) for at least 20 hours to fully precipitate.
9	Steps 7 and 8 were reproduced for the second steel dust sample.
10	After 20 hours of mixture precipitation, the supernatant liquid of the first slag sample was decanted through a weighed filter keeping most of the precipitate in the beaker. **Note:** A supernatant liquid sample was separated and stocked for further analysis.
11	Filtration process continued until the beaker seemed cleared of mixture. The precipitate was washed with three portions of deionized water.
12	A crucible, containing the precipitate, was dried at 104 °C for 2 hours (with 30 minutes intermediate weightings) until the mass of the crucible with the precipitate had not a considerable changed.
13	Steps 10-12 were reproduced for the second slag and both steel dust samples.

Appendix D- Protocol description for Carbonation tests developed during Experimental Work

Step	Description
1	Preparation of filter crucibles and equipment.
2	Dry at 550 °C the slag sample.
3	Preparation of 5M NH_4Cl aqueous solution.
4	Add 500 ml of the NH_4Cl aqueous solution to the 100 g of slag sample at room temperature and stir the mixture constantly for 1 hour.
5	Taking 10 ml samples at 5, 10, 20, 40 and 60 min after addition of the slag.
6	Record temperature and pH of the solution.
7	Leave mixture for at least 2 hours to fully sedimentation.
8	Decant the supernatant liquid through weighed filters keeping most of the precipitate in the beaker.
9	Wash with deionized water the final solid, dry at 550 °C and weight the precipitate and analyze it with XRF and XRD to determine the elemental composition and to obtain information on the chemical structure of the materials.
10	Absorption of CO_2.
11	Connect the CO_2 tank to the test tube with the rich ++ions solution, allowing CO_2 to be bubbled through the solution for as long as needed. Set the flow at 150 ml/min of CO_2 using a rotameter.
12	Taking 10 ml samples of the solution every 10 minutes after addition of the slag, for ICP analysis.
13	Record temperature and pH of the solution during the mixing.
14	Filter and wash the precipitate.
15	Dry at 550 °C and weight the resulting solid salt precipitates and analyze them by SEM (Scanning Electron Microscope).

Appendix E- Aspen Plus simulation model of the LWA pilot plant

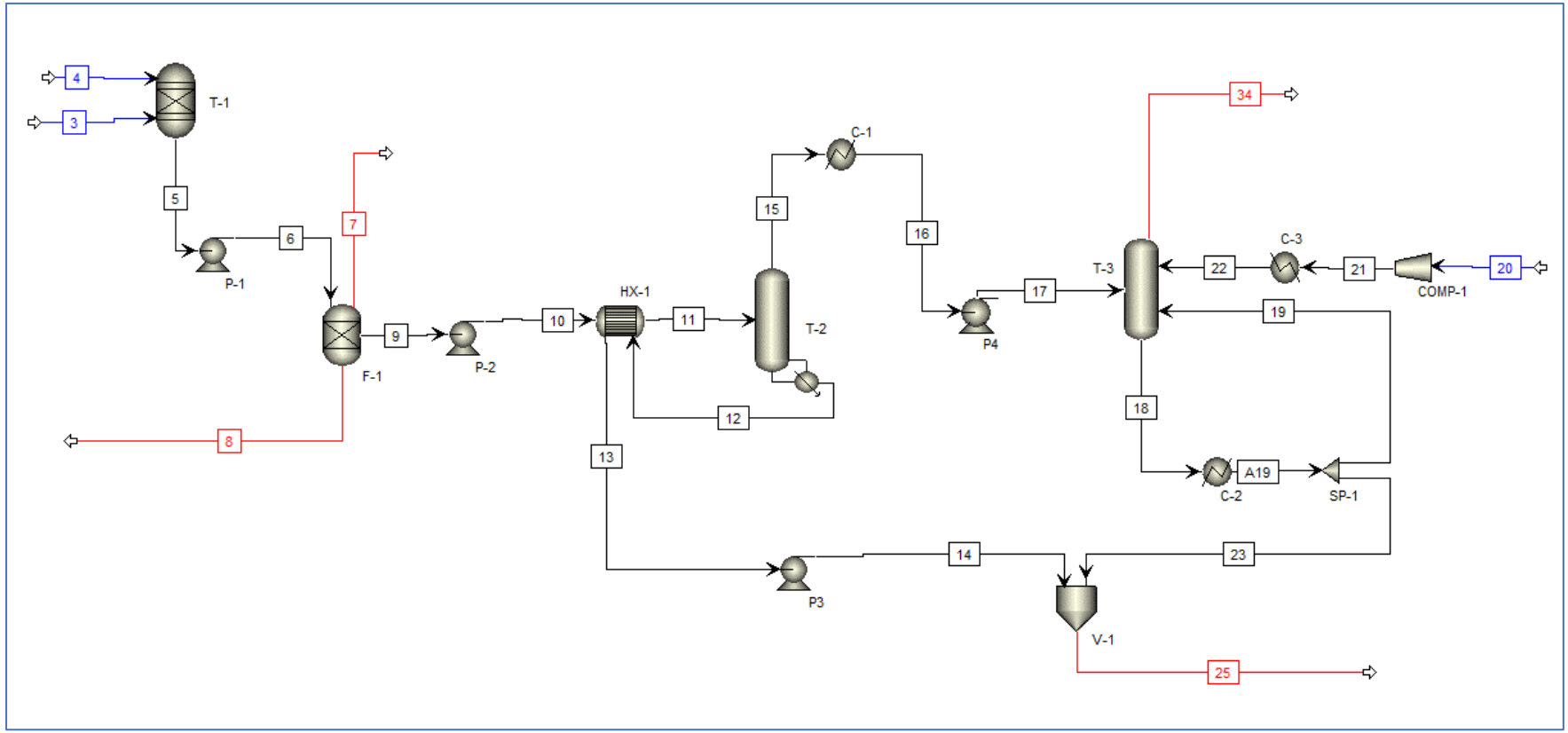

Appendix F- Stream results of the LWA pilot plant simulated in Aspen Plus.

		Streams											
	Unit	3	4	5	6	7	8	9	10	11	12	13	14
Temperature	C	25	107	118	118		30	30	30	138	152	32	32
Pressure	bar	1	1	1	2		2	2	4	4	4	4	5
Molar Vapor Fraction		0	0	0	0	0	0	0	0	0	0	0	0
Mole Flows	kmol/hr	13	696	714	714		8	706	706	706	655	655	655
Mass Flows	kg/hr	710	13,655	14,365	14,365		426	13,939	13,939	13,939	13,020	13,020	13,020
H2O	kg/hr		10,245	10,336	10,336			10,336	10,336	10,336	9,574	9,574	9,574
CAO	kg/hr	710		426	426		426						
CO2	kg/hr												
NH4CL	kg/hr												
NH4OH	kg/hr												
CACL2	kg/hr												
CA++	kg/hr			203	203			203	203	203	203	203	203
H3O+	kg/hr		0.10	3.27E-05	3.28E-05			1.88E-07	1.89E-07	9.31E-05	1.50E-03	2.31E-06	2.32E-06
NH4+	kg/hr		1,150	967	967			967	967	967	967	967	967
HCL	kg/hr		3.90E-04	1.96E-17	1.97E-17			1.42E-20	1.43E-20	4.11E-07	1.53E-15	1.62E-19	1.63E-19
CACO3(S)	kg/hr												
CACL2(S)	kg/hr												
HCO3-	kg/hr												
CL-	kg/hr		2,260	2,260	2,260			2,260	2,260	2,260	2,260	2,260	2,260
CO3--	kg/hr												
NH3	kg/hr		0.09	173	173			172	172	173	16	16	16
CAOH+	kg/hr			0.02	0.02			1.79E-02	1.79E-02	1.27E-02	1.20E-03	1.49E-03	1.49E-03
AMMON(S)	kg/hr												
CALCI(S)	kg/hr												
OH-	kg/hr		4.73E-07	1.55E-03	1.55E-03			4.61E-03	4.60E-03	1.02E-03	8.75E-05	4.26E-04	4.25E-04
NH2COO-	kg/hr												
SALT1	kg/hr												

		Streams											
	Unit	15	16	17	18	A19	19	20	21	22	23	25	34
Temperature	C	146	45	45	104	25	25	60	226	25	25	36	106
Pressure	bar	4	2	6	5	5	5	1	5	5	5	5	5
Molar Vapor Fraction		1	0	0	0	0	0	1	1	1	0	0	1
Mole Flows	kmol/hr	52	52	52	77	77	27	5	5	5	50	701	1
Mass Flows	kg/hr	919	919	919	1,734	1,734	607	227	227	227	1,127	14,147	18
H2O	kg/hr	762	762	762	1,081	1,114	390	4	4	4	724	10,251	2
CAO	kg/hr												
CO2	kg/hr				3	0.01	3.65E-03	223	223	223	0.01	0.03	11
NH4CL	kg/hr												
NH4OH	kg/hr												
CACL2	kg/hr												
CA++	kg/hr											14	
H3O+	kg/hr		3.90E-12	3.98E-12	5.81E-07	2.09E-08	7.33E-09			1.55E-05	1.36E-08	1.64E-05	
NH4+	kg/hr		0.04	0.04	89	107	37				69	1,139	
HCL	kg/hr	2.54E-05	1.34E-29	1.37E-29	4.02E-26	3.04E-28	1.06E-28				1.97E-28	1.03E-18	2.79E-17
CACO3(S)	kg/hr											472	
CACL2(S)	kg/hr												
HCO3-	kg/hr				165	76	27			4.96E-05	49	5	
CL-	kg/hr		2.47E-05	2.47E-05	3.80E-05	3.80E-05	1.33E-05				2.47E-05	2,260	
CO3--	kg/hr				4	19	7			8.71E-12	12	0.02	
NH3	kg/hr	157	157	157	73	34	12				22	6	5
CAOH+	kg/hr											2.21E-05	
AMMON(S)	kg/hr												
CALCI(S)	kg/hr												
OH-	kg/hr		3.98E-02	3.98E-02	1.34E-03	4.24E-04	1.48E-04			1.91E-12	2.75E-04	1.25E-04	
NH2COO-	kg/hr				127	242	85				157	0.43	
SALT1	kg/hr				192	142	50				92		

Appendix G- Aspen Plus simulation model of the PCC pilot plant

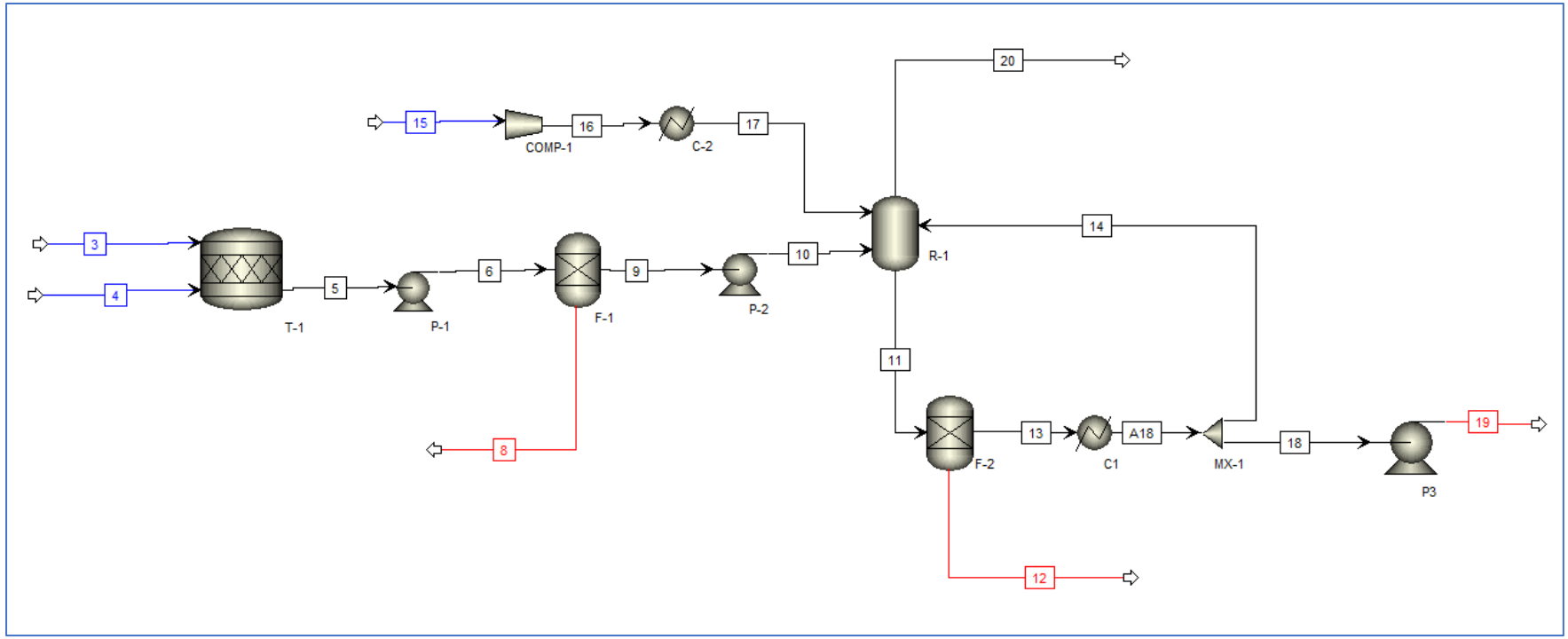

Appendix H- Stream results of the PCC pilot plant simulated in Aspen Plus.

		Streams											
	Unit	3	4	5	6	8	10	11	12	13	14	15	16
Temperature	C	25	25	30	30	30	30	25	25	25	25	60	131
Pressure	bar	1	1	1	2	2	3	3	3	3	1	2	3
Molar Vapor Fraction		0	0	0	0	0	0	0	0	0	0	1	1
Mole Flows	kmol/hr	95	1,431	1,536	1,536	85	1,451	14,227	21	14,206	12,785	11	11
Mass Flows	**kg/hr**	**5,612**	**28,059**	**33,671**	**33,671**	**5,028**	**28,643**	**280,259**	**1,200**	**279,058**	**251,150**	**466**	**466**
H2O	kg/hr		21,052	21,240	21,240		21,240	208,787	200	208,588	187,727	8	8
CAO	kg/hr	1,459		875	875	875							
CO2	kg/hr							1	2.02E-07	1	0.56	458.04	458
NH4CL	kg/hr												
NH4OH	kg/hr												
CACL2	kg/hr												
CA++	kg/hr			417	417		417	158	1.10E-03	158	142		
H3O+	kg/hr		1.42E-02	3.79E-07	3.80E-07		3.81E-07	2.74E-04	4.26E-10	2.74E-04	2.46E-04		
NH4+	kg/hr		2,362.87	1,987.44	1,987		1,987	23,555		23,555	21,200		
HCL	kg/hr		6.12E-16	2.85E-20	2.86E-20		2.87E-20	1.20E-17		1.20E-17	1.08E-17		
CACO3(S)	kg/hr							1,016	1,001	16	14		
CACL2(S)	kg/hr												
HCO3-	kg/hr							225	1.15E-03	2.24E+02	202		
CL-	kg/hr		4.64E+03	4.64E+03	4.64E+03		4.64E+03	46,438		46,438	4.18E+04		
CO3--	kg/hr							1	5.17E-04	7.94E-01	1		
NH3	kg/hr		0.01	354	354		354	63		63	57		
CAOH+	kg/hr			0.04	0.04		0.04	1.36E-04	2.83E-06	1.35E-04	1.22E-04		
AMMON(S)	kg/hr												
CALCI(S)	kg/hr												
OH-	kg/hr		3.11E-07	9.49E-03	9.49E-03		9.48E-03	1.55E-03	3.19E-04	1.55E-03	1.40E-03		
NH2COO-	kg/hr							15		15	13		

		Streams			
	Unit	17	A18	18	19
Temperature	C	25	25	25	25
Pressure	bar	1	1	1	2
Molar Vapor Fraction		1	0	0	0
Mole Flows	kmol/hr	11	14,206	1,421	1,421
Mass Flows	**kg/hr**	**466**	**279,058**	**27,906**	**27,906**
H2O	kg/hr	7	208,588	20,859	20,859
CAO	kg/hr				
CO2	kg/hr	458	1	0.06	0.06
NH4CL	kg/hr				
NH4OH	kg/hr				
CACL2	kg/hr				
CA++	kg/hr		158	16	16
H3O+	kg/hr	2.92E-06	2.74E-04	2.74E-05	2.74E-05
NH4+	kg/hr		23,555.28	2,355.53	2,356
HCL	kg/hr		1.20E-17	1.20E-18	1.21E-18
CACO3(S)	kg/hr		16	2	2
CACL2(S)	kg/hr				
HCO3-	kg/hr	9.36E-06	224	22	22
CL-	kg/hr		4.64E+04	4.64E+03	4.64E+03
CO3--	kg/hr	3.68E-12	1	0.08	0.08
NH3	kg/hr		63	6	6
CAOH+	kg/hr		1.35E-04	1.35E-05	1.36E-05
AMMON(S)	kg/hr				
CALCI(S)	kg/hr				
OH-	kg/hr	1.80E-12	1.55E-03	1.55E-04	1.55E-04
NH2COO-	kg/hr		15	1	1